12-HYDROXYSTEARIC ACID-BASED IN SITU FORMING ORGANOGELS: DEVELOPMENT AND CHARACTERIZATION

Dissertation

zur Erlangung des
Doktorgrades der Naturwissenschaften (Dr. rer. nat.)

der

Naturwissenschaftlichen Fakultät I – Biowissenschaften –

der Martin-Luther-Universität
Halle-Wittenberg

vorgelegt

von Herrn Dipl.-Pharm. Martin Windorf
geb. am 17. Mai 1988 in Rudolstadt

Gutachter:

1. Prof. Dr. Karsten Mäder
2. Prof. Dr. Lea Ann Dailey
3. PD Dr. Michael Hacker

Datum der öffentlichen Verteidigung: 14.08.2017

In der Wissenschaft gleichen wir alle nur den Kindern,
die am Rande des Wissens hier und da einen Kiesel aufheben,
während sich der weite Ozean des Unbekannten vor unseren Augen erstreckt.

Original von Sir Isaac Newton (1643-1727)

TABLE OF CONTENT

Table of Content I
Abbreviations and Symbols III
1 Introduction 1
1.1 Parenteral Depot Formulations 1
1.1.1 General Aspects 1
1.1.2 Benefits and Challenges of Depot Formulations 2
1.1.3 How to build long-acting Medicines? 3
1.2 Organogels 8
1.2.1 Oily Solutions as Vehicles 8
1.2.2 LMOGs as Thickening Agents 9
1.2.3 *In Situ* Forming Organogels (ISFOs) 12
1.3 Aims and Objectives 14
2 Materials 15
2.1 12-Hydroxystearic acid (12-HSA) 15
2.2 Vegetable Oils 18
2.3 Organic Solvents 18
2.4 Active Pharmaceutical Ingredients (APIs) 18
2.5 Further Excipients and Materials 19
3 Methods 21
3.1 Formulation Development 21
3.1.1 High Performance Thin Layer Chromatography (HPTLC) 21
3.1.2 Texture Analysis 22
3.1.3 Miscibility of Organic Solvents with Water and Oils 23
3.1.4 Solubility of 12-HSA in Organic Solvents 23
3.1.5 Preparation of Formulations and Stability Testing 24
3.1.6 Selection of Formulations for Characterization 24
3.2 *In Vitro* Characterization 25
3.2.1 Texture Analysis 25
3.2.2 Conductometric Experiments 26
3.2.3 Electron Paramagnetic Resonance (EPR) 26
3.2.4 Proton Nuclear Magnetic Resonance Relaxometry (^{1}H-NMR) 27
3.2.5 Oscillating Rheology 28
3.2.6 Cytotoxicity 30

3.2.7 Lipase Degradation Experiments 33
3.3 *In Vivo* Characterization 33
3.3.1 Animal Care 33
3.3.2 Magnet Resonance Imaging (MRI) 34
3.3.3 Ultrasound Imaging (USI) 35
3.3.4 Enzyme-Linked Immunosorbent Assay (ELISA) 36
4 Results and Discussion 37
4.1 Formulation Development 37
4.1.1 Selection of the 12-Hydroxystearic acid 37
4.1.2 Selection of the Organic Solvent 41
4.1.3 Selection of the Oil 44
4.2 *In Vitro* Characterization 50
4.2.1 Injectability 50
4.2.2 Release of Solvent 53
4.2.3 Microviscosity 59
4.2.4 Macroviscosity 64
4.2.5 Cytotoxicity 68
4.2.6 Enzymatic Degradation 78
4.3 *In Vivo* Characterization 83
4.3.1 Implant Degradation 84
4.3.2 Release of APIs 93
5 Summary and Perspectives 102
References VII
Deutsche Zusammenfassung XXII
Danksagung XXVI
Lebenslauf XXVII
Publikationsliste XXVIII
Selbstständigkeitserklärung XXX

ABBREVIATIONS AND SYMBOLS

% [m/m]	Percentage by weight
% [v/v]	Percentage by volume
12-HSA	12-Hydroxystearic acid
3D	Three-dimensional
^{1}H-NMR	Proton nuclear magnetic resonance
2P	2-Pyrrolidone
ad	fill up (lat. *adde*)
API	Active pharmaceutical ingredient
AUC	Area under the curve
bidest.	bidestilled
Corr.	Corresponding/ corresponds
δ	Loss angle
demin.	demineralized
DMSO	Dimethyl sulfoxide
EA	Ethyl acetate
EDTA	Ethylenediaminetetraacetic acid
ELISA	Enzyme-linked immunosorbent assay
EPR	Electron paramagnetic resonance
FCS	Fetal calf serum
FDA	U.S. Food and drug administration
G'	Storage modulus
G"	Loss modulus
GF	Glycofurol
GnRH	Gonadotropin-releasing hormone
HD-PMI	2-Heptadecyl-2,3,4,5,5-pentamethyl-imidazoline-1-oxyl
HPTLC	High performance thin layer chromatography
IC_{50}	Half maximal inhibitory concentration

i.m.	Intramuscular (lat. *intra musculus*)
i.v.	Intravenous (lat. *intra vena*)
ISFI	*In situ* forming implant
ISFM	*In situ* forming microparticle
ISFO	*In situ* forming organogel
KCl	Potassium chloride
LAF	Laminar air flow
LD_{50}	Median lethal dose
LH	Luteinizing hormone
LMOG	Low molecular weight organogelator
LOG P	Octanol-water partition coefficient
LPL	Lipoprotein lipase
LVR	Linear visco-elastic range
MEM	Minimal essential medium
MCT	Medium-chain triglycerides
mMEM	Modified minimal essential medium (see Table 6, p. 19 f.)
MRI	Magnet resonance imaging
MTT	3-(4,5-Dimethylthiazol-2-yl)-2,5-diphenyltetrazolium bromide
MWCO	Molecular weight cut off
NaCl	Sodium chloride
Neg. ctrl.	Negative control (sample)
NMP	*N*-Methyl-2-pyrrolidone
OD	Optical density
PBS	Phosphate buffered saline
PEG	Polyethylene glycol
Ph. Eur.	*Pharmacopoea Europaea*
PLA	Polylactic acid
PLGA	Poly(DL-lactide-co-glycolide)

PTFE	Polytetraflourethylene
R_f	Ratio of fronts
rpm	Revolutions per minute
SAFiN	Self-assembly fibrillar network
s.c.	Subcutaneous (lat. *subcutaneus*)
SD	Standard deviation
SRB	Sulforhodamine B
τ_c	Rotational correlation time
TSE	Turbo-spin-echo
T_1	Longitudinal relaxation time (spin-lattice)
T_2	Transverse relaxation time (spin-spin)
T_E	Time of echo
TLC	Thin layer chromatography
T_R	Time of repetition
USI	Ultrasound imaging
η	Dynamic viscosity
η^*	Complex viscosity
ZMG	Zentrum für Medizinische Grundlagenforschung

1 INTRODUCTION

1.1 PARENTERAL DEPOT FORMULATIONS

1.1.1 GENERAL ASPECTS

"Parenteral preparations are sterile preparations intended for administration by injection, infusion or implantation into the human or animal body."[1] Therefore, parenteral drugs have to comply with several quality tests, such as uniformity of content, sterility, bacterial endotoxins/ pyrogens and sub-visual particles. Additional excipients may be required in order to adjust the pH, to make the preparation isotonic with blood, to prevent deterioration of the API (active pharmaceutical ingredient) and to provide adequate antimicrobial properties. The *Ph. Eur. (Pharmacopoea Europaea)* defines the following categories of parenteral preparations:

- Injections;
- Infusions;
- Concentrates for injections or infusions;
- Powders for injections or infusions;
- Gels for injections;
- Implants.

The term *depot formulation* is not explicitly mentioned since it relates to the duration of the API release instead of the type of administration (injection, infusion) or the state of the formulation (concentrate, powder, gel, implant). Depot drugs are predominantly injected *i.m.* (intramuscular) or *s.c.* (subcutaneous), rarely *i.v.* (intravenous) (*e.g.* PEGylated antibodies). Depot formulations are counterparts of immediate-release dosage forms (*e.g.* uncoated tablets, hard capsules, preparations for inhalation and most *i.v.* applied parenteral drugs) as they release the API over prolonged periods of days to months. Typical applications include chronic diseases and long-term medications (*e.g.* hormone replacement, chemotherapy, rheumatoid arthritis, contraception).[2] Once applied it is hardly possible to remove a depot drug from the body. Hence, they are suitable for neuroleptic therapies as well. Thereby, non-compliant patients, who are often found with schizophrenia, cannot neglect or discontinue their medication.[3]

1.1.2 BENEFITS AND CHALLENGES OF DEPOT FORMULATIONS

BENEFITS

Compared to immediate-release drugs, depot dosage forms exhibit numerous advantages.[2,4,5] They allow continuous API release and thus prevent undesirable side effects caused by fluctuating plasma levels. In addition, frequent injections or long-term infusions are avoided, which improves the patient's compliance. Through the circumvention of both, the gastrointestinal tract and the first liver passage, food effects and variable intestinal resorption processes are bypassed. Hence, the bioavailability of unstable APIs (*e.g.* proteins, peptides) and APIs with a high first-pass metabolism can be increased. Furthermore, local injections (*e.g.* into the eye, gingival pocket) and therapies of difficult-to-access areas (*e.g*. joints) are feasible and avoid undesirable side effects caused by high systemic plasma levels.[6–8] Finally, by selecting suitable excipients, customized release profiles and release durations can be achieved.

CHALLENGES

Nearly all disadvantages of depot dosage forms relate to the impairment of either the patient's compliance or the drug safety. Oral dosage forms are often preferred since parenteral formulations bypass natural barriers (*i.e.* stomach, gut). Consequently, the latter have to fulfill the highest requirements concerning quality attributes in order to protect the patient's health. Injections often cause pain and tissue damage (*i.e.* bleedings, hematoma) at the site of injection.[9] This can be reduced by using low-viscous aqueous formulations, small cannulas, low injection volumes and a low injection speed. However, most parameters are fixed by the formulation itself and can hardly be influenced.

Avoiding *i.v.* administration of depot formulations is mandatory. Otherwise, vascular occlusions are likely to occur, which may cause embolisms or the death of limbs. Incorrect administration or unintentional failure of a depot drug can also lead to a sudden release of the entire quantity of API provided for the complete dosage interval. Consequently, side effects or even intoxications are most likely. Therefore, depot formulations are only developed for APIs with broad therapeutic indices and injections usually have to be done by physicians or medical staff. Thus, the patient's effort increases, whereas the therapy compliance decreases. Additionally, the operator must be specially trained in the administration. Since injected depots are very difficult to remove, hypersensitivities and allergic reactions of the patient should be ruled out in

advance or, if necessary, a small quantity of drug should be administered prior to test.[4] Finally, many depot formulations are inappropriate for terminal sterilization and thus require an aseptic production, which increases the manufacturer's efforts. Nonetheless, nearly all drugs recalled between 1980-2000 due to non-sterility were produced via aseptic processing.[10]

KEYS TO SUCCESSFUL DEPOT FORMULATIONS

As a result of the emering market of biopharmaceuticals (*i.e.* drugs containing antibodies, proteins, nucleic acids) over the past three decades, research and development in the field of parenteral drugs has clearly proceeded.[11–13] These technologically challenging drugs require excipients of special quality and manufacturing processes of particular care. Existing achievements of both factors were finally taken over by manufacturers and authorities as state-of-the-art and transferred to parenteral medicines in general. Thereby, the effort demanded by health authorities increases constantly.[14] It will be crucial in the development of new depot formulations to prefer robust and well-controllable production processes to complex and multistage processes. Selecting suitable excipients is also of special importance, with the principle of *simple and safe* being very well received.

An ideal depot formulation should meet the following criteria:

- Simple production (*i.e.* few steps, terminal sterilization, high stability);
- Patient-friendly administration *(i.e.* ready-to-use formulation, small cannulas);
- Biocompatibility of ingredients (*i.e.* low potential for side effects);
- Biodegradability of carrier material (*i.e*. residual-free resorbability);
- Controlled release of API (*i.e.* low initial burst effect, zero-order release, low variability, low risk for failure).

1.1.3 HOW TO BUILD LONG-ACTING MEDICINES?

Prolonging the effective period of an API can be achieved by different, mostly chemical and galenic principles. However, the site of injection and intended co-medications are affecting the effective period as well. Hydrophilic and low-molecular APIs will predominantly be cleared by blood vessels of the *i.m.* tissue, whereas macromolecules and lipophilic APIs will be rather removed from the *s.c.* tissue by lymphatic vessels.[15] Administration of a local vasoconstrictor (*e.g.* adrenaline) may slow down the

resorption of the API additionally.[16] In some cases, pharmacokinetic boosters exist. These APIs delay the elimination of the actual API from the body.[17]

CHEMICAL APPROACHES

Chemical modifications aim to reduce the water solubility of the API and thus to slow down their dissolution rate. Poorly water-soluble prodrugs are often produced by complex formation (*e.g.* zinc insulin) or esterification (*e.g.* testosterone enanthate, haloperidol decanoate).[18–20] Modifications of the pharmacologically active molecule itself are undesirable since they influence not only the pharmacokinetics but also the pharmacodynamics. In case of protein drugs for *i.v.* injection, the increase of the molecular weight by PEGylation and thus the delayed renal clearance has proven its worth.[21]

GALENIC APPROACHES

If chemical modifications of the API are not feasible to produce depot dosage forms, a variety of galenic approaches can be applied. Products of various principles are available on the market (Table 1, p. 5 f.). Poorly water-soluble APIs can be formulated as aqueous crystal suspension or oily solution. Well water-soluble APIs can be formulated as oily suspension. In suspensions, additional retarding effects can be achieved by the increase of the particle size, the change of the crystal modification and the addition of viscosity-increasing substances.[22] The APIs' release from oily solutions can also be influenced by the nature of the oil and the addition of organic solvents. In the recent past, the development of biodegradable polymeric materials has been the most central pillar in the research of depot dosage forms and already led to numerous new products, especially microparticulate formulations and implants.[23] Thereby, the API is embedded inside of the polymeric carrier (mostly co-polymers of lactic- and glycolic acid; *e.g.* PLGA (Poly(DL-lactide-co-glycolide))). After injection, the polymer slowly degrades and releases the API.[24] The polymeric structure (*e.g.* molecular weight, monomer ratio, stereochemistry, end-cap derivatization) provides a variety of opportunities to control the release.[25] However, using polyesters also has numerous intrinsic disadvantages significantly limiting their usability: polymer degradation during sterilization by moist and dry heat, the pH drop during polymer degradation irritating surrounding tissues and inactivating APIs, and the complex release kinetics.[26–32] The latter aspect is often based on the autocatalytic ester cleavage of the PLGA and is in contradiction to the possibilities mentioned to control the release.[33] Most common

polyester-based depot formulations are microparticles and implants. Drawbacks of these formulations are also the complex and expensive production of microparticles, their partially irreproducible reconstitution before administration as well as the patient-unfriendly injections of implants by means of large cannulas.[34–37]

Table 1 Approved parenteral depot products (table continues on the next page).[38,39]

	Product/ API	Carrier	Dosing frequency	Indication
Aqueous Suspensions	Celestan/ Betamethasone acetate, Betamethasone disodium phosphate	Water	1-2 weeks	Chronic inflammatory joint diseases
	Delphicort/ Triamcinolone-16,21-diacetate	Water	3-4 weeks	
	Lederlon/ Triamcinolone hexacetonide			
	Prednigalen/ Prednisolone acetate			
	Supertendin/ Dexametasone acetate, Lidocaine-HCl			
	Volon A/ Triamcinolone acetonide			
	Imap/ Fluspirilene	Water	1 week	Schizophrenia
	Zypadhera/ Olanzapine embonate	Water	2-4 weeks	
	Depo-Clinovir/ Medroxyprogesterone acetate	Water	3 months	Contraception
Oily Solutions	Rheumon/ Etofenamate	MCT	one-time	Chronic inflammatory joint diseases
	Ciatyl-Z Acuphase/ Zuclopenthixol acetate	MCT	2-3 days	Acute psychosis
	Ciatyl-Z Depot/ Zuclopenthixol decanoate	MCT	2-4 weeks	Schizophrenia
	Fluanxol Depot/ Flupentixol decanoate	MCT	2-4 weeks	
	Haldol/ Haloperidol decanoate	Sesame oil, benzyl alcohol	4 weeks	
	Lyogen Depot/ Fluphenazine decanoate	Sesame oil	2-4 weeks	
	Testosteron Depot/ Testosterone enanthate	Peanut oil	2-4 weeks	Testosterone deficiency
	Testoviron/ Testosterone enanthate	Castor oil, benzyl benzoate	2-4 Weeks	
	Nebido/ Testosterone undecanoate	Castor oil, benzyl benzoate	10-14 weeks	
	Faslodex/ Fulvestrant	Castor oil, benzyl benzoate, benzyl alcohol, ethanol	4 weeks	Mammary carcinoma
	Noristerat/ Norethisterone enanthate	Castor oil, benzyl benzoate	2-3 months	Contraception
	Androcur Depot/ Cyproterone acetate	Castor oil, benzyl benzoate	1-2 weeks	Prostate cancer, men paraphilia, flare-up of GnRH-agonists

	Product/ API	Carrier	Dosing frequency	Indication
Microparticles	Enantone/ Leuprolide acetate	PLGA	1 month	Prostate cancer, endometriosis, central precocious puberty
	Trenantone/ Leuprolide acetate	PLA	3 months	
	Sixantone/ Leuprolide acetate	PLA	6 months	
	Decapeptyl/ Triptorelin acetate	PLGA	1 month	
	Pamorelin/ Triptorelin embonate	PLGA	1 and 3 months	Prostate cancer
	Salvacyl/ Triptorelin embonate	PLGA	3 months	Men paraphilia
	Risperdal Consta/ Risperidone	PLGA	2 weeks	Schizophrenia
	Sandostatin LAR/ Octreotide acetate	PLGA	4 weeks	Akromegaly, carcinoid syndrome
Implants (preformed)	Gliadel/ Carmustine	Polyanhydride copolymer	one-time	Malignant glioma
	Zoladex/ Goserelin acetate	PLGA	1 and 3 months	Prostate cancer, endometriosis
	Profact Depot/ Buserelin acetate	PLGA	2 and 3 months	Prostate cancer
	Leuprone/ Leuprolide acetate	PLGA or PLA	1 and 3 months	
	Ozurdex/ Dexamethasone	PLGA	6 months	Macular edema
	Vantas/ Histrelin acetate	Acrylic copolymer[a]	12 months	Prostate cancer
	Implanon/ Etonogestrel	Ethylene vinylacetate copolymer[a]	36 months	Contraception
ISFI	Eligard/ Leuprolide acetate	PLGA, NMP	1, 3, 4 and 6 months	Prostate cancer

[a] Non-biodegradable carrier material.

IN SITU FORMING IMPLANTS (ISFIs)

One interesting technology already commercialized by the product Eligard, is based on the principle of *in situ* solidification (Figure 1, p. 7).[40–44] This ISFI (*In Situ* Forming Implant) is composed of the biodegradable and water-insoluble polymer PLGA, which is dissolved in the organic solvent NMP (*N*-Methyl-2-pyrrolidone) to form a high-viscous but injectable formulation. Before administration, this solution is mixed with the API leuprolide acetate, leading to a solution or suspension (dose-dependent). Once *s.c.* injected, diffusion of the solvent into the surrounding aqueous body fluid (trigger) leads to the precipitation of the polymer and to the formation of a solid implant. Subsequently, the API is released while the polymeric depot biodegrades.[24,32] By using different monomer ratios, release periods of 1, 3, 4 or 6 months can be achieved. Main

advantages of this formulation over microparticles and (preformed) implants are the simple manufacturing process including scale-up and the administration with smaller cannulas.[45]

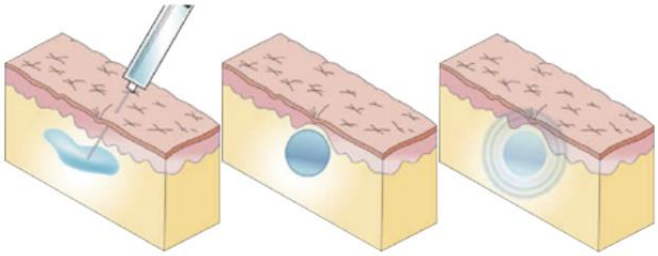

Figure 1 ***Principle of Eligard: After injection of the liquid formulation, the depot solidifies in situ. Due to the biodegradation of the PLGA, the API is released over 1, 3, 4 or 6 months.[46]***

Main obstacles of PLGA-based ISFIs in general and Eligard in particular are the hardly predictable release kinetic of the API and the toxicity of the organic solvents.[32,45,47–49] For the dissolution of the hydrophobic PLGA, only non-aqueous solvents, such as NMP, DMSO, PEG, GF, 2P, EA are suitable.[49,50] However, they all possess dose-dependent toxicity.[51] Considerable approaches to improve the compatibility are the search for alternative, biocompatible solvents and the reduction in solvent doses. The latter option also includes the search for alternative biodegradable polymers.[52,53] Furthermore, inherent and thus hardly influencing disadvantages of PLGA-based ISFIs are the initial burst release of the API caused by the solvent exchange as well as the variability in the shape of the solidified depots.[54,55] Both lead to complex and difficult-to-predict release profiles of the API. Particularly with larger depots, the polymer degradation is hard to control due to autocatalytic hydrolysis inside of the implants.[33,56] As for microparticles and (preformed) implants, the accumulation of acidic degradation products (*i.e.* lactic and glycolic acid) often leads to local irritation and stability issues of the active ingredient.[27–29] Consequently, this formulation is only suitable for APIs with a broad therapeutic index.[49] Another inconvenient and expensive factor concerning Eligard is the primary packaging in the form of 2 syringes in order to protect the API from degradation in the NMP during storage.[57] As a result, an effortful mixing procedure by medical staff is required to achieve the formulation ready-to-use.

1.2 ORGANOGELS

1.2.1 OILY SOLUTIONS AS VEHICLES

Organogels are gelled organic liquids or oils by means of gelator molecules. The oil serves as matrix material regarding the gelator. Considered in isolation, oils and oily solutions are often applied to achieve a sustained release of lipophilic APIs.[58,59] Carrier materials are usually vegetable oils, such as castor oil, sesame oil or peanut oil or semi-synthetic ones like MCT.[60] Parenterally administered, these oils are well-tolerated and low-irritant.[22] Influenced by oxygen, oils containing high contents of polyunsaturated fatty acids (*e.g.* linseed oil, soybean oil) can easily oxidize, build hydroperoxides and thus affect both the human tissue and the API.[61] Therefore, oils with a high saturation level and a high content of naturally contained antioxidants (*e.g.* tocopherol) are to be preferred. Due to the usage of highly purified, refined oils and proper storage (dark, cool, inert gas purging), irritation-causing hydroperoxides and hypersensitivity-causing allergenic contaminations are of minor significance.[62] In contrast to aqueous suspensions and hydrogels, oily solutions are water-free and particularly suitable for hydrolysis-sensitive APIs. Moreover, the adjustment of both pH and isotonicity as well as the addition of preservatives are unnecessary. However, especially castor oil-based formulations often require additives of organic solvents, such as benzyl benzoate or benzyl alcohol to reduce its high viscosity. During production, reduced viscosities allow quicker dissolution of the API by moderate stirring. Without organic solvents, this step would either take a long time or the high intake of air bubbles caused by a higher stirring rate would negatively affect both the microbial stability and the sterile filterability of the solution. Reducing the viscosity additionally improves the injectability via small cannulas. In some cases, the organic solvent also prevents premature recrystallization of the API. By using the moderately water-miscible benzyl alcohol, a certain diffusion of this solvent into the surrounding aqueous tissue fluid can be expected after injection. Since this oily depot remains completely liquid *in vivo*, such a formulation does not represent a typical ISFI.

Although oily solutions are highly biocompatible and well-studied, the retention of the API is usually limited to approximately 4 weeks (Table 1, p. 5 f.). Regarding dissolved APIs with moderate lipophilicity, the release within this period is predominantly diffusion-controlled and dependent on the distribution between oil and tissue fluids.[62–64,64] With increasing lipophilicity, the API enters the aqueous tissue fluid at the depot's

interface more slowly.[65] By using very lipophilic APIs, the rate of the release is predominantly controlled by the degradation of the oil.[64] Both the lipolytic cleavage of the triglycerides and the resorption of small oil droplets via the lymphatic system are described.[62] Very lipophilic and high-molecular APIs are primarily absorbed by the lymphatic route as well.[66] Assuming a given volume of depot, the release from oily solutions is additionally influenced by the shape of the depot; the higher the volume-specific surface, the quicker the rate of the release is, since diffusion paths will shorten. Therefore, all factors affecting the shape of the depot (*e.g.* injection volume/ speed/ site, body movement, external bumps) influence the release of the API as well.[64,67] Moreover, the viscosity of the oil affects the shape after injection and thus the release of particulate, undissolved APIs. Among oily solutions the product Nebido allows a dosing interval of 10-14 weeks. This long-term release is caused, on the one hand, by the very lipophilic undecylic acid ester of the testosterone. Therefore, the release is primarily controlled by the degradation of the oil. On the other hand, a single dose contains 4 mL instead of the usually applied 1 mL (equal concentration of API).[38,68] Thus, the release of the API accompanied by the degradation of the oil is prolonged.

1.2.2 LMOGs AS THICKENING AGENTS

LMOGs (low molecular weight organogelators) are monomeric compounds, which are capable of building colloidal arrangements in an organic solvent or oil and thereby to gelate. Resulting organogels can be considered as solids or semi-solids pervaded with the 3D self-assembly fibrillar network (SAFiN) of the LMOG.[69–72] Figure 2 (p. 10) shows examples of organogelators. Although most organogelators are LMOGs, several polymeric gelling agents exist (*e.g.* ethyl cellulose). However, all polymeric gelators are non-biodegradable and are thus unsuitable in terms of parenteral depot formulations but interesting for food industries.[73–75] Unlike polymeric gelling agents, LMOG molecules of the SAFiN are specifically connected via non-covalent interactions, such as hydrogen bonds, van der Waals forces, π-stacking or London forces.[71,76] The resulting fibers of the network and their junction zones provide rigidity to the microstructure. Thus, the organic liquid is immobilized by the SAFiN and thereby prevented from flowing.[77,78] Concerning gelation, the solubility of the LMOG in the organic liquid to be gelled is crucial. On the one hand, a certain solubility is necessary so that the substance behaves not only as sediment. On the other hand, the affinity of the LMOG must be lower to the organic liquid than to identical molecules in order to

build a SAFiN. Both LMOG and the liquid have to be considered by evaluating the ability to form organogels.[70,79,80]

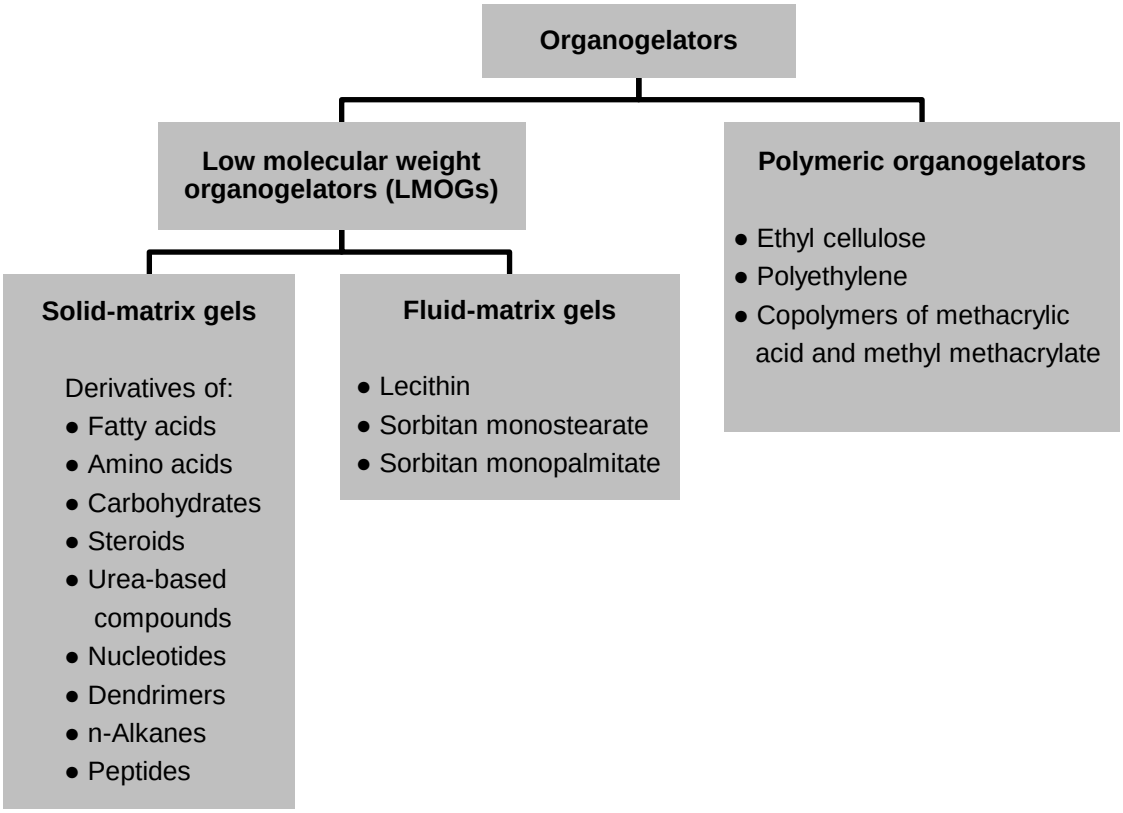

Figure 2 ***Overview of organogelators. Since the class of solid-matrix organogelators includes various heterogen types of molecules, several examples have been selected.[70,71,81]***

Based on the kinetic characteristic of the fibrillar network set up, LMOGs can be divided into solid- and fluid-matrix organogels (Figure 3, p. 11). Solid-matrix gels are typically prepared by dissolving the gelator in the heated organic liquid. Upon cooling, the solution supersaturates and molecules of the LMOG self-assemble into aggregates to form a permanent, most often crystalline network, in which junction points of pseudo-crystalline microdomains arise (sol-gel-transition). Solid-matrix organogels aggregate into high-order structures and are thus described as strong and more robust than fluid-matrix gels. Moreover, chirality of the gelator molecule is supposed to affect both growth and stability of the fibrillar network. In contrast, fluid-matrix organogels are mainly prepared by mixing the amphiphilic molecule with organic solvent to form reverse micelles. Upon the addition of small quantities of polar solvents, cylindrical reverse micelles start to grow until they entangle into a transient gelling network. The

formed organogels exhibit a “worm-like” or “polymer-like” structure in which junction points are simple chain entanglements. Gelator molecules of the micelles are dynamically exchanged with gelator molecules dissolved inside of the bulk liquid. The resulting less ordered structure with additional chain breaking and constant remodeling leads to rather weak gels compared to solid-matrix organogels.[70,71,81,82]

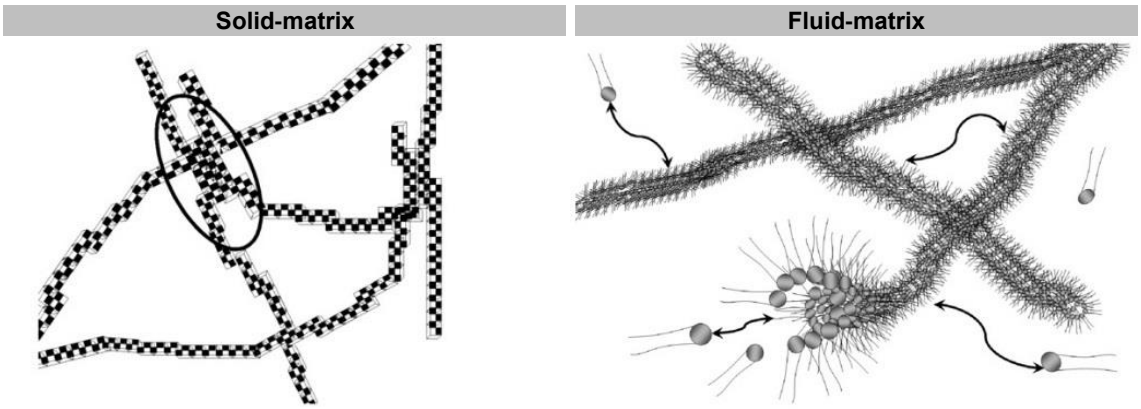

Figure 3 ***Left: Solid-matrix gel structure with robust and permanent solid-like network. Junction points are pseudo-crystalline microdomains (circled). Right: Fluid-matrix gel structure with transient network and junction points of simple chain entanglements. Dynamic exchange of gelator molecules and chain breaking/ recombination may occur (arrows).[70,81]***

Since organogels are to be considered as gelled oily solutions, they offer additional advantageous properties:

- By gelation, the release of undissolved and high-molecular dissolved APIs can be additionally delayed;
- Organogel depots are less susceptible to deformation after injection. Thus, implant shapes and release profiles are more reproducible;
- If the API is in particulate state, sedimentation is inhibited and reconstitution before administration can be omitted.

However, there are several disadvantages in using organogels instead of oily solutions:

- First, caused by their amphiphilic structure, fluid-matrix LMOGs often lead to irritations. Moreover, they are rather weak compared to solid-matrix organogels.
- Second, thermolabile APIs might not tolerate elevated temperatures during the manufacture of solid-matrix organogels.

- Third, gelation always leads to higher injection forces, especially when using small cannulas.
- Fourth, as a consequence of the mechanical stress and the resulting collapse of the SAFiN during injection, the gels' viscosity and thus the retention of the API decrease.
- Fifth, the incorporation of an API into organogels can cause competitive non-covalent interactions with the LMOG leading to liquefaction of the gel. Thus, organogels made of LMOGs will be incompatible with certain APIs.

1.2.3 *IN SITU* FORMING ORGANOGELS (ISFOs)

In order to overcome the mentioned disadvantages 2-4 of solid-matrix organogels (inappropriate for thermolabile APIs, high injection force, rheodestruction during injection), one strategy attains growing interest.[49,71,82–84] By adding a hydrophilic organic solvent that is miscible with the matrix oil, the LMOG's network structure can be disrupted and the gel liquefies. Thus, the viscosity decreases and the injectability via cannulas is enhanced. If the solvent is at least partly miscible with water, diffusion into the aqueous tissue fluid will occur (trigger). Thereby, the LMOG remains inside of the oily phase and its solubility is exceeded whereby organogelation starts *in situ*. Consequently, molecules of the LMOG build up the SAFiN and a solid depot arises at the site of injection. Since the principle of depot formation is comparable to polymer-based ISFI (*e.g.* Eligard, chapter 1.1.3, p. 3 ff.), but with liquid oil as matrix material instead of a solid polymer, this type of formulation is called ISFO (*In Situ* Forming Organogel). ISFOs can be considered as a subcategory of ISFIs. However, the term *ISFI* is still rather connected with polymer-based ISFIs. Accurately expressed, both ISFOs and polymer-based ISFIs are subcategories of ISFIs since *in situ* means the process of formation, whereas organogel and polymer correspond to the matrix material.

ISFOs combine advantages of both oily solutions and polymer-based ISFIs. The carrier material consists of refined vegetable oils, which are well-tolerated, enzymatically biodegradable and more inexpensive than their polymeric counterparts. The oil's degradation products (*i.e.* di-/monoglycerides, glycerol and fatty acids) are biocompatible as well. By the addition of organic solvents as crystallization inhibitors, the liquid state of the formulation can be maintained during storage and injection. Thus, lower injection forces are required compared to the high-viscous polymer-based ISFIs.

Eventually, gelled oils can offer longer release periods than liquid oily solutions. The simple production and gentle manufacturing conditions regarding temperature and shear sensitive APIs are major advantages of ISFOs in contrast to preformed organogels and polymer-based ISFI. Due to their lower viscosities compared to polymer-based-ISFIs, even sterile filtration instead of gamma sterilization may be possible. Since the organic solvent is only responsible to keep the LMOG dissolved in the oil phase, less solvent is necessary compared to dissolve the entire quantity of polymer (*e.g.* PLGA) concerning polymeric ISFIs. Challenging issues regarding ISFOs are, in turn, the toxicity of the organic solvent and the influence of the API on the stability of the LMOGs' solid-matrix network.

Several research approaches have been already investigated:

- A solution of 20 % of *N*-lauroyl-L-alanine methyl ester (LMOG), 14 % of ethanol and soybean oil was injected *s.c.* into rats. *In situ* gelation was evident 2 h after injection. Macroscopic observations after 9 days revealed no difference in the gel's integrity, whereas in the absence of the LMOG, soybean oil was cleared rapidly (< 24 h) from the site of injection.[83]
- *In vitro*, a formulation of 10 % of *N*-stearoyl-L-alanine methyl ester (LMOG), 10 % of NMP, 5 % of dispersed rivastigmine hydrogen tartrate particles and safflower showed low initial burst release of 10 % within the first 12 h but no further release within the following 6 days.[84]
- Using leuprolide acetate-loaded emulsions consisting of safflower oil, NMP, water, surfactants and either *N*-stearoyl-l-alanine methyl ester or N-stearoyl-l-alanine ethyl ester as LMOGs led to a pharmacological effect in rats over 35-50 days.[82]

1.3 AIMS AND OBJECTIVES

Drawing upon earlier research on parenteral depot formulations in general and on organogels in particular, this thesis attempts to develop an ISFO based on the LMOG 12-HSA (12-Hydroxystearic acid). Further excipients required should have a regulatory status or should be used already in the formulation of approved drugs for parenteral use. Selections of oils as matrix materials and organic solvents as crystallization inhibitors have been extensively investigated in order to meet the following criteria in the final formulation:

- Commercially available excipients of appropriate quality;
- Biocompatibility of ingredients and its metabolization products;
- Simple and reproducible production processes;
- Capability of terminal sterilization;
- Ease of injectability/ low-viscous formulation;
- Reliable *in situ* solidification effect;
- Complete biodegradability of carrier/ excipients.

Additional aims are desirable, but not mandatory:

- Sufficient storage stability;
- Low initial burst release of API;
- Controlled release of API over several months;
- Standard primary packaging (*e.g.* vial, ampule).

2 MATERIALS

2.1 12-HYDROXYSTEARIC ACID (12-HSA)

(*R*)-12-Hydroxystearic acid (12-HSA) is a white, greasy-feeling powder with an estimated water solubility of 0.33 mg/L at 25 °C and a Log P (octanol-water) of 6.4 (EPI Suite WSKOW v1.41, U.S. Environmental Protection Agency, USA). It is soluble in numerous organic solvents and shows a melting point at 81 °C.[85] The source material for its production is castor oil. After triglyceride hydrolysis, ricinoleic acid (C18:1 (ω-9), C12-OH) is extracted and hydrogenated leading to analytical grade 12-HSA. Technical-grade 12-HSA contains 15-35 % of stearic acid (C18:0) due to considerable contents of oleic acid (C18:1 (ω-9)), linoleic acid (C18:2 (ω-6)) and stearic acid (C18:0) which are linked with the glycerol of castor oil and transformed into stearic acid during hydrogenation.[22,86–89] Table 2 shows the 12-HSA products investigated in this thesis.

Table 2 Commercially available 12-HSA grades investigated in this thesis.

Trade name	Source	Remark
12-Hydroxystearic acid	Larodan, Sweden	Analytical grade
12-Hydroxystearic acid	Sigma-Aldrich, Germany	Analytical grade
12-HSA Flakes 81	Alberdingk Boley, Germany	Technical grade
Casid HSA	Vertellus, USA	Technical grade
Sternoil 12-HSA	Berg + Schmidt, Germany	Technical grade

12-HSA is a prototypical and well-known LMOG. It is commercially available, accepted as a biocompatible material and its potential to gel a variety of organic liquids and oils is intensively explored.[72,81,88–94] According to the available literature, most of these gels are prepared by melting 12-HSA with the organic liquid/ oil.[73] With cooling, the solubility of 12-HSA decreases, nucleation starts and crystal growth of fibrillary and branched structures occurs leading to a 3D network structure with the liquid/ oil entrapped.[95,96] General aspects concerning these SAFiN structures are described in chapter 1.2.2 (p. 9 ff.).

On the molecular level, the ability of organogelation can be reduced to the self-assembly of 12-HSA inside of the oil phase through intermolecular hydrogen bonds.[90,91] Specifically, carboxylic head groups dimerize and form cyclic head-to-head contacts (Figure 4, p. 16).[71,93] Secondary hydroxyl groups act as additional non-covalent

connecting elements.[97] The limited conformational freedom of the 12-hydroxyl group results in a zigzag H-bonding network, which is key for the fiber stability and causative for the unique crystallization characteristic.[89] Generally, the incorporation of polar additives (*e.g.* the API and/ or excipients) possessing competitive H-bonding groups needs to be avoided. Otherwise they would affect the self-assembly of the 12-HSA and finally weaken the stability of the gels.[98,99]

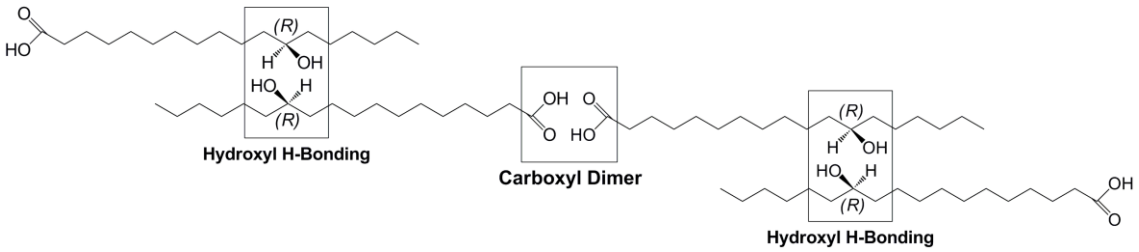

Figure 4 Postulated arrangement of (R)-12-HSA in the SAFiN of organogels.[97]

On the supramolecular level, organogels with low concentrations of 12-HSA appear transparent, whereas highly concentrated gels are turbid. The higher the concentration of 12-HSA is, the thicker the fibers will be and the more junction zones inside of the SAFiN will develop. Both larger aggregates and increased branching result in increased light diffraction and consequently stronger turbidity.[97] In contrast to 12-HSA, stearic acid, 12-methyl hydroxystearic acid and dihydroxy fatty acids are incapable of forming SAFiNs.[86,89,93,98] Due to the low molecular weight, small quantities of 12-HSA are necessary to gel non-polar liquids and to prevent them from flowing: 0.4 % in hexane[79], 0.5 % in canola oil[100] and 0.7 % in MCT[89]. However, different preparation conditions and the use of either analytical or technical grade 12-HSA do not permit a direct comparison of these concentrations.

Furthermore, the chirality of (*R*)-12-HSA is of great importance in order to ensure gelation. Although chirality in general is neither necessary nor sufficient for organogelation, enantiopure molecules are often better LMOGs than their racemic mixtures.[70] By using racemic 12-HSA, the carboxyl head groups do not dimerize in the oily phase. Thus, extended H-bonding networks cannot arise. Hence, the strength of the gel decreases due to the limited crystal growth.[86,95] Therefore, in mineral oil, less than 1 % of optically active (*R*)-12-HSA is sufficient for gelation, whereas 2 % of racemic (*RS*)-12-HSA is required.[71,89,95]

12-HSA organogels also exhibit thermoreversibility; gel-sol-gel transitions can arbitrarily often be repeated without changing the properties of the 12-HSA.[91,101] However, the gel's manufacturing temperature directly affects the crystallization process and thus the properties of the gel.[92,96] After melting 12-HSA in canola oil, a high cooling rate of 30 °C/min leads to impaired carboxyl dimerization during crystallization.[87] This results in less ordered crystals with highly branched structures having a small pore/ mesh size. These gels provide an enhanced oil-binding capacity with no syneresis. However, the elasticity of these gels is low due to the limited time to form an extended network structure.[87] In contrast, a low cooling rate of only 1 °C/min yields in a fibrillar LMOG network with minimal branching. The storage modulus is comparatively high, whereas oil inclusion is low due to the reduced capillary forces caused by the larger network meshes.[87,98,100]

Based on their viscoelastic properties, 12-HSA organogels are also sensitive to shear.[102] Elasticity of organogels in general depends on the quantity of LMOG, the strength and degree of the molecular interactions and the properties of the oily phase.[87] When the network structure of silicone oil gels containing 2 % of 12-HSA is destroyed by shear, the elasticity is recovered only up to 70 %, based on the storage modulus.[86,93] Hence, solidified organogels (*i.e.* preformed gels) produced by melting and subsequent cooling require the use of low-gauge (high diameter) cannulas for parenteral injection. Otherwise, the injection would lead to the rheodestruction of the organogels and therefore affect the gels' biodegradation properties and also the release of the API.

2.2 VEGETABLE OILS

Table 3 ***Vegetable oils used as matrix material for the preparation of ISFOs. All oils are in accordance with Ph. Eur. 9.0.***

Oil	Source	Remark
Medium-chain triglycerides (MCT)	Caesar & Loretz, Germany	Semisynthetic
Peanut oil	Caesar & Loretz, Germany	Refined grade
Sesame oil	Caesar & Loretz, Germany	Refined grade
Soybean oil	Caesar & Loretz, Germany	Refined grade

2.3 ORGANIC SOLVENTS

Table 4 ***Organic solvents used for the preparation of ISFOs to dissolve 12-HSA and to enable the in situ solidification by means of (partial) water miscibility.***

Organic solvent	Source	Purity
2-Pyrrolidone (2P)	BASF, Germany	≥ 99.0 %
Ethyl acetate (EA)	Carl Roth, Germany	≥ 99.8 %
***N*-Methyl-2-pyrrolidone (NMP)**	Carl Roth, Germany	≥ 99.8 %
Dimethyl sulfoxide (DMSO)	Grüssing, Germany	≥ 99.5 %
Glycofurol (GF)	Merck, Germany	≥ 98.0 %
Polyethylene glycol 400 (PEG 400)	Sigma-Aldrich, Germany	≥ 99.0 %

2.4 ACTIVE PHARMACEUTICAL INGREDIENTS (APIs)

Table 5 ***Model APIs selected for in vivo characterization.***

API	Source	Purity
Testosterone enanthate	Sigma-Aldrich, Germany	Analytical grade
Leuprolide acetate[a]	Chemos, Germany	98.3 %

[a] Micronized before use: CryoMill (Retsch, Germany), Adapter No. 02.706.0303 for the use of 2 mL reaction vessels (Safe-Lock Tubes, 2.0 mL, Eppendorf, Germany), one 4 mm steel ball per tube, -196 °C, 25 Hz, 60 s, 20 mg of substance each tube; obtained particle size < 30 μm (d90 < 10 μm).

2.5 FURTHER EXCIPIENTS AND MATERIALS

Table 6 Further objects and their origin (table continues on the next page).

Substance/ Trade name	Source	Remark
Acetic acid	Carl Roth, Germany	Purity 100 %
Aqua ad injectabilia	B. Braun, Germany	For Testosterone ELISA
***Aqua* bidest.**	Institute of Pharmacy, Martin-Luther-Universität Halle-Wittenberg, Germany	Produced by bidestillation
***Aqua* demin.**	Institute of Pharmacy, Martin-Luther-Universität Halle-Wittenberg, Germany	Produced by ion exchange and reverse osmosis
Copper sulfate pentahydrate	Carl Roth, Germany	Purity ≥ 99.5 %
Di-Sodium hydrogen phosphate	Grüssing, Germany	Purity 99 %
Fetal calf serum	Biochrom, Germany	
HD-PMI	Institute of Chemical Kinetics and Combustion, Russia	Spin probe, M_r 395.7 g/mol
Hexane	Carl Roth, Germany	Purity ≥ 99 %
Hydrochloric acid	Carl Roth, Germany	Purity 25 %
Injekt-F syringes	B. Braun, Germany	1 mL, silicone oil-free, single-use
Isoflurane (Forene)	Abbott, Germany	For veterinary use
Isopropyl alcohol	Sigma-Aldrich, Germany	Purity 99.5 %
Lipoprotein lipase	Sigma-Aldrich, Germany	From *Burkholderia sp.*, 1293 U/mg
MEM	Sigma-Aldrich, Germany	With Earle's salts, L-glutamine and sodium bicarbonate
Methanol	Carl Roth, Germany	Purity ≥ 99.9 %
mMEM	modified MEM	MEM supplemented with 15 % [v/v] of FCS, non-essential amino acids solution, 1 mM sodium pyruvate, 1 % [v/v] Penicillin-Streptomycin solution
Non-essential amino acid solution	Sigma-Aldrich, Germany	100 x concentrated
PBS	Produced with *aqua* demin.	pH 7.4, 137 mM NaCl, 2.7 mM KCl, 12 mM total phosphate, preserved with 0.05 % [m/m] of sodium azide (unless otherwise stated)
Penicillin-Streptomycin solution	Merck, Germany	10000 U/mL and 10 mg/mL
Phosphoric acid	Carl Roth, Germany	Purity 85 %
Potassium chloride	Grüssing, Germany	Purity 99 %
Potassium dihydrogen phosphate	Carl Roth, Germany	Purity ≥ 98 %
Resazurin sodium salt	Sigma-Aldrich, Germany	Purity 80 %
SKH1-*Hr^{hr}* mice (male)	ZMG, Martin-Luther-Universität Halle-Wittenberg, Germany	Originally ordered from Charles River, USA
Sodium azide	Sigma-Aldrich, Germany	

Substance/ Trade name	Source	Remark
Sodium chloride	Grüssing, Germany	Purity 99.5 %
Sodium pyruvate solution	Sigma-Aldrich, Germany	100 mM
Spectra-Por 1 Dialysis Tubing	Sigma-Aldrich, Germany	MWCO 6.5-8 kDa, CE membrane
Spectra-Por Float-A-Lyzer G2	Sigma-Aldrich, Germany	5 mL, MWCO 20 kDa, CE membrane
Stearic acid	Sigma-Aldrich, Germany	Purity 95 %
Sterican cannulas	B. Braun, Germany	21 G x $^{7}/_{8}$″, 23 G x $^{2}/_{5}$″, 25 G x $^{5}/_{8}$″, 27 G x $^{3}/_{4}$″
Sulforhodamine B (SRB)	Sigma-Aldrich, Germany	Purity 75 %
Testosterone rat/ mouse ELISA	Demeditec, Germany	
Thiazolyl Blue Tetrazolium Bromide (MTT)	Sigma-Aldrich, Germany	Purity 98 %
Trichlormethane	Carl Roth, Germany	Purity ≥ 99.9 %
Trichloroacetic acid	Carl Roth, Germany	Purity ≥ 99.0 %
Trypsin-EDTA solution	Sigma-Aldrich, Germany	1x, 0.5 g/L porcine trypsin, 0.2 g/L EDTA, 4Na/L of Hanks' balanced salt solution, phenol red
Tris	Carl Roth, Germany	Purity ≥ 99.8 %
Ultrasound contact gel	Caesar & Loretz, Germany	

3 METHODS

Unless otherwise stated in this work, data are generally displayed as medians and ranges as small sample sizes mostly prohibit the unconsidered calculation of means and standard deviations without testing for normal distribution (Gaussian). Furthermore, all experiments are to be considered as pilot study in order to generate data as a basis for further studies.

Although the core body temperature of 37 °C in healthy humans exceeds the body surface temperature of 32-34 °C (measured in the skin), all the *in vitro* experiments conducted to simulate *in vivo* conditions were performed at 37 °C. This procedure reflects the scientific consensus in this research area.

3.1 FORMULATION DEVELOPMENT

3.1.1 HIGH PERFORMANCE THIN LAYER CHROMATOGRAPHY (HPTLC)

In order to analyze the content of 12-HSA of products from various suppliers, HPTLC and spectrodensitometric measurements were performed. The origin flakes of 12-HSA (Table 2, p. 15) were crushed in a mortar. Samples were dissolved in chloroform/ methanol (2:1, v/v) to obtain a concentration of 500 *µ*g/mL. 1.5 mL screw-cap glasses with PTFE-lined caps were used for storage. The organic solutions were plotted (1, 5 and 20 *µ*L each) on a silica gel 60 F 254 GLP HPTLC plate (Merck, Germany) using an Automatic TLC Sampler (ATS 4, CAMAG, Switzerland). The elution was performed at 27 °C with various mobile phases of decreasing polarity using an Automated Multiple Development Chamber (AMD 2, CAMAG, Switzerland). Table 7 (p. 22) shows the mobile phase compositions and migration distances of each elution step.

Subsequently, the separated lipids were stained by the use of a copper sulphate solution (10 % $CuSO_4$ x 5 H_2O, 8 % H_3PO_4 (85 %), 5 % methanol, *aqua* bidest., all m/m). The plates were plunged in the solution for 20 s and then heated to 150 °C for 20 min in an oven. The quantification was performed by measuring the absorption at 546 nm using a TLC Scanner 3 (CAMAG, Switzerland). The software

WinCATS 1.4.2.8121 (CAMAG, Switzerland) was used for peak identification, baseline correction and peak area calculations.

Table 7 Elution gradient for the HPTLC plates.

Step	n-Hexane [%, v/v]	Ethyl acetate [%, v/v]	Migration distance [mm]	Drying time [min]
1	70	30	20.0	1.5
2	73	27	25.1	1.5
3	76	24	30.2	1.5
4	79	21	35.3	1.5
5	82	18	40.4	1.5
6	85	15	45.5	1.5
7	88	12	50.6	1.5
8	91	9	55.7	1.5
9	94	6	60.8	1.5
10	97	3	65.9	1.5
11	100	0	71.0	1.5

3.1.2 TEXTURE ANALYSIS

The Bloom test is a standard empirical method for quality control issues of gelatin and gels for pharmaceutical applications.[103,104] It was modified to examine the ability of the gel formation by the use of different 12-HSA grades. Following recent studies, peanut oil was selected as oil in this approach.[105] Mixtures of peanut oil and 12-HSA (total weight of 1.5 g) were prepared in 4 mL screw-cap glasses. The glasses were placed in a preheated 80 °C metal block thermostat and shaken for 5 min at 1,000 rpm (SC20, Torrey Pines Scientific, USA). Afterward, the homogeneous, melted solutions were cooled to 20 °C at a rate of 1 °C/min. Thereby, the gelling temperature was passed and the gels were formed.

The required force to push a metal cylinder with a constant velocity into the gel was measured using the TextureAnalyzer (CT3-4500, Brookfield-Rheotec, Germany) (Figure 5, p. 23). The samples were placed onto a stage (accessory TA-RT-KIT, Brookfield-Rheotec, Germany). Experiments were conducted at 20 °C using the deformation mode with a cylinder of 4 mm in diameter (accessory TA44, Brookfield-Rheotec, Germany) and a scan velocity of 0.05 mm/s. The trigger force was adjusted to 0.005 N. While lowering the cylinder, 5 measurements/s were recorded. The test

finished after a covered distance of 3 mm starting from the trigger point. Data recording and processing were carried out with the software TexturePro CT V1.4 Build 17 (Brookfield-Rheotec, Germany).

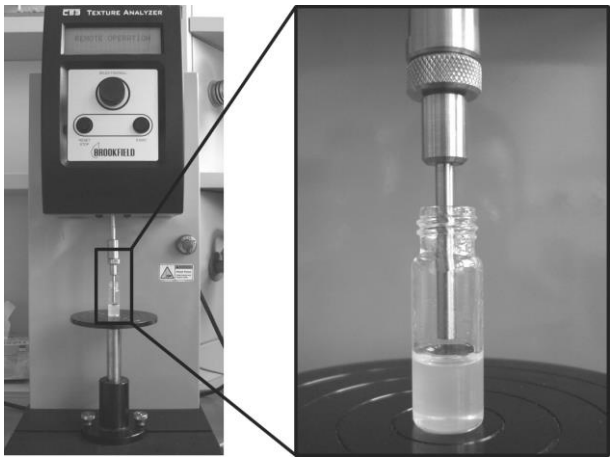

Figure 5 ***Setup of the texture analysis (left) with the gel in the glass and the metal cylinder coming from the top and penetrating into the gel with a constant velocity (right).***

3.1.3 MISCIBILITY OF ORGANIC SOLVENTS WITH WATER AND OILS

In order to achieve both the production of a liquid and homogeneous formulation and the *in situ* solidification inside of the *s.c.* tissue, the organic solvent used for the dissolution of 12-HSA has to be completely miscible with the matrix oil and at least partially miscible with the aqueous tissue fluid. Therefore, a gravimetrical mixing experiment was performed. Approximately 1 g of oil or *aqua* demin. was accurately weighed at 20 °C into 4 mL screw-cap glasses followed by the addition of the organic solvent. Dual Asymmetric Centrifugation (Speedmixer DAC 150 SP, Hauschild, Germany) was applied at 3,000 rpm for 30 s to ensure mixtures free from air bubbles. Thereby, the rotational motion around the center of the centrifuge is overlapped by the backward rotation of the glass itself to achieve a high mixing quality.[106] The mixtures were stored for 28 days at 20 °C in a climate chamber (B6760, Heraeus, Germany). Afterward, the samples were visually evaluated in order to identify the maximum content of organic solvent which is miscible with the oil/ *aqua* demin. without occurrence of phase separation or cloudy opacities.

3.1.4 SOLUBILITY OF 12-HSA IN ORGANIC SOLVENTS

Ingredients of *in situ* formulations for parenteral use should preferably be dissolved to pass cannulas of a low inner diameter. However, the use of organic solvents should be

reduced to a minimum. For solubility determination of 12-HSA in organic solvents, 12-HSA from the manufacturer Larodan was used. Samples were prepared by weighing 12-HSA and solvents in 4 mL screw-cap glasses at 20 °C. After vortex mixing (MS 3 basic, IKA, Germany) until 12-HSA had dissolved, the closed glasses were stored for 6 months at 20 °C in a climate chamber (B6760, Heraeus, Germany). Finally, the samples were visually checked for recrystallization of 12-HSA or gelation of the solvent. The samples with the highest concentration of 12-HSA, which were still in a clearly dissolved, single-phase state, indicated the solubility of 12-HSA searched for.

3.1.5 PREPARATION OF FORMULATIONS AND STABILITY TESTING

A storage stability test was implemented to select the appropriate mixtures of 12-HSA, organic solvent and vegetable oil for further *in vitro* and *in vivo* investigations. *In situ* formulations used in this thesis were prepared in 4 mL screw-cap glasses according to compositions shown in Table 12-Table 15 (p. 46 f.); 12-HSA was first dissolved in NMP at 20 °C and then blended with the oil by vortex mixing at 3,000 rpm for 30 s (MS 3 basic, IKA, Germany).

The closed screw-cap glasses were stored for 6 months at 20 °C in a climate chamber (B6760, Heraeus, Germany) and afterward visually checked. Gelation of the mixture, flocculation of 12-HSA and separation of the liquid phases indicated instabilities. Solely homogeneous, single-phase solutions were further investigated. Finally, 500 µL of the samples were injected (Injekt-F, Sterican 21 G, B. Braun, Germany) into 5 mL of PBS at 37 °C. After 72 h at 37 °C and while gently shaking at 30 rpm (SW23, Julabo, Germany), the implants were carefully removed from the PBS by using a metal spatula. A form-stable implant body with the entire quantity of oil solidified and without remaining oil droplets on the PBS surface indicated suitable compositions.

3.1.6 SELECTION OF FORMULATIONS FOR CHARACTERIZATION

Table 8 (p. 25) anticipates the compositions of the *in situ* formulations finally selected for both *in vitro* and *in vivo* characterization. The name of the formulations refers to the concentration of 12-HSA relating to the content of peanut oil (*i.e.* disregarding the content of the NMP, since NMP diffuses out of the formulation upon contact with water). Peanut oil as implant matrix material, NMP as organic solvent and 12-HSA by Larodan as LMOG were suitable components according to the results of the formulation

development (chapter 4.1, p. 37 ff.). The preparation of the formulations corresponds to the procedure previously described (chapter 3.1.5, p. 24).

Formulations for testing cytotoxicity (chapter 3.2.6, p. 30 ff.) and *in vivo* characterization (chapter 3.3, p. 33 ff.) were prepared under aseptic conditions in a laminar air flow (LAF) cabinet (HeraSafe KS 18, Heraeus, Germany). Equipment coming into contact with the ingredients of the formulations was sterilized by dry heat at 160 °C for 2 h (ST 6060D, Heraeus, Germany).

Table 8 ***Composition of the most suitable in situ formulations. The name of each formulation refers to the concentration of 12-HSA concerning the quantity of peanut oil.***

Name of the formulation in this thesis	**3 % ISFO**	**5 % ISFO**	**7 % ISFO**
12-HSA [%, m/m]	2.73	4.41	6.00
NMP [%, m/m]	8.84	11.74	14.34
Peanut oil [%, m/m]	88.43	83.85	79.66

3.2 *IN VITRO* CHARACTERIZATION

3.2.1 TEXTURE ANALYSIS

Texture analysis was performed to measure the required force for the ejection of the developed ISFOs and to evaluate their injectability. ISFOs were filled into syringes (Injekt-F, B. Braun, Germany) equipped with cannulas of different inner diameters (Sterican, B. Braun, Germany). A solid metal tripod was used to fasten the syringe vertically at the grip wings with the cannula facing downward. Force-distance profiles were recorded (TextureAnalyzer CT3-4500, Brookfield-Rheotec, Germany) for the injection into a beaker and the *s.c.* tissue of a chicken wing by moving down the punch (accessory TA4, Brookfield-Rheotec, Germany) on the plunger of the syringe. The injection velocity was controlled by the punch velocity. Experiments were conducted at 20 °C. The deformation mode was applied and the trigger force adjusted to 0.005 N. While lowering the punch, 60 measurements/s were recorded. The test finished after the ejection of 500 µL. To calculate the injection force, the data points of the force plateau (*i.e.* after the initial elastic range), obtained from the ejection of 200 µL of formulation, were averaged.

3.2.2 CONDUCTOMETRIC EXPERIMENTS

Conductivity measurements were performed to determine the release kinetic of the NMP from the *in situ* formulations. This straightforward method is particularly useful when measuring the concentration of NMP in the surrounding buffer. *In situ* formulations were injected (Injekt-F, Sterican 25 G, B. Braun, Germany) into 2.5 g of PBS at 37 °C in a quantity corresponding to 500 mg of peanut oil. All samples were then stored in closed 10 mL glasses at 37 °C and while gently shaking at 30 rpm (SW23, Julabo, Germany). Diffusion of the NMP into the PBS led to the *in situ* solidification of the implant. In order to monitor the progress of the NMP release, the surrounding medium was taken at predetermined points in time by aspirating with a syringe equipped with a 19 G cannula (Injekt-F and Sterican, B. Braun, Germany). The electrical conductivity of the NMP containing PBS was then measured at 37 °C (S230 SevenCompact, Mettler Toledo, Switzerland). Afterward, the medium was returned into the implant containing glass to continue the NMP release.

3.2.3 ELECTRON PARAMAGNETIC RESONANCE (EPR)

Electron paramagnetic resonance was carried out to gain further in-depth information on the NMP release and the implants' microviscosities. This non-invasive method enables their determination from the inside of the implant by means of incorporated spin probes. Contrary to NMR, in which nuclei (*e.g.* ^{1}H, ^{13}C) are responsible for the absorption of radio waves (300 MHz – 1 GHz), EPR is based on the absorption of microwaves (1 GHz – 300 GHz) by electrons of paramagnetic compounds.[107] EPR-active samples possess unpaired electrons in the form of metal ions or free radicals. Electron pairs with two electrons sharing one orbital are EPR-silent, because of the mutual annihilation of the oppositely orientated spins (diamagnetism). Mostly, incorporated stable radicals serve as reporter molecules (spin probes) in pharmaceutically relevant samples.[108–110] Special applications are the determination of micropolarity, microviscosity, temperature, pH-value, partial oxygen pressure inside of tissues as well as compositions of multi-component systems.[26,111–116]

For NMP release experiments, *in situ* formulations were prepared in screw-cap glasses as described in chapter 3.1.5 (p. 24, first section). Prior to the preparation of these samples, the lipophilic spin probe HD-PMI (2-heptadecyl-2,3,4,5,5-pentamethyl-imidazoline-1-oxyl) was given into the glasses as a stock solution. The solvent trichlormethane was entirely evaporated (Vacuum Controller CVC 2, Vacuubrand,

Germany). Subsequently, the precipitated HD-PMI was dissolved in the *in situ* formulations by vortex mixing (MS 3 basic, IKA, Germany). The final concentration of HD-PMI was 0.25 mmol/kg related to the mass of the peanut oil. Pure peanut oil with the same concentration of HD-PMI was used as control. Dialysis tubes with a MWCO (molecular weight cut off) of 20 kDa and a defined cylindrical geometry (Float-A-Lyzer G2, Sigma-Aldrich, Germany) were rinsed for 5 min with PBS to hydrate the cellulose ester membrane and to remove water-soluble storage stabilizers. The tubes were then carefully filled with 1,000 mg of formulation and put into 10 mL of PBS at 37 °C. Before EPR measurements, the dialysis tubes were removed from the PBS and the adhesive liquid on the membrane was gently dabbed with a paper towel.

EPR measurements were conducted using an L-band spectrometer (Magnettech, Germany) with a microwave frequency of about 1.1-1.3 GHz connected with a re-entrant resonator. Measurement parameters were set as follows: field center 49.1 mT, scan range 6 mT, scan time 400 s, modulation amplitude 0.0125 mT. The peak amplitudes of the obtained spectra were analyzed with the software MultiPlot 2.0 (Magnettech, Germany).

In order to investigate the impact of 12-HSA on the microviscosity of NMP-peanut oil mixtures (chapter 4.2.3, p. 59 ff.), the samples were prepared as follows; firstly, the spin probe HD-PMI was given in 4 mL screw-cap glasses as a stock solution and then the solvent trichlormethane was entirely evaporated. Secondly, 12-HSA, NMP and peanut oil were weighed to obtain a concentration of HD-PMI of 0.25 mmol/kg related to the total mass of the sample. Finally, all samples, independently whether clearly dissolved or with undissolved 12-HSA flakes, were locked and placed in a preheated 80 °C metal block thermostat and shaken for 5 min at 1,000 rpm (SC20, Torrey Pines Scientific, USA). Immediately afterward, the hot samples were transferred into 0.5 mL reaction vessels and filled to the brim (Mμlti-SafeSeal Tubes, Carl Roth, Germany). The vessels were locked and cooled to 20 °C at a rate of 1 °C/min. The EPR measurements of the obtained homogeneous samples were conducted according to the protocol of the section above.

3.2.4 PROTON NUCLEAR MAGNETIC RESONANCE RELAXOMETRY (^{1}H-NMR)

^{1}H-NMR relaxometry was applied to obtain additional information on the microviscosity of the ISFOs, especially on the mobility of the entrapped oil. This non-destructive

method takes the advantage of protons in the sample having a magnetic moment. Therefore and compared to EPR, the incorporation of additional marker probes is unnecessary when using NMR.[117–123]

In order to investigate the impact of 12-HSA on the microviscosity of peanut oil and NMP-peanut oil mixtures, 1.5 g of each sample were prepared in 4 mL screw-cap glasses. The concentration of 12-HSA relates to the quantity of peanut oil. Afterward, all samples, independently whether clearly dissolved or with undissolved 12-HSA flakes, were locked and placed in a preheated 80 °C metal block thermostat and shaken for 5 min at 1,000 rpm (SC20, Torrey Pines Scientific, USA). Finally, the homogeneous samples were cooled to 20 °C at a rate of 1 °C/min. 12-HSA-free mixtures were used as controls and passed the same temperature cycle to guarantee comparability.

Relaxation experiments were carried out with a 20 MHz ^{1}H-NMR benchtop spectrometer (Maran DRX2, Oxford Instruments, UK) equipped with an air flow temperature regulation. Prior to the measurement, each sample was pre-tempered in the resonator for 15 min. The CPMG (Carr-Purcell-Meiboom-Gill) pulse sequence was applied for T_2 relaxation analysis with a relaxation delay time of 3 s. 3072 echoes were measured and 64 scans were averaged per pulse sequence. The raw data were fitted with the software WinDXP analysis (Oxford Instruments, UK) using the inverse Laplace transformation to calculate the T_2 relaxation distributions.

3.2.5 OSCILLATING RHEOLOGY

Viscosity measurements of visco-elastic materials, including organogels, are frequently performed using oscillatory rheometry. Thereby, the samples are exposed to a defined mechanical strain and are analyzed for their viscous and elastic properties. When using a cone-plate setup, samples have to exist in a wafer-like flat form. Hence, a self-constructed sample holder was built (Figure 6, p. 29, left); a dialysis membrane with a MWCO of 6.5-8 kDa (Spectra Por 1, Spectrum Laboratories, USA) was rinsed for 5 min with PBS to remove water-soluble storage stabilizers and to increase the flexibility. Subsequently, the membrane was placed tightly and single-layered over the broad end of a glass funnel and attached with elastic band.

After drying the membrane at ambient conditions, the funnel was taken upside down and 2,500 µL of the ISFOs were ejected with a syringe through the thin funnel opening

onto the membrane. In order to simulate the *in vivo* solidification, the sample holders were placed with the membrane site for 48 h into 200 mL of PBS at 37 °C to extract the NMP from the formulations. After 24 h the PBS was replaced by a fresh one. The solid and dried gel wafers with a height of 2 mm and a diameter of 40 mm were used for measurements (Figure 6, right).

Figure 6 ***A self-constructed sample holder consisting of a glass funnel equipped with a dialysis membrane (left), was built to realize the extraction of NMP. The ISFO is located inside of the funnel on the membrane. The solvent NMP leaves the formulation through the membrane into the surrounding PBS resulting in a solidified gel wafer (right).***

Furthermore, reference samples, designated as *preformed implants*, were prepared without the solvent NMP. Peanut oil and 12-HSA were melted in 4 mL screw-cap glasses in a preheated 80 °C metal block thermostat and shaken for 5 min at 1,000 rpm (SC20, Torrey Pines Scientific, USA). Afterward, the homogeneous melt was quickly aspirated in a pre-tempered 80 °C syringe and placed for additional 2 min in an oven of 80 °C to avoid premature recrystallization of 12-HSA. Finally, 2,500 µL of the melted formulations were ejected as explained above through the thin funnel opening onto the membrane. The solidification of the implants occurred due to temperature reduction to 20 °C at a rate of 1 °C/min.

Measurements were carried out with an oscillating rheometer (Physica MCR 301, Anton Paar, Austria) using a cone-plate kit of 24.982 mm in diameter (Figure 7, p. 30). The angle of the cone was 1.003° and the gap between cone top and plate was 48 µm. After lowering the cone in measuring position, the excess of implant at the edge was removed. To realize *in vivo* conditions, plate and cone were tempered to 37 °C. Firstly,

a deformation sweep test was carried out. Therefore, a low but constant shear rate of 1 s^{-1} and a deformation range of 0.01-100 % were adjusted in order to determine the linear visco-elastic range (LVR), in which the gels' structures remain intact. Secondly and based on the results of the deformation sweep test, the frequency sweep test was performed at a constant deformation of 0.5 % and a range of the shear rate of 0.1-100 s^{-1}. Since irreversible destruction of the gel during the deformation sweep test could not be excluded, a new sample was used for the frequency sweep test. Data were analyzed and relevant parameters calculated using the software Rheoplus (Anton Paar, Austria).

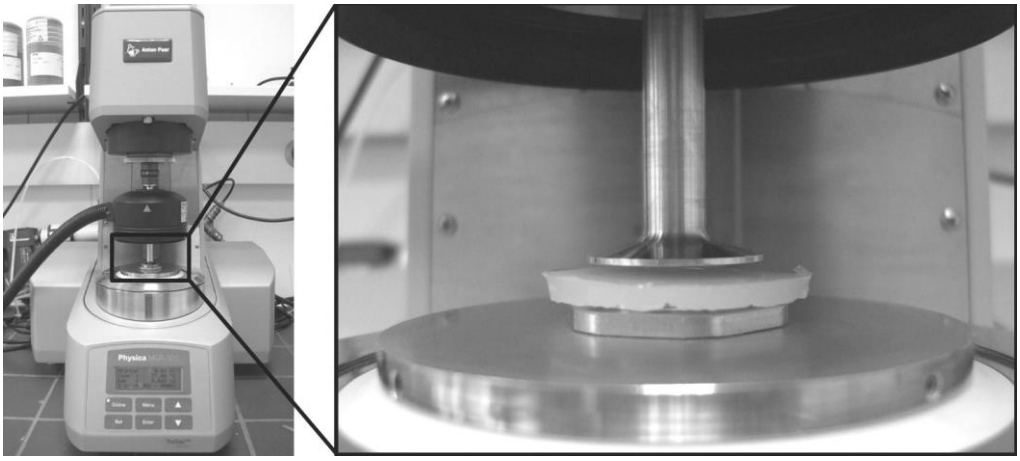

Figure 7 ***Setup of the oscillating cone-plate rheometer (left) with the flat gel wafer on the plate and the cone coming from the top and oscillating with defined deformation and shear rate (right).***

3.2.6 CYTOTOXICITY

Cytotoxicity testing of pharmaceutical dosage forms is crucial to help bridging the gap between *in vitro* and *in vivo* experiments. Even formulations consisting of substances which are already proven as non-toxic have to be tested for toxic effects when reassembled. Cytotoxicity of the ISFOs and NMP was investigated by SRB, MTT and Resazurin assays. Each test was carried out under sterile conditions (HeraSafe HS 12, Heraeus, Germany) and follows the same procedure: 1) preparation of the incubation medium; 2) incubation of the cells with the medium; 3) implementation of the test assay.

PREPARATION OF THE INCUBATION MEDIA

In order to distinguish between the potential toxicity of NMP and of the solidified implant (consisting of peanut oil and 12-HSA), two different incubation media were prepared. In the former case, a dilution series of NMP and mMEM (modified minimal essential medium) was used. In the latter case, 500 mg of the ISFOs were injected (Injekt-F, Sterican 25 G, B. Braun, Germany) into 4 mL of sterile PBS (without preservatives) and stored for 24 h at 37 °C in a 12-well plate (Tissue culture plate, TPP, Switzerland). Afterward, the NMP containing PBS was discarded and the solidified implants were carefully rinsed three times with 4 mL of fresh PBS (without preservatives) to remove adhesive NMP. Each implant was then incubated for 24 h at 37 °C in 4 mL of mMEM. Finally, a dilution series with the resulting implant extract and fresh mMEM was prepared.

CELL CULTURE AND INCUBATION

Human colon fibroblastic CCD-18Co cells (CRL-1459, ATCC, USA) were grown in mMEM at 37 °C in a humidified atmosphere of 5 % CO_2/ 95 % air (Function Line BB 16, Heraeus, Germany). Almost confluent cells were harvested by trypsin. Thereby, the medium was removed by rinsing the adherent cells with sterile PBS (without preservatives), followed by the incubation with trypsin/ EDTA for 5 min at 37 °C. The reaction was stopped by adding mMEM. After centrifugation of the cell suspension for 5 min at 1,300 rpm (Labofuge 400/ swing bucket rotor, Heraeus, Germany) the cells were resuspended in mMEM and dispensed in aliquots of 100 µL in 96-well plates (2,000 cells/well; Tissue culture plate, TPP, Switzerland). In the first and the last column, mMEM without cells was used for blank value determination. In the second column, non-treated cells in mMEM were used as neg. ctrl. (negative control).

After the cells had settled down and adherence had occurred (usually after 48 h), the incubation media were added in aliquots of 100 µL. Incubation with the extract dilutions of the solidified implants was carried out for 48 h at 37 °C in 5 %CO_2/ 95 % air atmosphere. Incubation with the NMP containing media was carried out at the same temperature and atmosphere using different time protocols (*long*, *sink* and *short;* Figure 22, Figure 24, Figure 25, p. 73 ff.) to investigate the time dependency and to simulate various *in vivo* conditions. Therefore, the medium was removed and replaced by NMP/ mMEM mixtures of the next following concentration. After 48 h of incubation, light microscopic images were recorded and the colors were inverted to improve

visualization of the cells (Axiovert 25, Carl Zeiss, Germany). Before applying the test assays, the incubation media were removed.

SULFORHODAMINE B ASSAY (SRB)

100 µL of a trichloroacetic acid solution (100 mg/mL) was added to each well to induce cell rupture and protein fixation and then incubated for 14 days at 5 °C. After washing four times with *aqua* bidest., the plates were air-dried at 20 °C. 100 µL of 4 µg/mL SRB dissolved in 1 % [v/v] of acetic acid was added and the plates were incubated 45 min at 20 °C to stain the proteins. Subsequently, the staining solution was removed and the plates were washed four times with 1 % [v/v] of acetic acid to remove unbound dye. After air-drying at 20 °C for 72 h, the bound dye was dissolved in 100 µL of 10 mM Tris buffer while gently shaking until a homogeneous staining had occurred. Absorption measurements were carried out immediately at 570 nm (SLT Spectra RainBow, Tecan, Switzerland). The absorption of the blank (only mMEM) was subtracted from the absorption of the negative control (cells plus mMEM) and the samples. The absorption of the negative control was set as 100 %.

MTT ASSAY

110 µL of a yellow MTT solution (500 µg MTT per mL of MEM) was added to each well and the plates were incubated for 4 h at 37 °C. Afterward, 100 µL of a solubilization solution (0.01 M HCl in isopropyl alcohol) was added and the plates were gently shaken at 20 °C until the metabolic formed dark blue MTT formazan crystals had dissolved. The absorption was measured immediately at 570 nm (SLT Spectra RainBow, Tecan, Switzerland). The absorption of the blank (only mMEM) was subtracted from the absorption of the negative control (cells plus mMEM) and the samples. The absorption of the negative control was set as 100 %.

RESAZURIN ASSAY

250 µL of a resazurin sodium solution (10 µg resazurin sodium per mL of MEM) was added to each well and the plates were incubated for 3.5 h at 37 °C. Subsequently, the fluorescence intensity was measured at 595 nm (excitation at 492 nm; SpectraFluor Plus, Tecan, Switzerland). The emission of the blank (only mMEM) was subtracted from the emission of the negative control (cells plus mMEM) and the samples. The emission of the negative control was set as 100 %.

3.2.7 LIPASE DEGRADATION EXPERIMENTS

When exposed to lipolytic enzymes, triglycerides are saponified to fatty acids, partial glycerides and glycerol. This *in vitro* investigation provides information about the duration of implant degradation in order to forecast the duration of the degradation *in vivo*. Therefore, 500 mg of the ISFOs were injected (Injekt-F, Sterican 25 G, B. Braun, Germany) into 3 mL of pre-tempered LPL (lipoprotein lipase) containing PBS at 37 °C. The samples were then stored in closed 10 mL glasses at 37 °C and while gently shaking at 30 rpm (SW23, Julabo, Germany). Every 48 h, the surrounding medium containing the degradation products was removed by aspirating with a syringe (Injekt-F, B. Braun, Germany) equipped with a 19 G cannula. While remaining inside of the glasses, the implants were carefully washed once with 3 mL of *aqua* demin. and then dried in a silica gel containing desiccator in vacuum until a constant weight was reached (usually after 4 h). The time-dependent degradation of the implants was determined by weighing (Extend ED224S, Sartorius, Germany) and calculating the weight loss with respect to the initial weight. Subsequently, freshly prepared LPL containing PBS was added to continue the lipolytic degradation of the implants.

3.3 *IN VIVO* CHARACTERIZATION

3.3.1 ANIMAL CARE

All *in vivo* experiments complied with regional regulations and guidelines and were approved (Approval No. 42502-2-1243 MLU-HAL) by the Animal Ethics Committee of the state Saxony-Anhalt (Germany) and the commissary of animal protection of the Martin-Luther-Universität Halle (Germany). Male SKH1-*Hr*^{hr} nude mice (euthymic and immunocompetent) were used as hairs disturb the ultrasound investigations. The mice were kept under controlled conditions (12 h light/ dark cycle, 24 °C, 65 % relative humidity, feed and water *ad libitum*) in groups of 2-5 animals per cage. At the start of the experiments, the mice had an age of 3-5 months and a body weight between 30-35 g.

INJECTIONS AND ANESTHESIA

For implant injection, mice were anesthetized with 1.5-2 % of isoflurane in oxygen at a flow of 2 L/min. With the mice lying on their back, 150 µL of the formulations were

slowly injected (approx. 15 µL/s, 26 G cannula) *s.c.* from *distal* into the *regio inguinalis* (Figure 27, p. 84). For API release experiments, the injected formulations contained a dose of 17 mg/kg testosterone enanthate (corr. 12 mg/kg testosterone) or 50 mg/kg leuprolide acetate. Placebo implants for MRI and USI experiments were administered into both sides to halve the total mouse number. After these injections, the mice were anesthetized for 30 min in supine position to allow the initial solidification of the implants with minimal spreading of the oil. During MRI and USI measurements, the mice were anesthetized at 2.5-4 % of isoflurane in oxygen (2 L/min flow) to avoid disturbing interferences caused by moving and breathing. Generally, anesthetized mice were placed on a tempered 37 °C silicon pad to prevent the body from cooling.

BLOOD SAMPLING

At predetermined points in time, blood samples of approximately 80 µL were collected in accordance with the GV-SOLAS regulations by puncturing the tail vein or the retro-orbital venous plexus.[124] Afterward, the blood samples were temporarily stored in reaction vessels (Safe-Lock Tubes, 0.5 mL, Eppendorf, Germany) for 1 h at 4 °C. After coagulation, the serum was obtained by centrifugation for 10 min at 13,000 rpm (Biofuge Fresco/ fixed-angle rotor, Heraeus, Germany) and stored in reaction vessels (Vials PCR 0.2 mL, Carl Roth, Germany) at -80 °C until the determination of the concentration of testosterone via ELISA (enzyme-linked immunosorbent assay; chapter 3.3.4, p. 36). On the basis of the circadian rhythm of the testosterone blood level, samples were always taken between 1-3 p.m.[125]

3.3.2 MAGNET RESONANCE IMAGING (MRI)

MRI is a predestined method to monitor the implant volume, shape alterations as well as the localization of inflammation during implant degradation. MRI enables pronounced contrasts in the presentation of soft tissues.

MRI experiments were performed with a 3 T scanner (Magnetom Skyra, Siemens, Germany) at a scan frequency of 123 MHz. The anesthetized mice underwent MRI in a whole-body rat coil (Stark Contrast, Germany) with an inner diameter of 70 mm. Scans were carried out before and at predetermined points in time after the injection of the formulations. A T_1-weighted TSE (turbo-spin-echo) sequence with an echo time (T_E) of 16 ms and a repetition time (T_R) of 751 ms was used. 30 slices with a thickness of 0.7 mm and an interstice gap of 0.07 mm were recorded. The field of view was

72 mm x 144 mm with a resolution of 384 x 768 pixels. *Coronal* records were selected for the evaluation. *Transversal* images helped to identify the implant if it had not been clearly evident in the *coronal* plane.

3.3.3 ULTRASOUND IMAGING (USI)

USI is an alternative method to visualize and quantify the implant degradation *in vivo*. Based on comparatively short scan times, USI is suitable when larger sample sizes are desired and additional characteristics, such as the implant shape or encapsulation phenomena, are also of interest. In principle, quartz crystals inside of a transducer emit ultrasound by means of electricity. These acoustic waves travel into the body, are reflected on the tissue and reach the crystals again. There, the acoustic energy is transformed back into electric energy (piezo electric effect). The image contrast is based on the degree of the reflection and the scattering of the waves at tissue interfaces and inhomogeneous tissues (acoustic impedance). Time and frequency of the returning waves are the parameters to generate the image; the longer the sound takes to come back, the deeper the tissue is located and the further down the software will plot the dot on the image. And the better the tissue reflects the ultrasound, the more energy comes back to the transducer and the brighter the dot will be. Strongly reflecting elastic materials (*e.g.* solids such as bones as well as gases in lung and intestine) appear bright. However, they prevent the propagation of the ultrasound and thus the visualization of the tissues located behind. In contrast, plastic materials (*e.g.* fluids, such as water and blood, contained in organs) show almost no reflection and appear dark. Consequently, these plastic materials can be permeated by ultrasound waves and hence even structures lying in the shadow of these tissues can be detected. Structures with both elastic and plastic properties (*e.g.* most of the internal organs, skin and connective tissue) reflect a proportion of the ultrasound and are partially penetrated by them. Consequently, they appear grey and provide further information on the images.[126–130]

Depending on the scientific issue, transducers of different frequencies are available. The higher the frequency of the emitted waves, the better the image resolution, but the lower the penetration depth is. Thereby, high-frequency transducers are highly suitable for the characterization of *s.c.* implants. The angle between the transducer and the object to be examined should be 90° in order to achieve a quantitative detection of the reflected waves. Short measurement durations and the high spatial resolution are more

beneficial compared to MRI. One serious drawback is the smaller size of the image, which could support overlooking relevant structures or information.

US imaging experiments were performed using a Vevo 2100 system (Visual Sonics, Canada) equipped with a linear MS 550D transducer (40 MHz) fastened in a 3D motor stage. The anesthetized mice were placed in supine position and ultrasound contact gel was dispersed on the skin above the implant. The B-Mode (brightness modulation) was used for implant localization. Subsequently, 3D-combined B-Mode was applied with a scan range of 25 mm. Thereby, the system creates a series of 196 *transversal* B-Mode slices within the scan range and calculates the 3D image. For volumetric measurements, the implant contours in each individual slice were manually drawn (step size: 0.51 mm) and the software Vevo 2100 1.4.0 (Visual Sonics, Canada) was used for image analysis and volume calculation.

3.3.4 ENZYME-LINKED IMMUNOSORBENT ASSAY (ELISA)

In order to characterize the release of testosterone enanthate and leuprolide acetate from the ISFOs, serum concentrations of testosterone in mice were determined. As explained in chapter 4.3.2 (p. 93 ff.), the *in vivo* testosterone serum level should be proportional concerning the released testosterone enanthate and inversely proportional concerning the released leuprolide acetate (except the initial testosterone peak of the flare-up phenomenon). For testosterone serum level measurements, a commercial ELISA adapted for blood samples of rats and mice was applied. This solid phase kit is based on the principle of competitive binding. An unknown concentration of testosterone present in the serum sample and a defined concentration of testosterone conjugated to horseradish peroxidase compete for the binding sites of the testosterone antiserum coated to the wells of a microplate. After incubation, washing and addition of the substrate solution, the concentration of testosterone is inversely proportional to the OD (optical density) measured (SLT Spectra RainBow, Tecan, Switzerland). The detailed assay procedure is described in the product information.[125] Each well requires 10 µL of serum. Values represent the mean from two measurements. Calibrator standards cover a range of 0.1-25 ng/mL and the test sensitivity is 0.066 ng/mL.

4 RESULTS AND DISCUSSION

4.1 FORMULATION DEVELOPMENT

4.1.1 SELECTION OF THE 12-HYDROXYSTEARIC ACID

CONTENT OF COMMERCIALLY AVAILABLE 12-HSA PRODUCTS

Initially, the content of 12-HSA of selected commercially available products has been determined. Due to its natural origin and elaborate isolation, impurities can be expected, particularly with the more inexpensive technical grade products. These impurities with deviating structures of 12-HSA may adversely affect the gelation process. In addition, by-products can differ in their composition and thus in their interfering interactions during gelation. A high content of 12-HSA corresponds with a high reproducibility for the formation of the gel. For the purpose of content determination, the individual components of the products have been separated on a silica gel plate. Subsequently, the areas under the curves (AUCs) of the relevant peaks have been quantified.

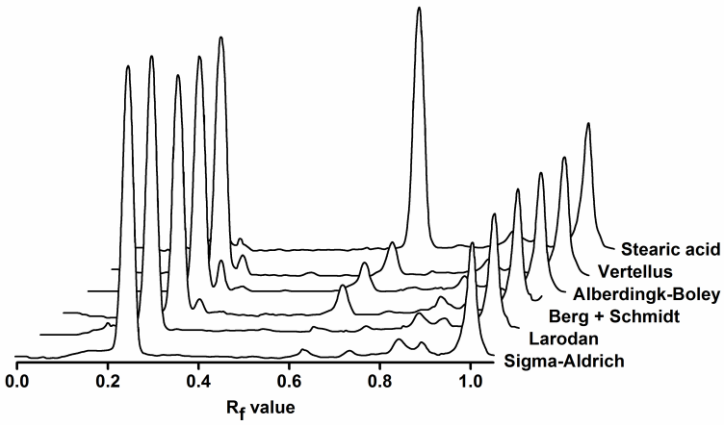

Figure 8 ***Chromatographic separation of the components present in the investigated 12-HSA products. 12-HSA appears at R_f 0.25. The most extensive by-product of the production is stearic acid appearing at R_f 0.62. Peaks above R_f 0.8 belong to components of the mobile phase or the silica gel plate.***

Figure 8 shows the separated individual components of the investigated 12-HSA products after application of 1 µL solution (corr. 0.5 µg powder). Chromatograms with an applied volume of 5 µL (corr. 2.5 µg powder) and of 20 µL (corr. 10 µg powder) are not shown. They merely helped to identify the peaks to be included in the calculation of the total AUC. Regardless of the applied sample volume and 12-HSA product

investigated, all peaks with R_f (ratio of fronts) > 0.8 showed identical AUC (area under the curve) values. Therefore, these three comparatively lipophilic ingredients do not belong to the products tested. Possibly these impurities originate from the mobile phase or the silica gel plate. Consequently, only the peaks of R_f 0-0.8 were considered to the calculation of the total AUC. Within this range, all products show multiple peaks. The more polar the compound, the lower the R_f is. For all commercial products, the main peak at R_f 0.25 corresponds to 12-HSA. Moreover, the analytical grade products of Sigma-Aldrich and Larodan show the lowest level of impurities. Stearic acid at R_f 0.62 represents the major contamination, especially in the products of Berg + Schmidt, Alberdingk-Boley and Vertellus. Except for 12-HSA and stearic acid, other substances were not further investigated.

Table 9 (p. 39) presents the calculated 12-HSA contents of the investigated products. Based on the chromatographic results with applied sample volumes of 1 µL and of 5 µL, proportionality between the applied sample volumes and the resulting AUCs has been confirmed. The chromatogram with an applied volume of 1 µL was used for content determination. The content of 12-HSA was calculated as the ratio of the 12-HSA AUC in relation to the total AUC between R_f 0-0.8. The analytical grade of Larodan possesses the highest content of 12-HSA with 98.1 %, which is in agreement with the specification. 12-HSA of Sigma-Aldrich, also specified as analytical grade, contains 96.3 % of 12-HSA, deviating from the specification. The technical 12-HSA grades of Berg + Schmidt, Alberdingk-Boley and Vertellus contain 80-85 % of 12-HSA. Stearic acid is their major contamination with about 11 %. However, several additional impurities exist in these three products. In conclusion, the isolation of 12-HSA after triglyceride hydrolysis and fatty acid hydrogenation has failed or was deliberately refrained at the technical grade 12-HSA products.

Fatty acids without a secondary hydroxyl group such as stearic acid, do not contribute to the formation of the gel as 12-HSA does. Due to the lack of this second connecting element they are not able to build extended LMOG networks via hydrogen bonds with other but identical molecules. If these non-hydroxy fatty acid contaminations do not even interfere with the gelation of 12-HSA, higher quantities of the technical grade products (*i.e.* Berg + Schmidt, Alberdingk-Boley, Vertellus) will be necessary to produce organogels with the same gel strength compared to the analytical grades (*i.e.* Sigma-Aldrich, Larodan). To illustrate, a gel containing 3 % [m/m] of 12-HSA of Larodan should have a similar strength than a 3.7 % [m/m] gel of Alberdingk-Boley, which

contains only about 4/5 of 12-HSA compared to Larodan. From this perspective, the products of Larodan and Sigma-Aldrich are more beneficial.

Table 9 ***Spectrodensiometric results received from the separation by HPTLC (Figure 8, p. 37). Percentage peak areas refer to the total AUCs in the range of R_f 0-0.8.***

Source Product	Specified purity [%]	R_f peak max [-]	Assigned substance	Peak area [%]
Sigma-Aldrich 12-Hydroxystearic acid	99	0.25	**12-HSA**	**96.3**
		0.63	Stearic acid	2.4
		0.74	Unknown	1.3
Larodan 12-Hydroxystearic acid	> 98	0.25	**12-HSA**	**98.1**
		0.61	Stearic acid	0.4
		0.72	Unknown	1.5
Berg + Schmidt Sternoil 12-HSA	85	0.25	**12-HSA**	**84.9**
		0.30	Unknown	3.5
		0.62	Stearic acid	10.7
		0.72	Unknown	0.9
Alberdingk-Boley 12-HSA Flakes 81	83-90	0.25	**12-HSA**	**80.0**
		0.30	Unknown	5.9
		0.35	Unknown	1.2
		0.61	Stearic acid	11.6
		0.73	Unknown	1.3
Vertellus Casid HSA	Not specified	0.24	**12-HSA**	**81.3**
		0.29	Unknown	5.1
		0.44	Unknown	1.8
		0.62	Stearic acid	10.9
		0.71	Unknown	0.9
Sigma-Aldrich Stearic acid[a]	95	0.19	Unknown	12.7
		0.63	Stearic acid	86.3
		0.72	Unknown	1.0

[a] Reference substance for indication of stearic acid impurities of the 12-HSA products.

GEL STRENGTH OF 12-HSA-BASED ORGANOGELS

Texture analysis was performed in order to investigate the mechanical properties of the organogels. The experiment focuses on the influence of the different contents of 12-HSA of the selected commercial products on the strength of the gels. The gels of analytical grade products, with a higher content of 12-HSA, should result in more rigid gels than those of the technical grade products. Based on previous studies, peanut oil has been selected as oily matrix, which was co-heated with 12-HSA above its melting point, homogenized and subsequently cooled below the gelling temperature.[105]

During measurement, a metal cylinder penetrates with a constant velocity of 0.05 mm/s into the gel. The force of the gel against the cylinder was recorded as a function of the penetration depth (Figure 9, p. 41, left). The resulting curves can be divided into two sections; the initial increase in force describes the elasticity of the gels. With increasing depth also the force increases. The higher the rise in this section, the more pronounced the solid state character of the sample is. Large penetration depths before the force plateau are primarily characteristic for elastic bodies. Within this first curve section, the structures of the gels remain intact. Penetration depth and velocity are insufficient to destroy the structure of the gel.

In the second section, called *force plateau*, the gels are situated in the viscous or plastic state. Here, the deflection of the cylinder exceeds the mechanical strength of the gels. In other words, the applied shear force exceeds the yield point, the structure of the gel collapses and the formulation starts to flow. The height of the force plateau reflects the number of 12-HSA molecules included in the gelation process. The higher the force, the more molecules are involved, the denser the fibrillar network and the more robust the structure of the gel is. This maximum force may only be increased by means of a higher penetration velocity or a larger diameter of the cylinder. Both parameters were constant in these experiments to directly compare the gels. Nonetheless, the structure of the gel collapses at the maximum force. For comparing the gel strength of various 12-HSA products, a representative section of 2 mm within the force plateau was selected and the average of the data points calculated (Figure 9, p. 41, left). This value corresponds to the applied force leading to the destruction of the gel.

By increasing the concentration of gelator, all products show a higher maximum force (Figure 9, p. 41, right). This is even observed, to a lesser extent, for the reference substance stearic acid, which is incapable of molecular cross-linking due to the lack of a secondary hydroxyl group. However, a higher concentration of stearic acid means a higher viscosity and consequently a higher resistance of the sample against the penetrating cylinder. The gels containing 3 % [m/m] of 12-HSA are almost equal in their maximum force, which is 0.6 N. Differences between the products were notable only at 5 % and 7 % [m/m] of 12-HSA. As expected, the forces measured in the gels produced with analytical 12-HSA grades (*i.e.* Sigma-Aldrich and Larodan) are higher than with the technical grade alternatives. The difference is all the more pronounced, the higher the applied *concentration* of 12-HSA is. This is due to the different *contents* of the 12-

HSA (Table 9, p. 39). The higher the applied concentration to gel the oil, the stronger the influence of the required force is, if a large content of non-12-HSA impurities is present. The gel, which proved to be most robust with a force of about 2 N, contains 7 % [m/m] of 12-HSA of Sigma-Aldrich. In comparison, the gel with 12-HSA by Larodan results in a lower force measured, despite the slightly higher content of 12-HSA. These findings suggest that the content of 12-HSA is not exclusively decisive for the strength of the gel, but also the composition of the impurities.

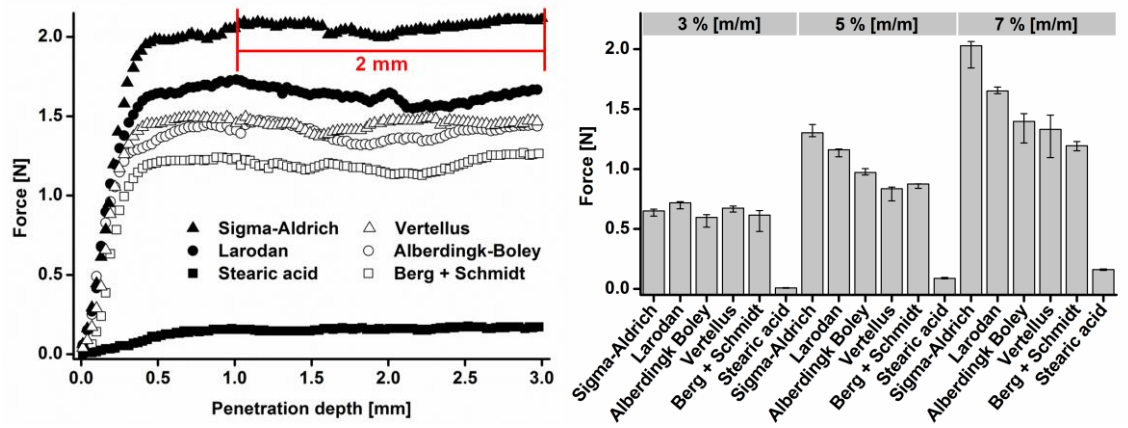

Figure 9 ***Left: Exemplary force path of the texture analysis during penetration of the cylinder into the gels consisting of peanut oil and 7 % [m/m] of 12-HSA from selected sources or stearic acid. Data points of 2 mm of the force plateau were averaged for force calculation. Right: Applied force of the penetrating cylinder into the gels at 20 °C and depending on the source of 12-HSA performed at 3 %, 5 % and 7 % [all m/m] of 12-HSA or stearic acid. Data represent medians ± ranges, n=3.***

Based on the results of the 12-HSA content determination as well as the strength of the gels, solely 12-HSA by Larodan has been used in the further course of this work. This commercial product possesses the highest content of 12-HSA. Other reasons concerning this decision were the direct contact with the manufacturer (Sigma-Aldrich is just the supplier of 12-HSA, the manufacturer has not been announced), the continued availability and the cost-effectiveness.

4.1.2 SELECTION OF THE ORGANIC SOLVENT

Using 12-HSA to gel numerous lipophilic liquids has already been described in chapter 2.1 (p. 15 ff.) and has also been shown in the previous chapter exemplified by peanut oil. By heating both components above the melting point of 12-HSA and subsequent cooling, dimensionally stable gel bodies can easily be prepared. This

approach, however, has two major drawbacks regarding drug therapy. Firstly, it it applicable only for temperature-resistant APIs. Since many APIs exhibit polymorphism or thermal degradation, this results in a significant limitation of the broad applicability of an implant carrier. Secondly and more relevant to patient compliance, preformed and consequently bulky implants require surgeries or injections with thick cannulas and a high burden of pain as well as a considerable risk of complications.

Therefore, the formulations require the addition of a gelation inhibitor, which prevents the solidification of oil by 12-HSA *before* administration and thus facilitates the injection. This excipient (*i.e.* organic solvent) must have a high solvating power concerning 12-HSA in order to disrupt their intermolecular associations. Moreover, the solvent should be miscible with the oil itself and at least partially miscible with aqueous media. Once the liquid formulation is injected into the tissue, the organic solvent has to be extracted into the surrounding aqueous fluid. Simultaneously, the 12-HSA molecules assemble themselves and thereby gel the oil. This entire process is called *in situ precipitation*. Of course, only biocompatible solvents may be considered.

Table 10 ***Miscibility [mg/g] of organic solvents with aqua demin./ vegetable oils at 20 °C. Samples were prepared in steps of 10 mg of organic solvent within a range of 10-1000 mg per gram oil/ water.***

	***Aqua* demin.**	**MCT**	**Sesame oil**	**Peanut oil**	**Soybean oil**
NMP	1000	1000	1000	1000	1000
GF	1000	150	110	110	80
2P	1000	50	40	60	50
DMSO	1000	40	40	50	10
PEG 400	1000	< 10	10	10	< 10
EA	80	1000	1000	1000	1000

Table 10 shows the miscibility of several preselected organic solvents with vegetable oils, which were taken into account as matrix carrier. All solvents are already used in approved medicines for parenteral use or are described as biocompatible.[51,60] The oils are also found in commercial parenterals and classified as physiologically compatible.[60] In this test, miscibility referred solely to real molecular solutions.

With the exception of EA, all organic solvents are miscible with demineralized water in a ratio of 1:2 (*i.e.* 1+1). Therefore, they fulfill the required precondition for the

extractability into the aqueous medium. In contrast, EA is only partially water-miscible. However, it is soluble with all tested oils in a ratio of 1:2 (*i.e.* 1+1). Due to its pronounced lipophilicity and its higher affinity to oil than to water, the usage of EA could lead to an incomplete extraction into water after injection and hence to an incomplete solidification of the implant. PEG 400 turned out to be the most polar solvent. Turbid emulsions are obtained already below 10 mg/g of MCT and soybean oil. Therefore, it is unsuitable for the preparation of single-phase formulations. GF, 2P and DMSO are also very limited in their oil miscibility. Consequently, their suitability depends on the potential to dissolve 12-HSA. If the solubilizing power is high, a low content of solvent will be necessary to obtain the desired liquid and single-phase formulations. Otherwise, if the solubilizing power is low, the large content of solvent, which is necessary for the dissolution of 12-HSA, would be immiscible with the oily phase. Hence, a separate phase of dissolved 12-HSA dispersed in the oil would result. Such emulsions are more difficult to inject through thin cannulas. Interestingly and also reported in the literature, NMP was found to be completely miscible with water and all of the oils in a ratio of 1:2 (*i.e.* 1+1).[35,51] Even after storage at 20 °C for 28 days, phase separation of both NMP and oils was imperceptible. Thus, NMP preferably meets the criteria of water and oil miscibility.

Figure 10 (p. 44) shows the solubility of 12-HSA in the preselected organic solvents. Since 12-HSA is capable of gelling organic liquids, the method usually applied, with an excess of solid in the solvent and subsequent determination of the concentration in the supernatant, could not be carried out. Instead, a concentration series was prepared for each solvent. After storage at 20 °C for 6 months, the mixtures have visually been checked. The saturation solubility was indicated by the sample with the highest concentration of molecular dissolved 12-HSA. DMSO shows the highest solubility of 12-HSA with 47 % [m/m]. Also NMP proved to be a very powerful solvent with 42 % [m/m] of 12-HSA dissolved, whereas 2P was already gelled above 12 % [m/m] of 12-HSA. GF, PEG 400 and EA are non-solvents with less than 1 % of [m/m] 12-HSA dissolved. Here, the further addition of 12-HSA resulted in suspensions of 12-HSA in the solvent. Thereby, the amount of dissolved 12-HSA molecules is lower than the gelation concentration. By using these solvents, gelation could be obtained only by heating the suspension above the melting point of 12-HSA and subsequent cooling.

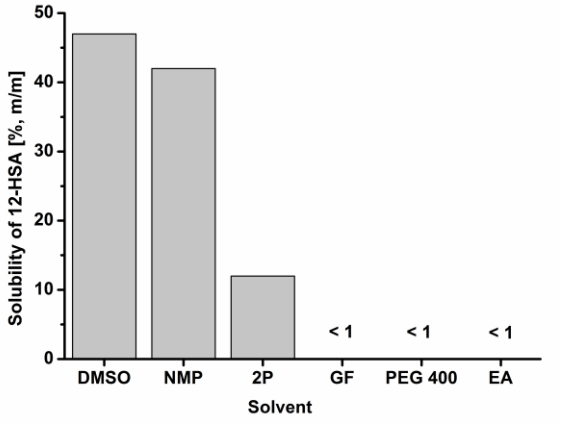

Figure 10 ***Solubility of 12-HSA by Larodan in organic solvents at 20 °C. The dissolved state remains at least for 6 months.***

To conclude, NMP has been selected as solvent for 12-HSA for all further experiments. Its high solvating power for 12-HSA may allow a sparing use concerning the *in situ* formulations. Moreover, its miscibility with water and oil provides at least necessary requirements for the *in situ* solidifying effect.[131] Further experiments should clarify, whether and to what extent the NMP diffuses from 12-HSA-NMP-oil mixtures into the aqueous medium (chapter 4.2.2, p. 53 ff.). In addition, the accurate amount of NMP, which is necessary to prevent 12-HSA-NMP-oil mixtures from premature gelation, must be investigated. Since NMP is completely miscible with the oil, not all NMP molecules may be available for the dissolution of 12-HSA inside of this mixture. Thus, a further addition of NMP is likely and must be determined in order to keep the formulation liquid and single-phase before administration (chapter 4.1.3).

4.1.3 SELECTION OF THE OIL

Currently approved, long-acting pharmaceuticals for parenteral use can be divided into aqueous-, lipid- and polymer-based matrices (Table 1, p. 5 f.). Matrix lipids used are primarily sesame oil, peanut oil and castor oil. By refining (*i.e.* degumming, bleaching, deodorization and neutralization of free fatty acids) they significantly differ in their quality compared to natural unrefined oils.[132] Contrary to hydrogenated oils, double bonds remain completely preserved. Therefore, these oils require specific storage conditions (*i.e.* cool, closed, light protected) and have a limited shelf life. Other parenterally used oils are soybean oil and MCT. They are primarily contained in nanoemulsions for parenteral nutrition or in medicines with poorly water-soluble APIs.[60] However, pure oils are inadequate depot matrices due to their liquid state at body

temperature and hence their tendency to spread inside of the tissue after *s.c.*/ *i.m.* injection. For example, peanut oil-based depot solutions with testosterone enanthate cover a release period of only 2-4 weeks and show large variations in plasma levels.[133]

This chapter determines the most suitable oil for producing storage-stable mixtures of 12-HSA, NMP and oil. The simple 2-stage preparation (1. step: dissolution of 12-HSA in NMP; 2. step: addition of oil and vortex homogenization; chapter 3.1.5, p. 24) is already a substantial advantage compared to the expensive and less robust manufacturing process of microparticles and the technically-complex extrusion methods for the production of preformed implants. After 6 months of storage at 20 °C, the mixtures were visually checked. Subsequently, liquid and single-phase formulations were injected into PBS and analyzed concerning their solidification characteristics (Table 12-Table 15, p. 46 f.). The outcome can be grouped into 4 categories (Table 11). Useful in terms of further *in vitro* examinations are only these mixtures in a liquid and single-phase state after storage, which solidify completely after injection into PBS, without showing individual liquid oil droplets floating on the PBS surface.

Table 11 ***Legend of Table 12-Table 15 (p. 46 f.). 12-HSA from Larodan was used. The stated concentrations of 12-HSA refer to the quantity of oil (i.e. after NMP release).***

	Amount of 12-HSA exceeds solubility in NMP
	Precipitation of 12-HSA in the 12-HSA-NMP-oil mixture during 6 months at 20 °C
	Liquid single-phase mixture for at least 6 months, but unstable implant after injection into PBS
	Liquid single-phase mixture for at least 6 months and complete solidification after injection into PBS → “workspace”

Table 12 12-HSA-NMP-oil mixtures with MCT. For explanation see Table 11 (p. 45).

7 % [m/m] 12-HSA										
6 % [m/m] 12-HSA										
5 % [m/m] 12-HSA										
4 % [m/m] 12-HSA										
3 % [m/m] 12-HSA										
2 % [m/m] 12-HSA										
1 % [m/m] 12-HSA										
NMP [mg]	**10**	**20**	**30**	**40**	**50**	**60**	**70**	**80**	**90**	**100**
MCT [mg]	**500**									

Table 13 12-HSA-NMP-oil mixtures with peanut oil. For explanation see Table 11 (p. 45).

7 % [m/m] 12-HSA										
6 % [m/m] 12-HSA										
5 % [m/m] 12-HSA										
4 % [m/m] 12-HSA										
3 % [m/m] 12-HSA										
2 % [m/m] 12-HSA										
1 % [m/m] 12-HSA										
NMP [mg]	**10**	**20**	**30**	**40**	**50**	**60**	**70**	**80**	**90**	**100**
Peanut oil [mg]	**500**									

Table 14 12-HSA-NMP-oil mixtures with sesame oil. For explanation see Table 11 (p. 45).

7 % [m/m] 12-HSA										
6 % [m/m] 12-HSA										
5 % [m/m] 12-HSA										
4 % [m/m] 12-HSA										
3 % [m/m] 12-HSA										
2 % [m/m] 12-HSA										
1 % [m/m] 12-HSA										
NMP [mg]	**10**	**20**	**30**	**40**	**50**	**60**	**70**	**80**	**90**	**100**
Sesame oil [mg]	**500**									

Table 15 12-HSA-NMP-oil mixtures with soybean oil. For explanation see Table 11 (p. 45).

7 % [m/m] 12-HSA										
6 % [m/m] 12-HSA										
5 % [m/m] 12-HSA										
4 % [m/m] 12-HSA										
3 % [m/m] 12-HSA										
2 % [m/m] 12-HSA										
1 % [m/m] 12-HSA										
NMP [mg]	**10**	**20**	**30**	**40**	**50**	**60**	**70**	**80**	**90**	**100**
Soybean oil [mg]	**500**									

Generally, a minimum quantity of 12-HSA is necessary to build solid implants. This quantity of 12-HSA, in turn, required a certain quantity of NMP to prevent the formulations from premature gelation. The higher the concentration of 12-HSA, the higher the addition of NMP must be, regardless of the oil used. Despite their initially liquid state directly after production, some formulations proved to be non-injectable after storage due to precipitation of 12-HSA or gelation of the oil (*e.g.* Table 12, p. 46: 3 % [m/m] of 12-HSA/ 30 mg of NMP). Thereby, the high miscibility of NMP with the oil required a further addition of NMP to completely dissolve the 12-HSA and to keep the mixture liquid.

Differences between the oils tested arose with regard to the “workspace” caused by their different fatty acid finger prints (Table 16, p. 49). MCT is a semi-synthetic oil, exclusively containing the fatty acids 8:0, 10:0 and 12:0 and thus making this oil markedly less lipophilic than the other three selected oils. Therefore, its polarity is the most comparable to the polarity of 12-HSA. Thus, it is a better solvent concerning 12-HSA than the other oils and consequently a higher concentration of 12-HSA is necessary to exceed the solubility and to induce gelation. At least 6 % [m/m] of 12-HSA has been necessary to gel the oil completely after injection into PBS (Table 12, p. 46). In order to keep the formulations containing 6 % [m/m] of 12-HSA liquid during a 6-month period, 70 mg of NMP were necessary using MCT, whereas 80 mg of NMP were required in case of the natural oils. However, MCT-based ISFOs spread strongly on the surface of PBS, even at high 12-HSA concentrations. The large surface-to-volume ratio of these ISFOs causes unstable gel bodies up to 5 % [m/m] of 12-HSA. Furthermore, the rather flat gel wafers, obtained at 6 % [m/m] of 12-HSA or even more, were very sensitive toward mechanical strain. MCT as matrix oil for the production of ISFOs was found to be rather inappropriate.

Fatty acid finger prints of peanut oil and sesame oil are comparatively similar, apart from the fractions with more than 18 carbon atoms (Table 16, p. 49). As expected, the formulations investigated with these oils show almost identical results (Table 13-Table 14, p. 46 f.). Peanut oil is slightly more lipophilic due to the higher proportion of fatty acids with long carbon chains. Therefore, at a given concentration of 12-HSA, the peanut oil-based mixtures should require more of NMP to inhibit gelation. This minor difference was demonstrated only for the formulations with 1 % and 4 % [m/m] of 12-HSA. At these concentrations, the peanut oil-based mixtures, in which the solubility of 12-HSA is lower compared to the sesame oil-based mixtures, required marginally more

NMP to avoid recrystallization of 12-HSA. Already 12 h after injection into PBS, dimensionally stable gel bodies with approximately spherical shape were formed with both oils. Even at the low 12-HSA concentration of 3 % [m/m], the implants could easily be removed from the glasses without disruption or spreading on the surface of the PBS.

Due to the high content of polyunsaturated fatty acids, soybean oil is nutritionally valuable, but also susceptible to oxidative expiry.[22] In particular, the threefold unsaturated linoleic acid is present primarily in the soybean oil. Within the “workspace”, solid implants were formed after injection into PBS and spreading did not occur. However, unlike peanut oil and sesame oil, at least 4 % [m/m] of 12-HSA were necessary to gel the oil completely.

Table 16 Fatty acid composition [%] of the investigated oils.[134]

Fatty acid	MCT	Peanut oil[a]	Sesame oil	Soybean oil
< C16	100.0	< 0.2	< 0.1	< 0.3
16:0		8.0-14.0	7.9-12.0	8.0-13.5
16:1		< 0.2	< 0.2	< 0.2
18:0		1.0-4.5	4.5-6.7	2.0-5.4
18:1		35.0-69.0	34.4-42.3	17.0-30.0
18:2		12.0-43.0	36.9-45.5	48.0-59.0
18:3		< 0.3	0.2-1.0	4.5-11.0
20:0		1.0-2.0	0.3-0.7	0.1-0.6
20:1		0.7-1.7	< 0.3	< 0.5
22:0		1.5-4.5	< 1.1	< 0.7
22:1		< 0.3	< 0.05	< 0.3
24:0		0.5-2.5	< 0.3	< 0.5

[a] Composition strongly depends on the origin.

In summary, peanut oil has been selected for all further experiments as matrix lipid. This oil allows the production of solid implants already at 3 % [m/m] of 12-HSA. It is a common oily vehicle for sustained release parenterals and evidently well-tolerated for a long time.[22,135,136] Peanut oil is extracted from the seeds of the peanut plant (*Arachis hypogaea L*) and available in adequate quality, as claimed by respective pharmacopoeia monographs. Despite significant levels of unsaturated fatty acids and due to the naturally contained antioxidant tocopherol, peanut oil is durable under light

and air exclusion over a long time. Since sesame oil contains less tocopherol than peanut oil, the latter was preferred in this work. In contrast to crude or cold-pressed peanut oil for nutrition, contaminations of aflatoxins and Ara h-proteins, which often cause allergic reactions, are primarily removed during refinement.[137,138]

For further *in vitro* and *in vivo* characterization, the peanut oil-based formulations containing 3 %, 5 % and 7 % [m/m] of 12-HSA with the lowest corresponding content of NMP have been investigated (chapter 3.1.6, p. 24 f.).

4.2 *IN VITRO* CHARACTERIZATION

4.2.1 INJECTABILITY

The mere thought of receiving an injection by means of a syringe can provoke fears among patients and often contribute to non-compliance concerning intended therapies. Therefore, the use of thin cannulas significantly improves the patients' compliance.[139] On the other hand, the formulation to be injected must be able to flow through the small cross section of the cannula. This condition often constitutes the critical step in developing sustained release medicines, such as aqueous suspensions, oily solutions, microparticles or polymer implants. In order to ensure injectability and to avoid trauma at the site of injection, the viscosity and perhaps the particles' size of the formulation have to be adapted.[22] Nevertheless, the choice of an adequate cannula size also depends on the aspired velocity of injection as well as the maximum injection force applied by the user.

Table 17 (p. 51) shows the cross-sectional dimensions of the cannulas used for the following injection force determinations. Generally, the higher the Gauge value, the thinner and the more preferable the cannula is. Commercial oil-based solutions and microparticulate formulations are administered with 19-25 G cannulas.[22,140] Preformed implants require the use of 14-16 G cannulas, whereas one of the few available ISFIs (Eligard) still needs 18-20 G cannulas due to the high viscosity of this polymeric solution.[57] Further approaches to decrease the injection forces by preparing ISFMs (*In Situ* Forming Microparticles) were successful, but take the risk of coalescence and possibly cause blockages.[51,139]

Table 17 Cross-sectional dimensions of the applied cannulas.[141]

Cannula size [Gauge]	Outer diameter [mm]	Inner diameter [mm]	Flow area [mm²]
21	0.80	0.57	0.26
23	0.60	0.39	0.12
25	0.50	0.29	0.07
27	0.40	0.22	0.04

Measurements in this study were carried out by applying three practical and application-oriented injection velocities each into a beaker (*i.e.* against the external air pressure) and into the *s.c.* tissue of a chicken wing (*i.e.* against the pressure of the tissue) (Figure 11, p. 52).

In general, the thinner the cannula and the higher the injection velocity, the higher the applied shear stress is and the higher the required force to eject the formulation. The ejection of pure water, as a comparative value to the ISFOs, requires approximately 1.4 N, regardless of the cannula size and the injection rate. However, these data do not confirm its recognized Newtonian flow characteristic, since the same force is required to just eject air, which equally corresponds to the syringe's resistance. In order to present real injection forces, this basic force was deliberately not subtracted in the following. Interestingly, using the 21 G cannula at the lowest injection rate of 10 µL/s, less force is necessary to eject peanut oil and the ISFOs into the beaker compared to eject either air or water. By applying this comparatively low shear stress, the lubricating effect of the oil occurs and therefore decreases the friction between the plunger and the case of the syringe.

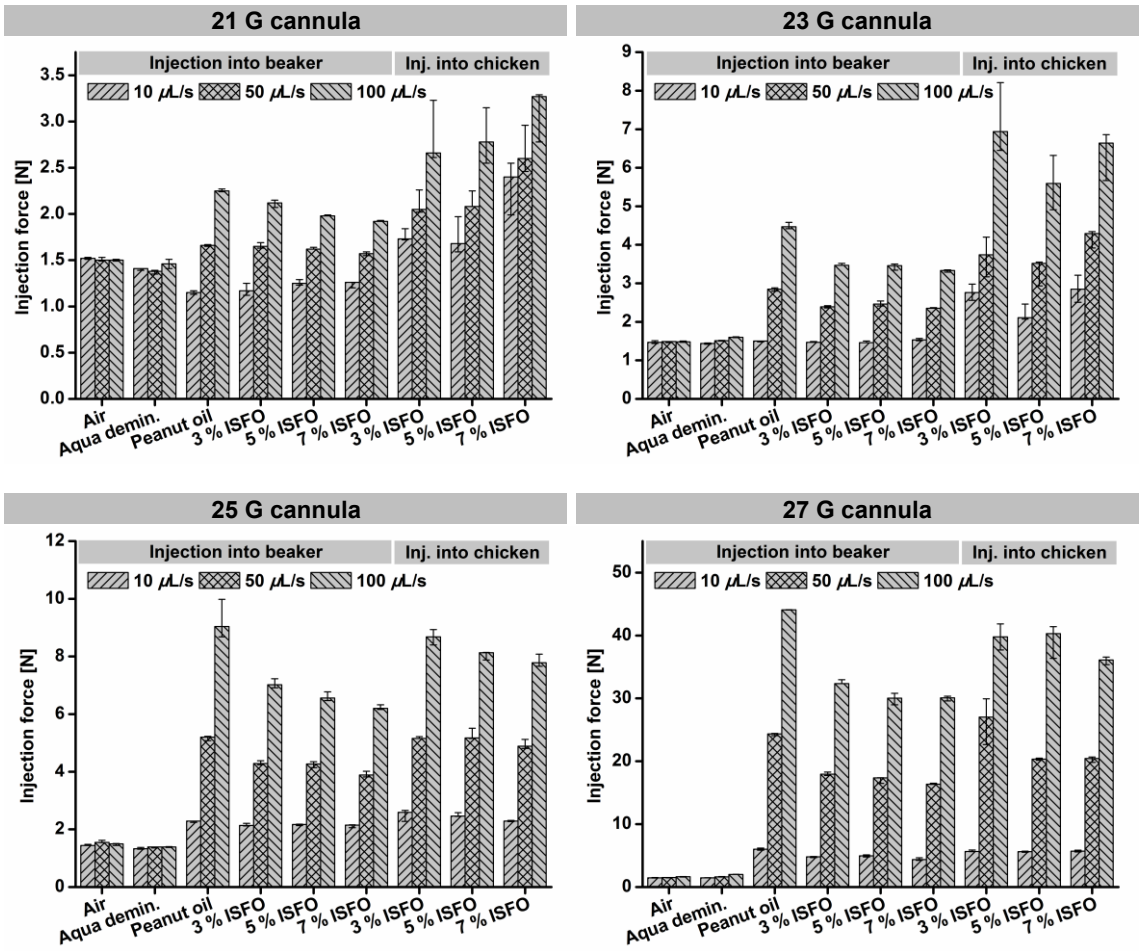

Figure 11 ***Required forces for the injection of ISFOs and reference samples at 20 °C depending on the injection rate performed with 21 G (top left), 23 G (top right), 25 G (bottom left) and 27 G (bottom right) cannulas. Data represent medians ± ranges, n=3.***

The ISFOs as well as pure peanut oil show a dependence of the injection rate on the injection force due to their non-Newtonian flow properties. The higher the injection rate and the thinner the cannula, the higher the required force is. Compared to pure peanut oil, slightly lower forces are needed for the ejection of the ISFOs. This is due to the addition of NMP which decreases the overall viscosity stronger than the addition of 12-HSA increases it. Furthermore, the higher the content of NMP in the ISFOs (Table 8, p. 25), the lower the viscosity is and the lower the necessary ejection forces are. Hence, the 7 % ISFO with its highest content of NMP is the most suitable formulation for injection. For the administration into the chicken slightly higher forces are needed compared to the injection into the beaker. This observation is caused by the limited *s.c.* space and the backpressure of the surrounding tissue and has also been reported for other injectable formulations.[139]

Correlations between injection forces *in vitro* and *in vivo* have already been demonstrated.[139] Accordingly, forces of 0-10 N are classified as *very easily injectable*, 10-25 N means *easily injectable* and 25-50 N means just *injectable*. All of the developed ISFOs require injection forces below 40 N and are thus considered to be injectable. By the use of 25 G cannulas, very low injection forces of less than 9 N are required for all ISFOs and injection rates, providing the possibility of a further reduction in needle size. Using 27 G cannulas for the injection of the 3 % ISFO into the chicken required forces of merely 6 N (10 µL/s), 27 N (50 µL/s) and 40 N (100 µL/s). For comparison, a 40 % [m/m] solution of PLGA in organic solvent administered with a 21 G cannula required a force of 100 N, which means *difficult to inject* concerning the classification mentioned above.[139] Taken together, the results of this investigation impressively confirmed the ease of injectability of the developed ISFOs, especially by the use of very thin cannulas, which promises patient-friendly injections.

4.2.2 RELEASE OF SOLVENT

CONDUCTOMETRY

After administering the ISFOs, the extraction of NMP into the surrounding aqueous tissue fluid is the basis for the *in situ* solidification. The more NMP leaves the ISFO, the more 12-HSA precipitates and contributes to the gelation of the oil. Hence, a complete and reproducible extraction of NMP is desired. Furthermore, the quicker the NMP diffuses out of the oily matrix, the quicker a solid carrier appears. This prevents the deformation of the initially liquid formulation by external mechanical strain (*e.g.* bump, pressure) and minimizes the diversity of implant shapes, which would cause unreproducible API release profiles. Therefore, conductometrical measurements were performed in order to determine both extent and velocity of the extraction of NMP.

The experiment is based on the decrease in conductivity of a buffered solution by the addition of NMP (Figure 12, p. 54, top left). In contrast to EPR, where the “signal” originates from a spin probe inside of the implant, here (*i.e.* electrical conductivity) the information is gained from the outside of the implant by the addition of the buffer medium. However, permanent online measurements after the injection of the ISFO into PBS were impossible as high evaporation loss caused by open glasses would falsify the results. Hence, the extraction media were removed for determination and afterward added again to the formulations.

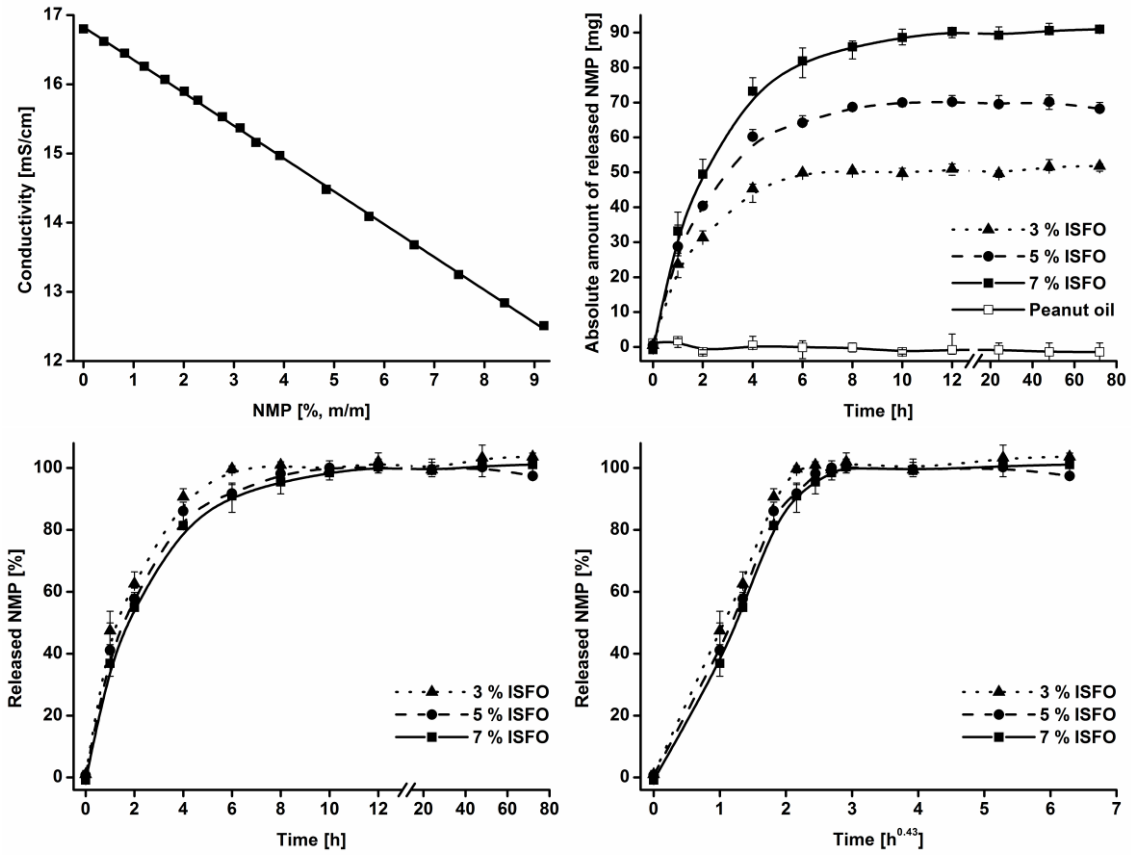

Figure 12 ***Top left: Electrical conductivity of PBS at 37 °C depending on the content of NMP (R^2=0.9995). Top right: Time-dependent NMP release from the ISFOs into PBS at 37 °C. Bottom left: Percentage release of NMP from the ISFOs into PBS at 37 °C. Bottom right: Korsmeyer-Peppas plot of the NMP release ($t^{0.43}$). Data represent medians ± ranges, n=3.***

Figure 12 (top right) illustrates the entire quantity of NMP diffusing from the ISFOs into the buffer within 6-12 h. Corresponding to the compositions (Table 8, p. 25), the 3 % ISFO contains 50 mg of NMP related to 500 mg of peanut oil. Analogously, the 5 % ISFO contains 70 mg of NMP and the 7 % ISFO contains 90 mg of NMP. As NMP is completely water-miscible as well as the maximum achievable concentration is merely 3.5 % [m/m] (*i.e.* 90 mg of NMP dissolved in 2.5 g of PBS), a buffer exchange during solvent extraction has been unnecessary. Up to 45 min after injection, the formulations have not been removable from the buffer, because of their still viscous state. Afterward, solid implants with stable surfaces have been formed. Due to their lower density compared to PBS, they floated on the buffer with a small area of the ISFOs standing out without any contact to the PBS. It should, therefore, be assumed that a complete rinse with PBS would even accelerate the release of NMP additionally.

In principle, two facts concerning the NMP release are highly interesting (Figure 12, p. 54, bottom left). Firstly, despite its 1:2 (*i.e.* 1+1) miscibility with water *and* peanut oil (Table 10, p. 42), the NMP diffuses completely into the buffer. Therefore, the greatest possible quantity of 12-HSA precipitates in the oil and contributes to the gelation. Secondly, the release kinetic is almost independent of the concentration of 12-HSA used. This could be explained by the fibrillar network structure of the 12-HSA. The formation of a bulk organogel with its low microviscosity (*i.e.* the viscosity on the molecular level) causes dissolved NMP molecules in the oil to be highly mobile and thus to diffuse easily to the interface. The density of the 12-HSA meshes does not play a major role due to the liquid oil interpenetrating this solid network.[90] The extraction of NMP is a process controlled by diffusion and depends on the NMP distribution between peanut oil and PBS.

Figure 12 (p. 54, bottom right) shows that during the first 4 h the extraction process follows approximately Korsmeyer & Peppas' kinetic for the diffusion controlled release out of stable, spherical objects, resulting in a linear connection between released NMP and time to the power of 0.43.[142] The density of the 12-HSA fiber network meshes from the inside of the implants toward its surfaces gradually increases. This probably leads to an extraction deceleration of the remaining 20 % of NMP from the 4th hour until the NMP release is finished. During this period, the graph also shows the slightly faster extraction with a decreasing concentration of 12-HSA. Nonetheless, the entire quantity of NMP leaves the oily matrix within several hours enabling a rapid and complete solidification of the oil. Furthermore, the implants showed a solid surface already 45 min after injection.

ELECTRON PARAMAGNETIC RESONANCE (EPR)

A further approach to monitor the extraction process of NMP is EPR. This non-invasive method requires a paramagnetic compound inside of the sample. Depending on the issue to be investigated, the chosen spin probe has to have specific physico-chemical properties. Based on the spectra obtained, various parameters can be calculated, allowing conclusions about the properties on the molecular level of the direct spin probe vicinity. For example, a high mobility of a dissolved spin probe, indicated by a low τ_c (rotational correlation time), implies a low microviscosity of the sample.[111,116] Therefore, direct influences on the microviscosity (*i.e.* the viscosity on the molecular level in the immediate vicinity of the probe) can be analyzed from the implants' inside.

Since the samples are neither altered nor damaged by the measurement, time profiles on one and the same formulation can be created during the extraction of NMP.

In case of the developed ISFOs, solvent extraction and gelation of the oil happen simultaneously, since only the NMP release leads to gelation of 12-HSA in the peanut oil. During this solidification process, the constantly changing composition of the formulation is accompanied by a notable increase of its *macro*viscosity, triggered by the precipitation of 12-HSA. However, this is not necessarily a measurable outcome on the molecular level (microviscosity). Chapter 4.2.4 (p. 64 ff.) enlightens the macroviscous implant properties by means of oscillating rheology, whereas chapter 4.2.3 (p. 59 ff.) examines the implants' *micro*viscosities by means of EPR and NMR relaxometry. HD-PMI was selected as spin probe for all EPR measurements in this thesis (Figure 13). Due to its pronounced lipophilicity (log P ~ 9), this molecule is water-insoluble and located solely inside of the peanut oil, even after the extraction of NMP.[143]

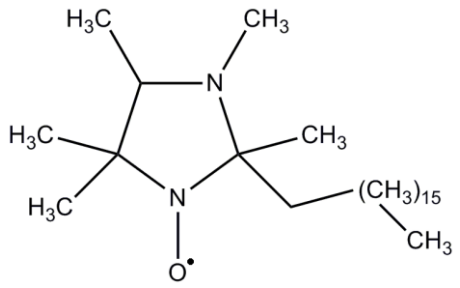

Figure 13 Chemical structure of the lipophilic nitroxide spin probe HD-PMI.

Figure 14 (p. 57, left) shows the typical three lines in the EPR spectrum of HD-PMI in both NMP and peanut oil. This hyperfine splitting is caused by the magnetic interaction of the probe's free electron and the nuclear spin of the connected nitrogen atom. Several parameters can be obtained from the spectra. Calculating the τ_c (rotational correlation time) in order to analyze the microviscosity strictly requires a spherical geometrical shape of the spin probe molecule. However, the long side chain with 17 carbon atoms prevents an isotropic rotation. Alternatively, the amplitude of the peak at the lowest magnetic field (amplitude 1) was set in relation to the amplitude of the peak at the center field (amplitude 2). The higher the peak 1/ peak 2 amplitude ratio, the higher the HD-PMI mobility is and the lower the microviscosity of the sample. In other words, the less NMP (low dynamic viscosity) is contained in the 12-HSA-NMP-peanut oil mixture (high dynamic viscosity), the lower amplitude 1 in relation to amplitude 2 is.

In general, calculating the peak 1/ peak 2 amplitude ratio allowed better and more clear results compared to the most often used peak 3/ peak 2 amplitude ratio or the analysis of line widths.

Figure 14 (right) presents the decrease of the peak 1/ peak 2 amplitude ratio while incubating the ISFOs in PBS. Before contact with PBS (*i.e.* 0 h), the 7 % ISFO shows the highest probe mobility with a ratio of approximately 65 %, followed by the 5 % ISFO at 62.5 % and the 3 % ISFO at about 60 %. The differences are based on the contents of NMP (Table 8, p. 25). The addition of NMP decreases the microviscosity of the liquid ISFOs more than the addition of 12-HSA increases it. Adding NMP leads to higher spin probe mobility and consequently to a greater amplitude ratio. This result correlates with the findings of the injectability measurements (Figure 11, p. 52). The more NMP is contained (lower dynamic viscosity compared to peanut oil), the lower microviscosity and macroviscosity of the liquid ISFOs are.

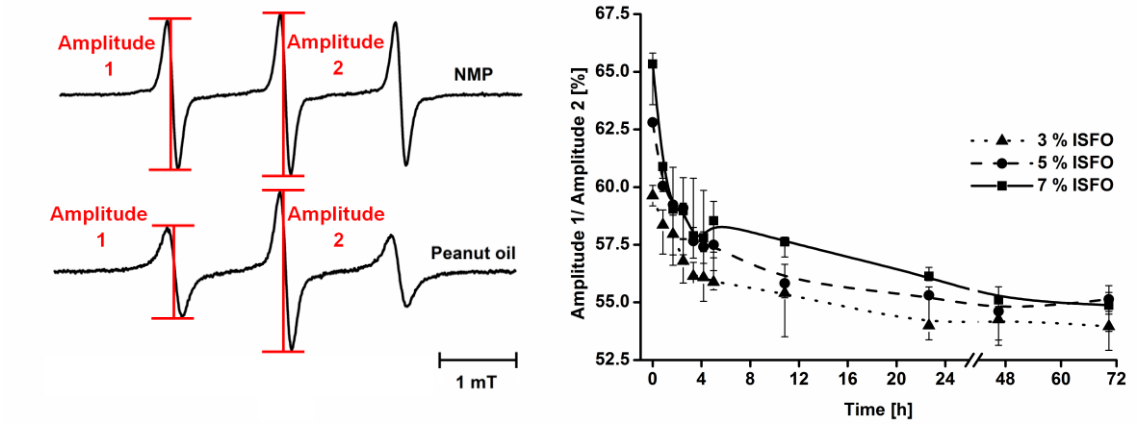

Figure 14 ***Left: EPR L-band spectra of the spin probe HD-PMI dissolved in NMP and peanut oil. The higher the peak 1/ peak 2 amplitude ratio, the higher the spin probe mobility is, which is accompanied by a low microviscosity of the sample. Right: Time-dependent amplitude ratios during the NMP release from the ISFOs into PBS at 37 °C using Float-A-Lyzer G2 dialysis devices. Data represent medians ± ranges, n=3.***

Dialysis tubes with a MWCO of 20 kDa were used for the incubation of the ISFOs in PBS. Thereby, the membrane permits the extraction of water-miscible NMP into the buffer as well as the retention of peanut oil and 12-HSA. Each ISFO shows a significant drop of the HD-PMI mobility during the first 4 h (Figure 14, right). In the following, the decrease slows down and all formulations achieve an equilibrium state of about 55 % after 48 h at the latest. These almost identical HD-PMI mobilities in the solidified

implants are independently from the concentration of 12-HSA and indicate a bulk gel structure, as it was concluded from the conductometric measurements (Figure 12, p. 54, bottom left). Thereby, the 12-HSA forms a 3D scaffold, which is completely penetrated by liquid peanut oil. The spin probe is dissolved in the oil, allowing free diffusion through the coherent oily matrix. The microviscosity of the oil remains unaffected by the gelation. Only the extraction of the majority of NMP during the first hours causes the decrease of the HD-PMI mobility and hence an increase of the formulations' microviscosities. This correlates with the results of the conductometric solvent extraction determination, where 80 % of NMP has been released after 4 h from all ISFOs (Figure 12, p. 54, bottom left).

Regarding polymeric ISFIs, several authors drew attention to API instabilities, polymer degradation and irregular API release profiles associated with incomplete or long-lasting NMP release. After 3 h, 40 % of NMP remained inside of the precipitated PLGA implant and still 26 % even after 24 h.[54,111] Independently from the polymers' molecular weight and their lactic-to-glycolic acid ratio, another study showed that at least 40 % of NMP have not been released from the implant within 7 days. Even more critical, the average molecular weight of PLGA (42.6 kDa) dissolved in NMP was halved within 10 days.[131] Moreover, PLGA-PEG-PLGA-based ISFIs still contained 25 % of NMP even after 6 days leading to comparatively mobile polymer chains, which accelerate the release of the API.[144] Other reports demonstrated the influence of the implant surface area. PLGA-based ISFIs with a small surface area contained 65 % of NMP after 3 h and 36 % after 24 h, whereas the threefold surface area accelerated the extraction process and nearly the entire quantity was released after 24 h.[145] Altogether, the literature data diverge significantly, primarily due to the different polymer types, the applied concentration of NMP as well as the shape and the surface area of the solidified implants. Hence, the fast and uniform NMP release from the developed ISFOs is an advantage compared to ISFIs as it is in a certain range independent of the concentration of the gelling agent and of the amount of NMP.

Comparing conductometric measurements (Figure 12, p. 54, top right) and EPR results (Figure 14, p. 57, right), a different time is observed to gain the equilibrium state of the NMP release (conductivity: 6-12 h; EPR: 24-48 h). This is probably caused by the free diffusion of the spin probe inside of the oily matrix. Thus, even after the NMP is entirely released, interactions of HD-PMI with 12-HSA, peanut oil or among HD-PMI molecules themselves are possible, which delay the equilibration time. Since the extraction of

NMP occurs at the interface of the ISFOs, the local concentration of 12-HSA is higher at the edge than at the implant inside. Accordingly, the 12-HSA fiber network is also denser there. These density inconsistencies could also delay the distribution of the spin probe.

4.2.3 MICROVISCOSITY

ELECTRON PARAMAGNETIC RESONANCE (EPR)

EPR was also applied to study the gels' microstructures. In the previous chapter, the mobility of the spin probe during the solvent extraction process has been investigated. Despite different concentrations of 12-HSA, the final equilibrium state of the solidified implants indicated their bulk gel structure due to the identical probe mobilities. However, with the higher concentration of 12-HSA at the implants' surface it might be possible that more HD-PMI molecules accumulate there and interact with each other. This would result in spin probe mobilities measured too low and consequently the implants' microviscosities would be estimated too high. In this experiment, the HD-PMI mobility has been investigated in *homogeneous* formulations, which have been prepared by co-melting 12-HSA, NMP and peanut oil directly in the sample holder and subsequent cooling. Figure 15 (p. 60) shows the HD-PMI mobility in 12-HSA-NMP-peanut oil mixtures. For comparison, samples without 12-HSA have also been prepared. In addition, the temperature dependence at 23 °C and 37 °C has been analyzed.

The relevant proportion of NMP in the ISFOs is in a range between 0-14.3 % [m/m] (Table 8, p. 25). Generally, increasing the concentration of NMP leads to enhanced mobility of the spin probe and thus the amplitude ratio is increased. There is no linear connection between the concentration of NMP and the amplitude ratio, which is shown by 12-HSA-free mixtures (Figure 15, p. 60, top left). Mixing NMP with peanut oil leads to volume contraction and thus the mixture's properties, such as density, microviscosity and macroviscosity, change nonlinearly dependent on the mixture ratio. As expected, raising the temperature decreases the viscosity of the mixtures and thus increases the mobility of the spin probe.[71] This temperature effect is even more pronounced for low concentrations of NMP. At high proportions above 50 % [m/m] of NMP, the influence of the temperature can be neglected. This observation can be explained by the fact that temperature affects the viscosity of oil stronger than the viscosity of NMP.

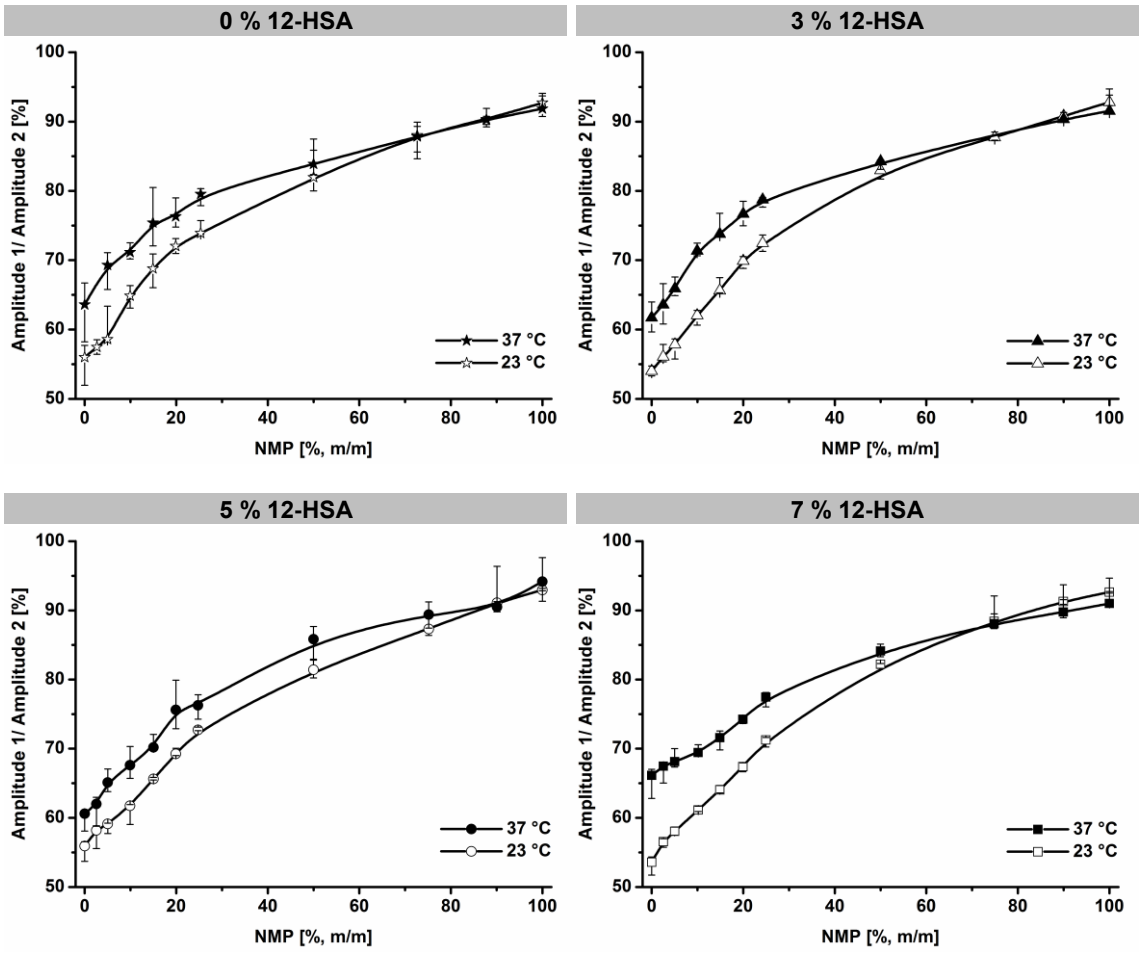

Figure 15 ***NMP concentration dependent amplitude ratios of peanut oil samples containing 0 % (top left), 3 % (top right), 5 % (bottom left) and 7 % [all m/m] (bottom right) of 12-HSA (relating to the quantity of peanut oil) and conducted at 23 °C and 37 °C. For amplitude ratio explanation see Figure 14, p. 57. Data represent medians ± ranges, n=4.***

By adjusting 23 °C, the sample without 12-HSA and 0 % [m/m] of NMP (*i.e.* pure peanut oil) shows an amplitude ratio of about 55 % (Figure 15, top left). The same value is obtained by the gelled oils containing 3 %, 5 % and 7 % [m/m] of 12-HSA with other conditions being equal (Figure 15). In other words, the probe mobility in the organogels is identical to that in pure liquid peanut oil. In conclusion, the organogels can be classified as real bulk gels, as it has already been proven (chapter 4.2.2, p. 53 ff.). The probe mobility in the oily bulk areas is completely free and unaffected from the 12-HSA fiber network. At this point, it is worth comparing these findings with the results of the rheological investigations concerning the organogels'

macroviscosities (chapter 4.2.4, p. 64 ff.). Thereby, complex viscosity and storage modulus considerably increase by increasing the concentration of 12-HSA.

By adjusting 37 °C, the amplitude ratios of the 12-HSA containing formulations with 0 % [m/m] of NMP are between 60-66 % (Figure 15, p. 60). Thus, these *homogeneous* gels show a lower microviscosity compared to the ISFOs with the same composition, but prepared by the extraction of NMP (amplitude ratio in equilibrium was 55 %; Figure 14, p. 57, right). Concerning administration, the experimental setup with the extraction of NMP is more realistic and leads to higher concentrations of 12-HSA at the interface. This could be explained with the diffusion of NMP out of the oil matrix. Thereby, also the probe may be transported to the interface, where the 12-HSA fiber network is denser than in the implant inside. Hence, inter- and intramolecular interactions between HD-PMI and 12-HSA might be possible leading to a lower mobility of some of the HD-PMI molecules. In EPR experiments as well as in all other probe techniques, always the specific place in a micro-heterogeneous sample is explored, where the probe is exactly located and which is affected by the presence of the probe. Thus, the EPR data correspond to the characteristics of the spin probe and are not always transferrable to the sample itself.

PROTON NUCLEAR MAGNETIC RESONANCE RELAXOMETRY (^{1}H-NMR)

^{1}H-NMR relaxometric measurements have been performed additionally in order to explore the microstructure of the developed ISFOs. To guarantee comparability with the EPR data, the samples were prepared identically by co-melting 12-HSA, NMP and peanut oil and subsequent cooling. This leads to a uniformly dense 12-HSA fiber network in the formulations. 12-HSA-free NMP-peanut oil mixtures served as controls. Since T_2 relaxation times of ^{1}H-hydrogen atoms are analyzed, the addition of “reporter molecules” (*i.e.* probes) to the samples as in EPR experiments is not necessary in ^{1}H-NMR relaxometry. The T_2 relaxation time depends on properties, such as density and microviscosity of the proton environment. The higher the microviscosity (*i.e.* the viscosity on the molecular level in the immediate vicinity of the protons), the lower the T_2 relaxation time is. Solids and immobilized liquids such as gels show stronger spin-spin interactions than liquid fluids and correspondingly possess shorter T_2 relaxation times.[111]

Figure 16 (p. 62) shows the T_2 relaxation time distributions of peanut oil depending on the concentrations of 12-HSA and NMP. For each figure, one major peak and at least

one side peak have been obtained. By applying 0 % [m/m] of NMP, the peak maxima of the main peaks appear at approximately 100 ms, independent of the concentration of 12-HSA. A content of NMP of 85 % [m/m] shifts the maximum of each peak to about 1,000 ms, indicating the lower microviscosity of the mixtures. The side peaks between 1-10 ms are irrelevant to the viscosity examinations due to their low peak amplitude. Most likely, they are attributed to surface phenomena between the mixtures and the screw-cap glasses.

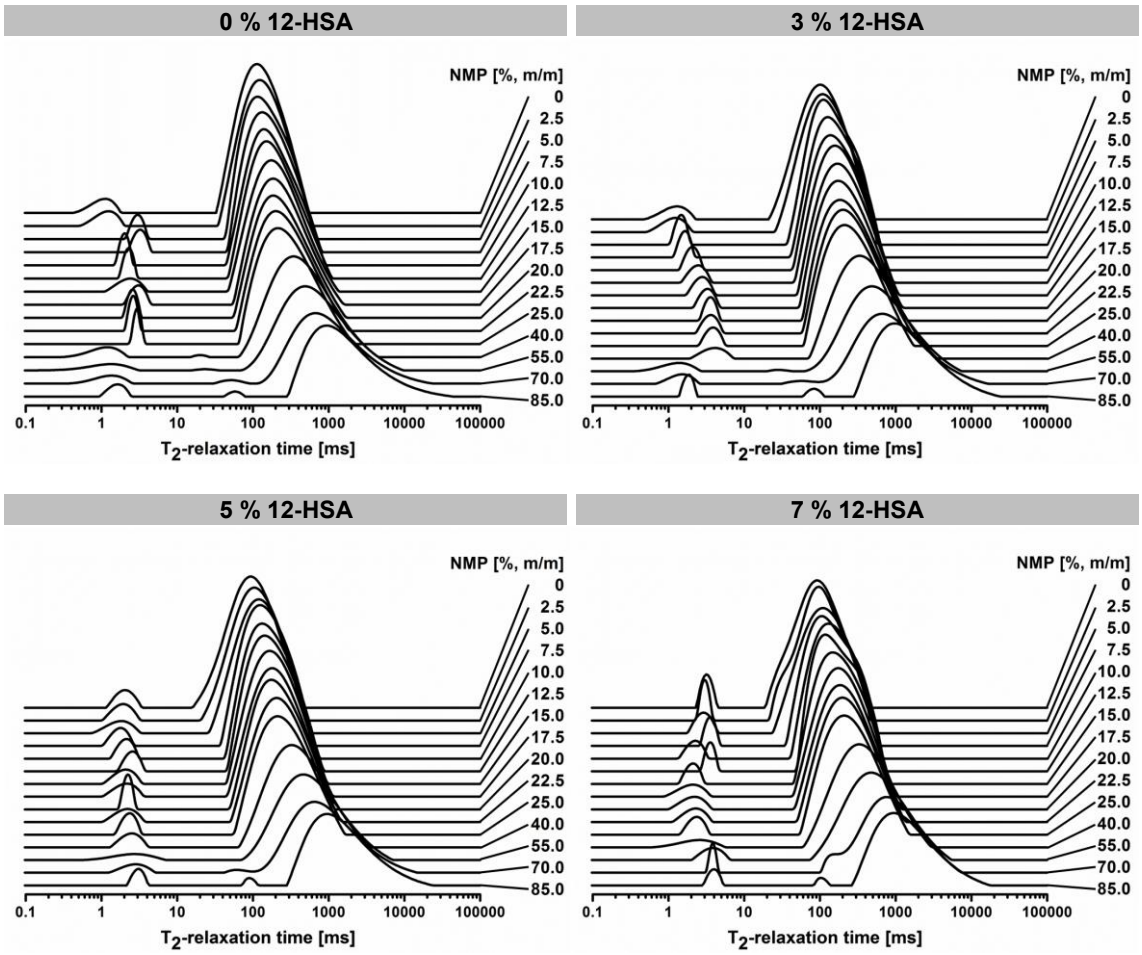

Figure 16 ***Distributions of T_2-relaxation times at 37 °C of peanut oil samples containing 0 % (top left), 3 % (top right), 5 % (bottom left) and 7 % [all m/m] (bottom right) of 12-HSA (relating to the quantity of peanut oil) depending on the concentration of NMP.***

As Figure 17 (p. 63, left) displays more clearly, 12-HSA-free NMP-peanut oil mixtures present almost equal relaxation time distributions as the 12-HSA containing mixtures. Consequently, T_2 relaxation times of the peak maxima are not influenced by the addition of 12-HSA. According to Table 13 (p. 46), 12-HSA containing mixtures are

liquid at high and already gelled at low concentrations of NMP. In the former case, the 12-HSA remains dissolved, whereas in the latter case precipitation already occurred and the 3D fibrillar network with the incorporated oil was formed. The relaxation times of the 12-HSA gels with 0 % [m/m] of NMP are identical to those of the liquid peanut oil (*i.e.* 0 % [m/m] of 12-HSA and 0 % [m/m] of NMP), indicating identical microviscosities. This confirms the previous findings of a bulk gel structure (chapter 4.2.2 and 4.2.3, p. 53 ff.). 12-HSA forms a wide-meshed scaffold with the highly mobile peanut oil in the space between the meshes. The oil's microviscosity in these bulk areas is equal to this of pure peanut oil, which is in agreement with other studies.[100,105] However, due to their different *macro*viscosities, the pure oil and the gelled oils showed different properties by applying oscillating rheology (chapter 4.2.4, p. 64 ff.). Furthermore, the addition of NMP decreases the microviscosity and thus increases the T_2 relaxation time. The shape of the curves (Figure 17, left) reveals the non-linear connection between the concentration of NMP and the T_2 relaxation time. This, in turn, is based on the volume contraction when mixing peanut oil and NMP as already demonstrated with the EPR experiments (Figure 15, p. 60). Thereby, the physico-chemical properties of the mixtures change nonlinearly with the increasing concentration of NMP.

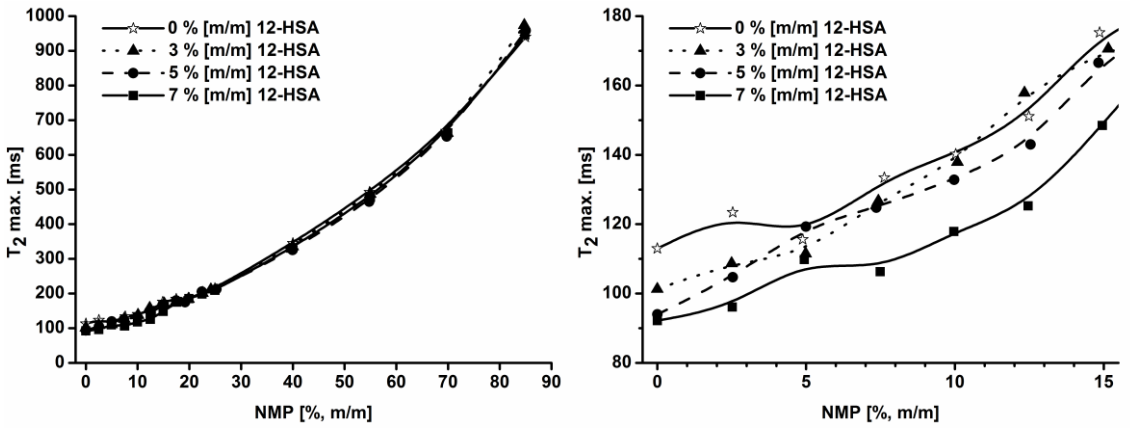

Figure 17 ***Left: Comparative presentation of T_2-relaxation times of the main peak maxima of Figure 16 (p. 62). Right: Enlarged section of the relevant concentration of NMP concerning ISFOs (Table 8, p. 25).***

The enlarged section of the relevant NMP range concerning the ISFOs (Figure 17, right) shows slight differences of the T_2 relaxation times between the organogels and the 12-HSA-free mixtures. However, the single values are within the digital resolution of the device and prevent the proper monitoring of the NMP extraction process.

4.2.4 MACROVISCOSITY

Gels are gelled liquids consisting of a matrix fluid and a gelling agent.[146] The gelling agent builds a 3D network or scaffold, which is completely penetrated by the matrix fluid.[76] This is also described by bicoherence. Approaching rheologically, gels represent ideal-elastic systems. After deformation, they return to their original state. However, this is only partially true for real gels. Due to a certain degree of flexibility, the scaffold is able to dodge low mechanical strain. However, when the yield point is exceeded, the structure of the scaffold collapses and the macroviscosity of the formulation decreases. Under these conditions, the formulation behaves viscously, denoting it as a *sol*. If this process is reversible, it will be called *gel-sol-gel transition*.

Determining macroviscosity, a sample is exposed to a certain degree of mechanical strain and its “response” is measured. Viscosity as an intrinsic resistance of the sample against external deformation depends on various parameters (*e.g.* temperature, pressure, pretreatment of the sample) and cannot be determined directly, since any shearing leads to a changing viscosity. Consequently, it is called *dynamic viscosity* in order to indicate that the viscosity of the absolute state of rest in a sample is immeasurable. The exact measurement conditions are always required for the interpretation and for the comparison of viscosities.

Rheological investigations of the ISFOs were performed after the extraction of NMP. It can be assumed that the 12-HSA scaffold at the implants’ surface is denser than in the implants’ inside. Homogeneous organogels, made by co-melting 12-HSA and peanut oil (so-called *preformed implants*), were also tested for comparison. To study only gels with intact fibrillar network structures (*i.e*. not the sol state), the applied strain must not exceed the samples’ yield points, where the formulations start to become viscous. The first step was the determination of the required deformation, which causes the gels to flow. For this purpose, the sample was placed onto a stationary plate and forced to deform by the oscillating cone. In *ideal-elastic* systems, the displacement of the cone (*i.e.* the deformation or strain) is proportional to the counteracting force of the formulation (*i.e.* the shear stress). Hence, the sinusoidal time-deformation curve is in-phase with the sinusoidal time-shear stress curve. Consequently, the loss angle δ (also known as phase shift angle) is 0°. The loss angle describes the relationship between the deformation (*i.e.* cone displacement) and shear stress (*i.e.* resistance of the sample). In *ideal-viscous* systems the time-shear stress curve is shifted by 90° in

relation to the time-deflection curve (*i.e.* δ=90°). Hence, the shear stress of the sample is the lowest when the cone displacement is the greatest. Accordingly, at a loss angle of 45° the system theoretically possesses 50 % of elastic and 50 % of viscous proportions.

Figure 18 (p. 66, left) shows the determined loss angles δ as a function of the deformation, by applying a low but constant oscillating shear rate of 1 s^{-1}. The constant loss angle of about 10°, up to a deformation of 0.05 %, results from the predominantly elastic properties of all the formulations. In contrast, the loss angle of about 80° at a deformation of 100 % indicates a pronounced viscosity/ plasticity. In both states (*i.e.* unsheared and maximum deformation) neither ideal-elastic nor ideal-viscous characteristics, with loss angles of 0° and 90°, respectively, are observed. As it is known for most of the gels for pharmaceutical applications, also the ISFOs belong to visco-elastic materials.[147] Above 0.05 % of deformation, all formulations response to the increased strain with a loss of elasticity. Only the formulations containing 3 % [m/m] of 12-HSA prove to be slightly more elastic even at a higher deformation. Significant differences between ISFOs and preformed implants cannot be observed. Within the range of deformation between 1-10 %, the irregular curve shapes of the implants containing 5 % and 7 % [m/m] of 12-HSA cannot be explained in detail. Colloidal or liquid crystalline structures have likely being formed during measurement and cause these curve shapes. However, due to the fiber network structures that are already destroyed at that point, further investigations were not conducted.

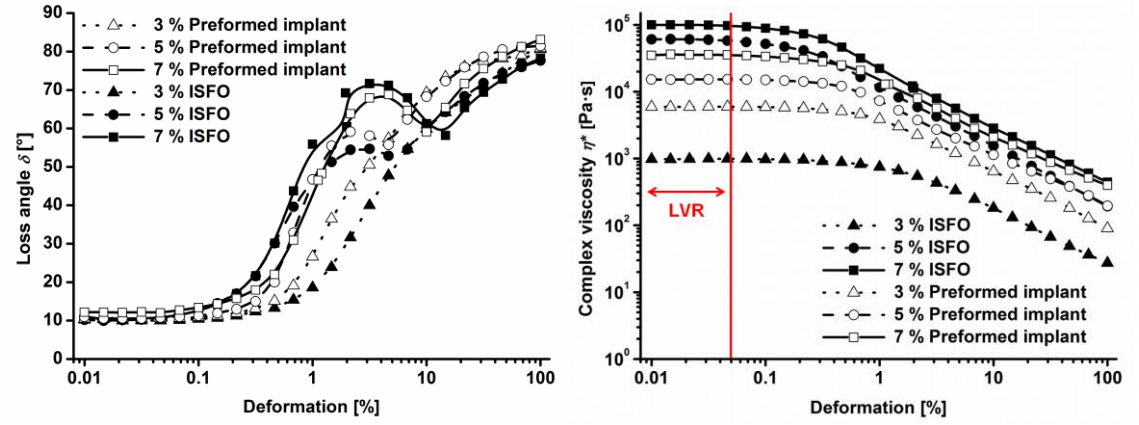

Figure 18 ***Deformation dependence of loss angle δ (left) and complex viscosity η* (right) at 37 °C and a default shear rate of 1 s^{-1}. All formulations remain intact up to a deformation of 0.05 % (linear visco-elastic range).***

The complex viscosity *η** (Figure 18, right) correlates with the results of the measurements of the loss angle. Up to a deformation of 0.05 % (*i.e.* LVR), the complex viscosity of the gels is unaffected by the deflection of the cone. Thus, the integrity of the 12-HSA-based fiber network structure is guaranteed within this range and the implants are stable and almost ideal-elastic. This comparatively narrow LVR has also been reported for similar 12-HSA containing formulations and also for other LMOGs.[84,105] At a higher deformation, the scaffold of the 12-HSA fibers collapses. The complex viscosity at a deformation of 100 % is reduced to only 1/30 of the initial values. As expected, the higher the concentration of 12-HSA, the higher the complex viscosity is. The meshes of the fiber network are closer together and make the gels more resistant to external strain. Interestingly, by applying equal concentrations of 12-HSA, the ISFOs show a significantly higher complex viscosity than the homogeneous preformed implants. Even the 5 % ISFO has a 1.5-fold higher complex viscosity within the LVR than the preformed implant containing 7 % [m/m] of 12-HSA. This result confirms the higher concentration of 12-HSA at the ISFOs' interface, which considerably increases their robustness. An exception of this observation represents the 3 % ISFO with a significantly lower complex viscosity than its preformed equivalent. However, this is consistent with the experiments in chapter 4.1.3 (p. 44 ff.). Although using 3 % [m/m] of 12-HSA is enough to gel the entire quantity of peanut oil, the implants turned out to be comparatively fragile to mechanical strain.

Figure 19 (p. 68) summarizes the results of the frequency sweep test. Based on the results of the deformation sweep test, a constant deformation of 0.05 % was set and

the shear rate of the cone has gradually been increased during measurements. As expected, the loss angles (Figure 19, p. 68, top left) are constant and low within the entire range of the shear rate.[71] The linear curves parallel to the x-axis confirm that the fibrillar network structures of all formulations remain intact during measurements. Accordingly, the storage modulus G' (representing the degree of elasticity) is proportional but higher than the loss modulus G'' (presenting the degree of plasticity), confirming the elastic properties of the formulations (Figure 19, p. 68, bottom). Furthermore, G' and G'' are almost independent of the applied shear rate, which is typical for gel structures.[71] However, G'' of each formulation exceeds 1/10 of G', indicating a rather poor elasticity in total.[84] In fact, the gel bodies appear rather like butter, which was just taken out of the refrigerator (*i.e.* solid but rheodestructive), and not like wine gum or gum, which are flexible and comparatively elastic. However, organogels with paraffin oil as oily matrix and 5 % [m/m] of 12-HSA showed a lower storage modulus of 60,000 Pa.[99] Even worse, using canola oil and 5 % [m/m] of 12-HSA result in a storage modulus of only 20,000 Pa, whereas the 5 % ISFO presents a storage modulus of about 250,000 Pa (Figure 19, p. 68, bottom left).[100]

A drop in complex viscosity η^* by increasing the shear rate is observable in Figure 19 (p. 68, top right). This is due to the almost constant shear stress of the intact gels within the entire range of the shear rate. The apparent loss of the complex viscosities is a theoretical loss that results from the calculation. It is not the result of the physical gels' viscosities. In other words, the resistance of the sample against external deformation of the cone remains constant even with an increase of the oscillating shear rate. If the increased shear rate led to the destruction of the gel structure, the storage modulus G' would noticeably drop, whereas the loss modulus G'' would considerably increase, but apparently this is not the case. In addition, the complex viscosity of the ISFOs at a given concentration of 12-HSA is higher than of the preformed implants, as it has already been obvious at the deformation sweep test (Figure 18, p. 66, right). In addition to the denser 12-HSA fiber network at the ISFOs' interface, the comparatively slow formation of the SAFiN during the extraction of NMP is responsible for the higher complex viscosity of the ISFOs. During the slow NMP release within 6-12 h, the 12-HSA molecules can arrange in a more organized way compared to the rapid cooling of the 12-HSA-peanut oil melt. Due to the fast cool down the resulting molecular mismatch of 12-HSA molecules leads to more branching and results in a lower

elasticity because of the limited time to build organized and extended network structures.[87]

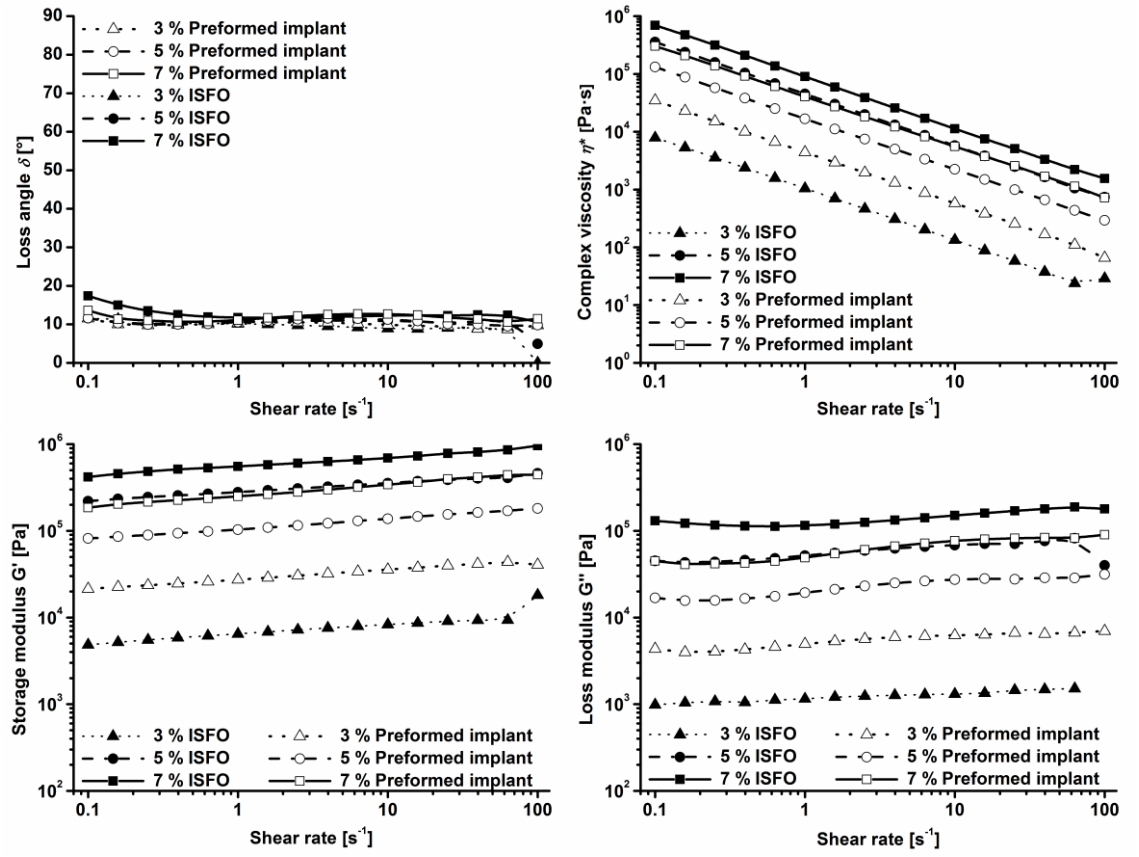

Figure 19 ***Shear rate dependence of loss angle δ (top left), complex viscosity η* (top right), storage modulus G' (bottom left) and loss modulus G'' (bottom right) at 37° C and a default deformation of 0.05 %.***

4.2.5 CYTOTOXICITY

SULFORHODAMINE B ASSAY (SRB)

This cytotoxicity assay allows conclusions regarding the total protein concentration in a cell culture. Originally, this assay had been used to determine the number of cells within a colony.[148,149] The dye SRB is capable of staining cellular proteins. Ionic bonding between the dye and basic amino acids occurs under acidic conditions. Unbound dye can be rinsed out afterward. Subsequently, bound dye is extracted in a basic medium. The optical density of the final solution correlates with the concentration of protein. For adherent cells, the test is also used to determine the toxicity of noxious substances. Cells respond to toxic substances with a decreased rate of protein synthesis and/ or a slower reproduction. Both lead to a decreased concentration of

protein in the treated cell colony compared to an untreated control. In case of serious cellular damage, cells may die directly. Thus, they detach from the ground of the plate and are rinsed out and discarded. Hence, their proteins do not contribute to the total amount of protein. Consequently, the more cells are affected adversely by noxious substances, the lower the detected concentration of protein is.

Figure 20 (p. 70) shows the optical densities measured after cell incubation with the extracts of the solidified ISFOs. The influence of the NMP has separately been examined due to its already known cytotoxic effect (Figure 22, p. 73). Cells in mMEM were used as a negative control and set as 100 %. In general, the solidified ISFOs consisting of 12-HSA and peanut oil are demonstrated to be excellently compatible with the cells. The diluted extracts of the 5 % ISFO and the 7 % ISFO (Figure 20, p. 70, bottom) show no reduction in the total amount of protein compared to the control group and can be regarded to be non-toxic. Investigating the extract of the 3 % ISFO (Figure 20, p. 70, top), about 80 % of proteins were detected after incubation with the 1:4 dilution. The loss of 20 % of proteins may be the result of several dead cells and/ or a down-regulated protein synthesis. However, an extent of 20 % should not be commented on too critically. 12-HSA is a component of various pharmaceutical excipients, especially non-ionic solubilizers, such as Kolliphor HS 15 and Kolliphor RH 40 (both BASF, Germany).[150,151] Their accepted toxicity profile justifies its use in a large number of drugs for parenteral and oral use.[60] The cytotoxic results also match those observed in an earlier study, whereby porous 12-HSA-soybean oil organogels proved to be very promising as scaffolds for the proliferation and colonialization of Chinese hamster ovary (CHO) fibroblast cells.[72]

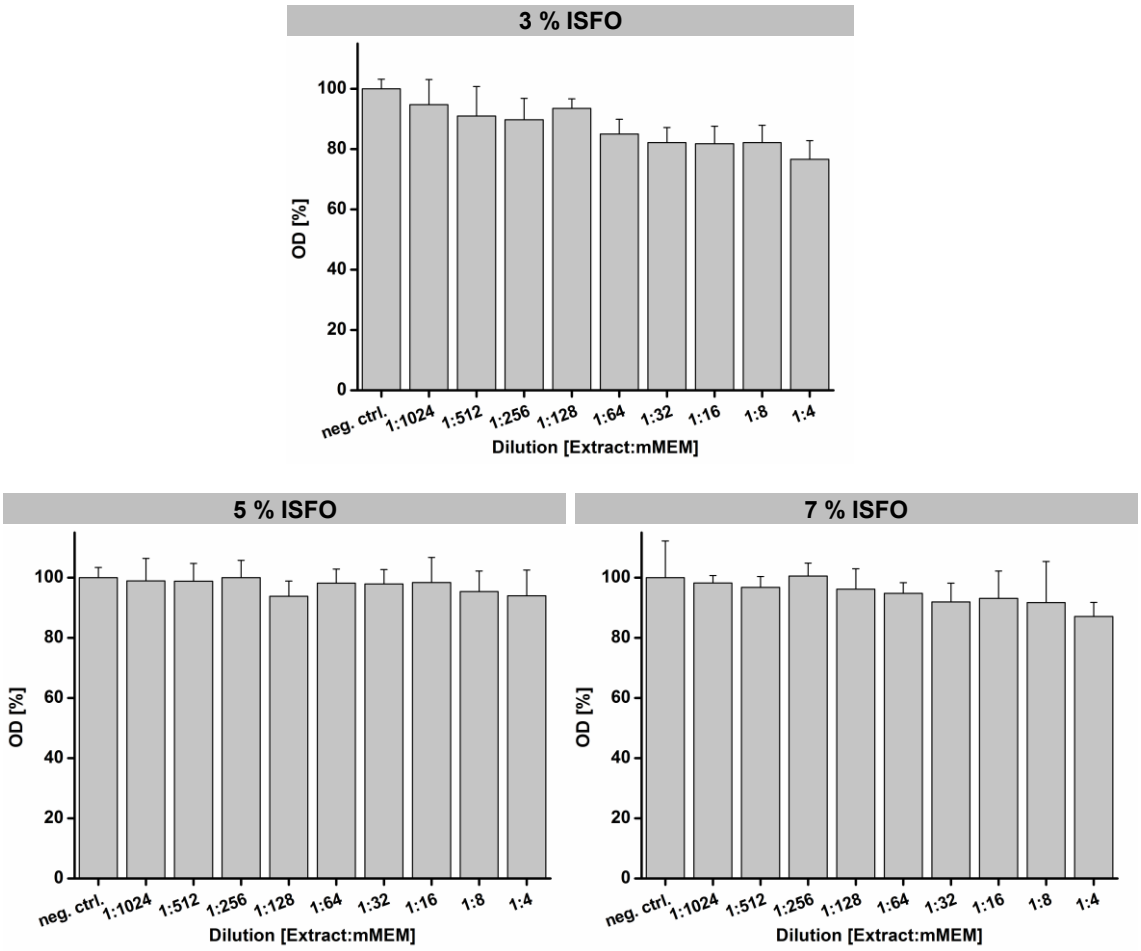

Figure 20 ***Optical densities measured 48 h after incubation of CCD-18Co cells with dilutions of the extracts [v/v] of the solidified ISFOs containing 3 % (top), 5 % (bottom left) and 7% [all m/m] (bottom right) of 12-HSA. Cells in mMEM were used as neg. ctrl. Data represent means ± SD, n=8.***

Untreated CCD-18Co cells have an elongated, fibrous shape and their ends are connected with other cells (Figure 21, p. 71, left), whereas dead cells have a round shape (Figure 23, p. 75, top right). Morphologically, the cells treated with the 1:4 extract dilution of the 3 % ISFO are identical to the untreated cells (Figure 21, p. 71). A decreased protein synthesis rate or a lower cell proliferation rate is, therefore, more likely than real cell necrosis. Cytotoxicity caused by 12-HSA can be excluded due to the observed tolerability of the extracts of the ISFOs containing 5 % and 7 % [m/m] of 12-HSA. The 3 % ISFO has probably loosened individual oil droplets from the interface, which led to surface effects with some cells during incubation in PBS. The significantly lower macroviscosity of the 3 % ISFO compared to the 5 % ISFO and the 7 % ISFO supports this assumption (chapter 4.2.4, p. 64 ff.).

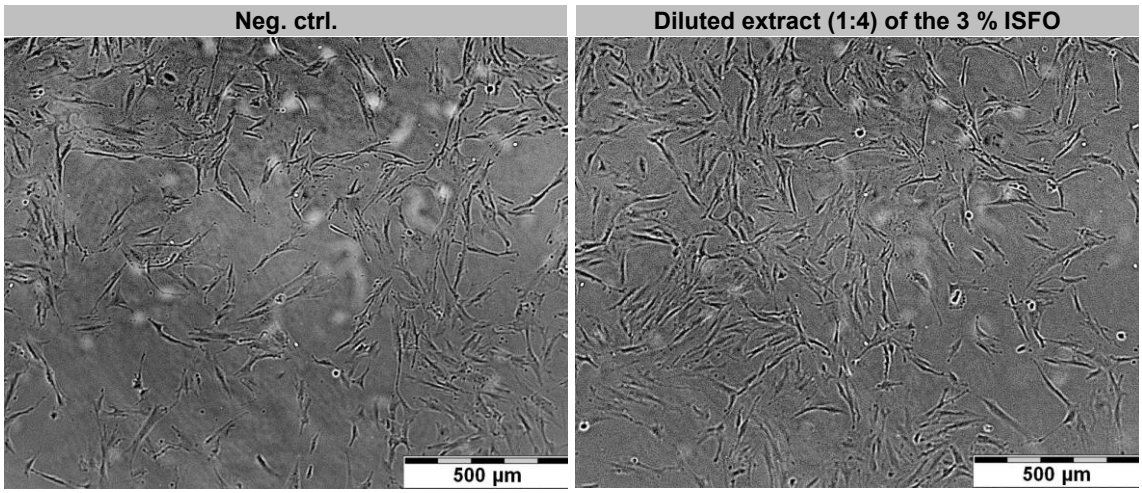

Figure 21 ***CCD-18Co cells (black) after 48 h of incubation with mMEM (left, neg. ctrl.) and with the mMEM diluted extract (1:4, v/v) of the solidified 3 % ISFO (right).***

NMP is used in FDA (U.S. Food and drug administration) approved formulations and is regarded as safe up to certain concentrations.[131] After administration, NMP rapidly distributes in human tissues and organs. Following metabolization by cytochrome P450, NMP and its hydroxylated and oxygenated metabolites are excreted by the kidneys within a few hours.[131,152] Unfortunately, toxicological data are often contradictory or difficult to compare. There are no toxicity data available for the *s.c.* and the *i.m.* administration of NMP relating to human beings.[45,49,152] Its LD_{50} (median lethal dose) for *i.v.* injection in rats is about 2.4 g/kg.[45] In animals, NMP often causes pain, local irritation, edema and muscle damage at the injection site.[41,49,111,153] In contrast, other findings demonstrated no acute toxicity in rhesus monkeys after injection of formulations containing NMP.[41] Furthermore, ISFOs with an amino acid-based LMOG, safflower oil and 10 % of NMP showed a high compatibility in rats with an inflammatory reaction between minimal and mild.[154] Moreover, most of the NMP related side effects are concentration dependent. In this work, the *s.c.* injection of 150 µL of the 7 % ISFO into a 30 g mouse (chapter 4.3, p. 83 ff.) contains approximately 20 mg of NMP (Table 8, p. 25). Assuming a patient of 80 kg, this quantity corresponds to the impractical mass of 53 g of pure NMP. This imbalance should generally be considered by the evaluation of the side effects in preclinical animal studies. Dealing with small contents of NMP in pharmaceutical parenterals is practicable but should be done in a reasonable way due to the unique solvating properties of this solvent. Hence, the developed ISFOs considerably contribute to the expansion of the applicability of parenteral *in situ* forming drug delivery systems.

Cytotoxic effects of NMP are already well known and described in the literature.[41,45,152,155,156] Using a potentially harmful substance for the development of a drug is often a compromise of various factors. The applied dose always determines the degree of unintended side effects. The approved human drug Eligard is available for *s.c.* administration with a 4-month depot effect. A single dose contains 30 mg of the API leuprolide acetate and 211.5 mg of the matrix polymer PLG, which is dissolved in 258.5 mg of NMP.[57] The majority of NMP will be released during the first hours after injection.[54,111] As a result of physical irritation, side effects, such as burning and paresthesia (very common), pain and bruising (common), pruritus (uncommon), ulceration (rare) and necrosis (very rare), occur at the site of injection.[157] Comparing the same mass of the matrix material (*i.e.* PLG in polymer implants and peanut oil in the ISFOs), the 7 % ISFO contains only 38 mg of NMP (Table 8, p. 25). This 7-fold higher amount of NMP in Eligard is necessary to dissolve the solid matrix polymer and to achieve a syringable solution. In contrast, the matrix of the ISFOs is peanut oil, which is already liquid and injectable at ambient conditions. The addition of NMP is only necessary to keep the comparatively low content of 16 mg of 12-HSA dissolved. Concerning the toxic NMP effects, a significant improvement of the side-effect profile of the developed ISFOs compared to the approved product Eligard can be expected.

Besides the concentration, the duration of the NMP exposure also affects the extent of local tissue irritation. The NMP is released out of the ISFOs into the surrounding *s.c.* tissue. Simultaneously, this absorption process is overlapped by the distribution of NMP into more distant structures and subsequently its metabolization and its renal excretion (*i.e*. its elimination). However, exact *in vivo* rates of absorption, distribution and elimination are unknown. Hence, by carrying out the cytotoxicity tests, three scenarios were tested exemplary: 1) incubation of the cells for 48 h at a constant concentration of NMP (*long procedure*); 2) incubating the cells for 6 h with a decreasing concentration of NMP, then 42 h with mMEM (*sink procedure*); 3) incubation of the cells for 2 h at a constant concentration of NMP, then 46 h with mMEM (*short procedure*). Thus, next to the concentration dependency the time dependency is also investigated. Figure 22 (p. 73) presents the results of the SRB assay.

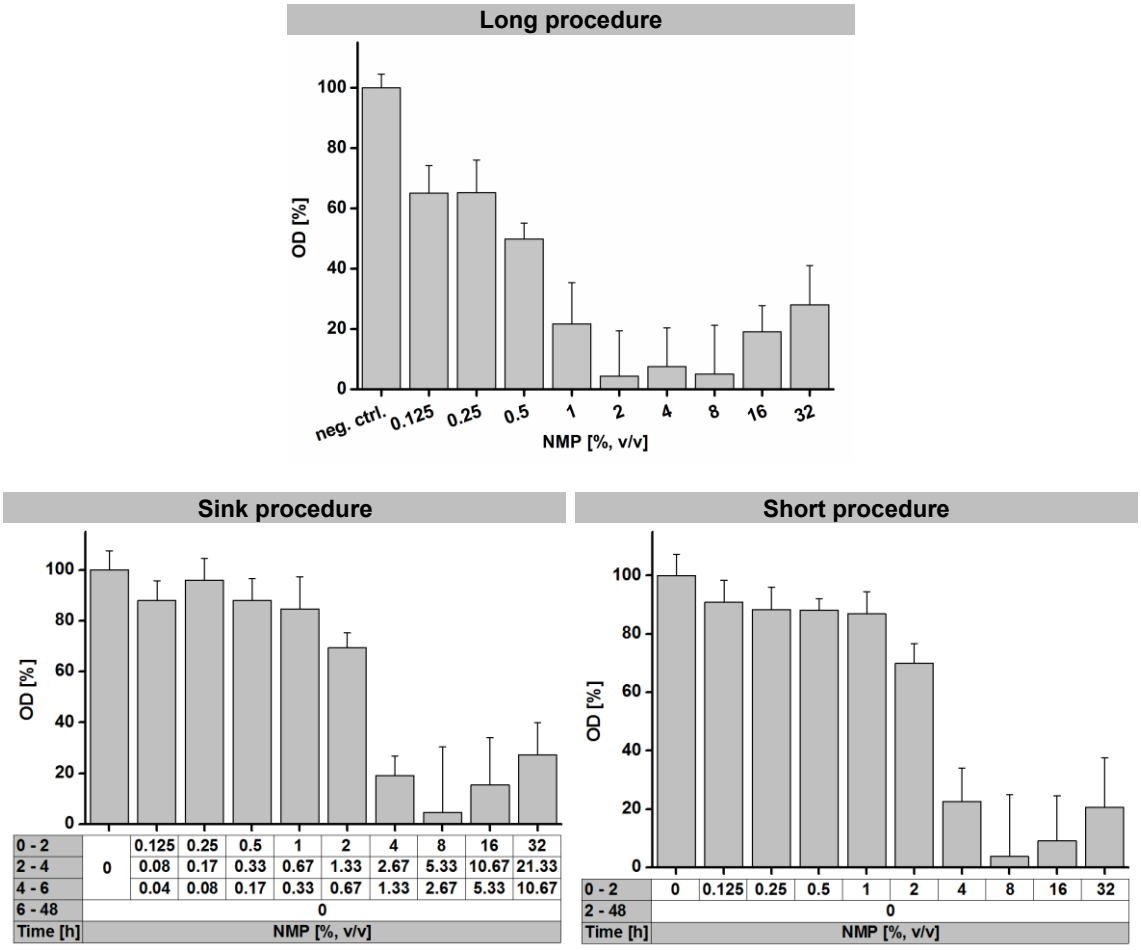

Figure 22 ***SRB assay: Optical densities measured after incubation of CCD-18Co cells with mMEM containing different NMP concentrations. Cells in mMEM were used as negative control. Top: Constant concentration of NMP for 48 h (long procedure). Bottom left: Decreasing concentration of NMP over 6 h, then 42 h mMEM (sink procedure). Bottom right: 2 h NMP exposition, then 46 h mMEM (short procedure). Data represent means ± SD, n=8.***

The treatment with NMP led to a decreased concentration of protein compared to the negative control in each of the three scenarios. As expected, the extent of cell damage depends on both concentration of NMP and exposition time. After incubation for 2 h in 1 % [v/v] of NMP, more than 80 % of the proteins were still present (*short procedure*), whereas only 20 % of the proteins were remaining after 48 h at the same concentration of NMP (*long procedure*). Incubating the cells with NMP dilutions of a declining concentration (*sink procedure*) led to identical protein concentrations as in the *short procedure*, despite the longer presence of NMP in total. Accordingly, the degree of cell damage was dependent on the highest applied concentration of NMP. The subsequent treatment with lower concentrations of NMP (*sink procedure*) did not lead to further cell

damage. For the first 2 h of incubation, the amount of proteins in cells treated with 0.125 % [v/v] of NMP equals the level of 1 % [v/v] of NMP (see both *sink* and *short procedure*). Within this concentration range, NMP is comparatively well-tolerated by the cells. However, already 4 % [v/v] of NMP results in a dramatic cellular damage, even at the short-term incubation of 2 h. Paradoxically, the protein concentration increases again from 8 % [v/v] of NMP to beyond in each of the three scenarios. In addition, no more time dependence is observable at these high concentrations of NMP. Incubation in 32 % [v/v] of NMP led to a protein concentration of about 25 %, irrespectively whether the cells were exposed to the solvent for 48 h (*long procedure*) or just for 2 h (*short procedure*).

The microscopic image of the cells after 48 h of treatment with NMP (*long procedure*) provides an explanation for the described paradoxical effect (Figure 23, p. 75). Incubation with 1 % [v/v] of NMP (Figure 23, p. 75, top left) leads to a significant cell rounding as an indicator of advanced lesions compared to the native, non-treated state (Figure 21, p. 71, left). At 4 % [v/v] of NMP (Figure 23, p. 75, top right), almost all cells are round and hence dead. These cells including their proteins are detached from the ground of the plate and are discarded during the washing process. Hence, their proteins do not contribute to the optical density measured. Interestingly, after incubation with 16 % [v/v] and 32 % [both v/v] of NMP (Figure 23, p. 75, bottom) hardly any round cells are visible. Their shape is similar to that of untreated cells. However, they appear narrower and slightly shrunken. Probably high concentrations of the NMP cause an osmotic effect and abruptly absorb the cellular fluid. The resulting denaturation of cellular proteins leads to the fixation of the cells on the ground of the plate. The cells morphology remains largely unaffected. Ultimately, these cells contributed to a false negative result, as they were detected by the test (Figure 22, p. 73). In order to attain certain knowledge of this effect and to support the results of the SRB assay, the metabolic activity of the NMP treated cells has been measured by applying both MTT and resazurin assay.

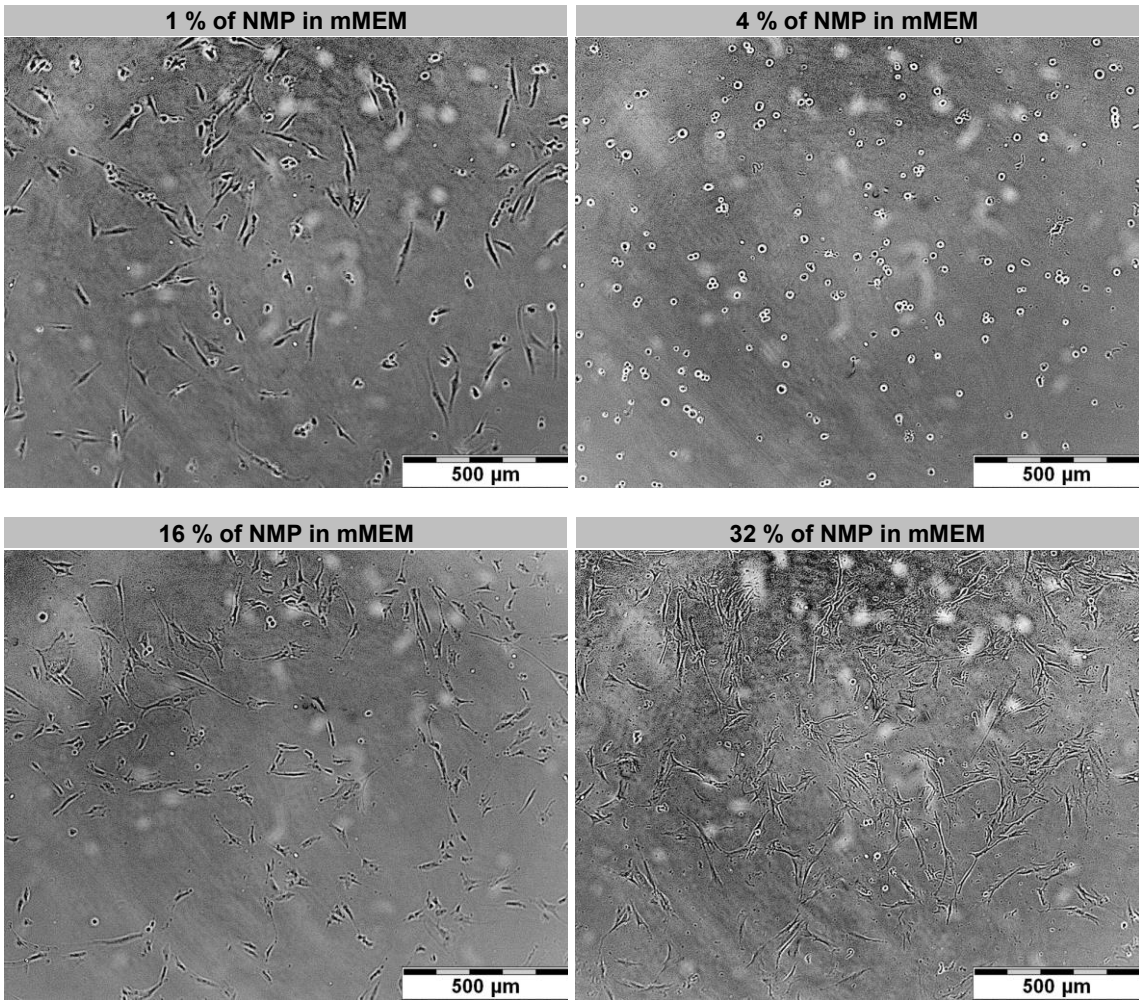

Figure 23 ***CCD-18Co cells (black) after 48 h of incubation with dilutions of 1 % (top left), 4 % (top right), 16 % (bottom left) and 32 % [all v/v] (bottom right) of NMP in mMEM.***

MTT ASSAY

This test is based on the conversion of yellow MTT to dark blue MTT formazan by mitochondrial dehydrogenases in living cells.[158] The distinction between living and dead cells enables an estimation of the toxicity of noxious substances. Figure 24 (p. 76) shows the optical densities measured, which correlate with the metabolic activity of the cells. The increase of the concentration of NMP and of the exposition time is both accompanied by a loss of metabolic activity. The results of the MTT assay led to similar values as for the SRB assay (Figure 22, p. 73). However, no re-increase in the metabolic activity was observed at 8 % [v/v] of NMP and beyond, as it was for the SRB assay. This confirms the assumption of a cell fixation on the ground of the plate caused by high concentrations of NMP. Hence, the cellular proteins of these cells contribute to

the total concentration of protein measured by the SRB assay. However, these cells were already dead.

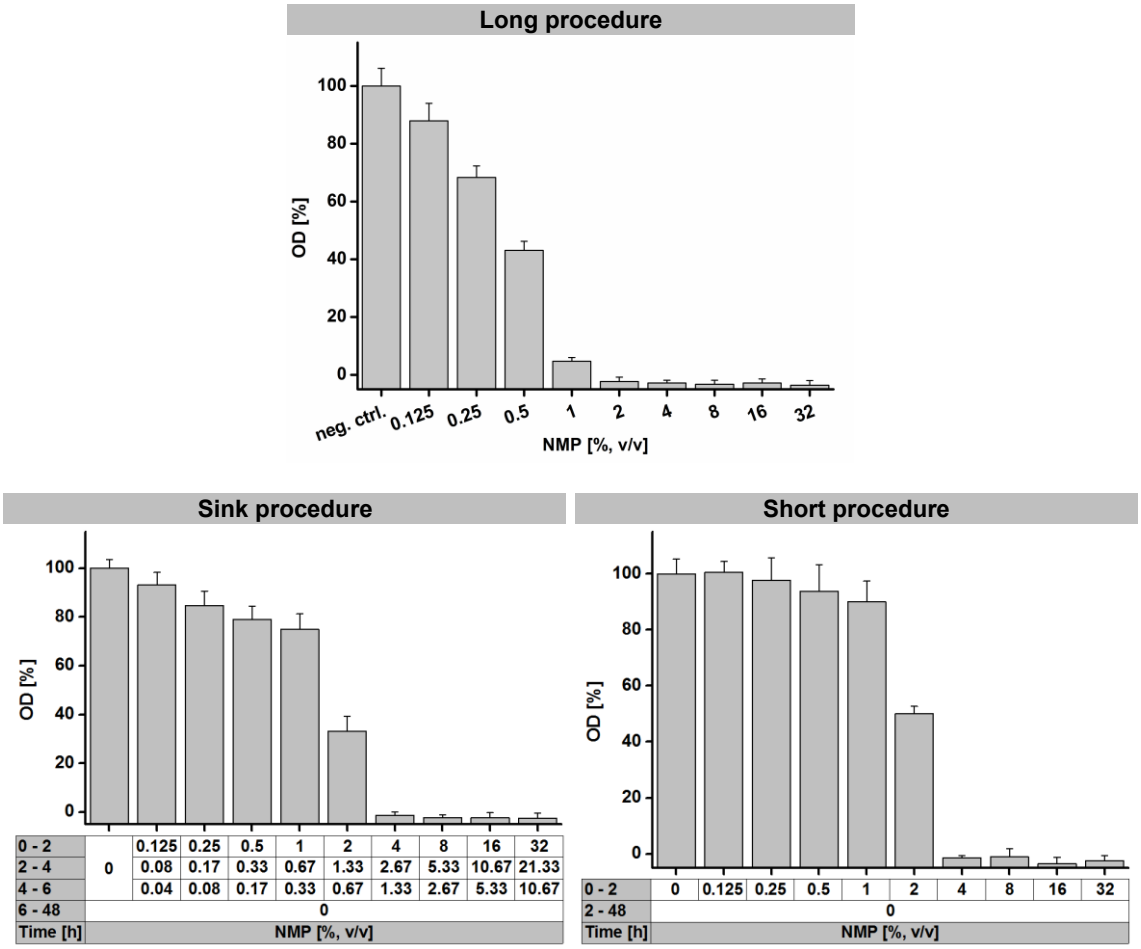

Figure 24 ***MTT assay: Optical densities measured after incubation of CCD-18Co cells with mMEM containing different NMP concentrations. Cells in mMEM were used as negative control. Top: Constant concentration of NMP for 48 h (long procedure). Bottom left: Decreasing concentration of NMP over 6 h, then 42 h mMEM (sink procedure). Bottom right: 2 h NMP exposition, then 46 h mMEM (short procedure). Data represent means ± SD, n=8.***

RESAZURIN ASSAY

The resazurin assay is, as well as the MTT assay, used to measure the metabolic activity of the cells. Living cells reduce the non-fluorescent blue resazurin to the fluorescent red resorufin.[159,160] The measured fluorescence intensity, in turn, allows conclusions concerning the cytotoxic effect of NMP. Figure 25 (p. 77) shows the measured OD, which correlates with the metabolic activity of the cells.

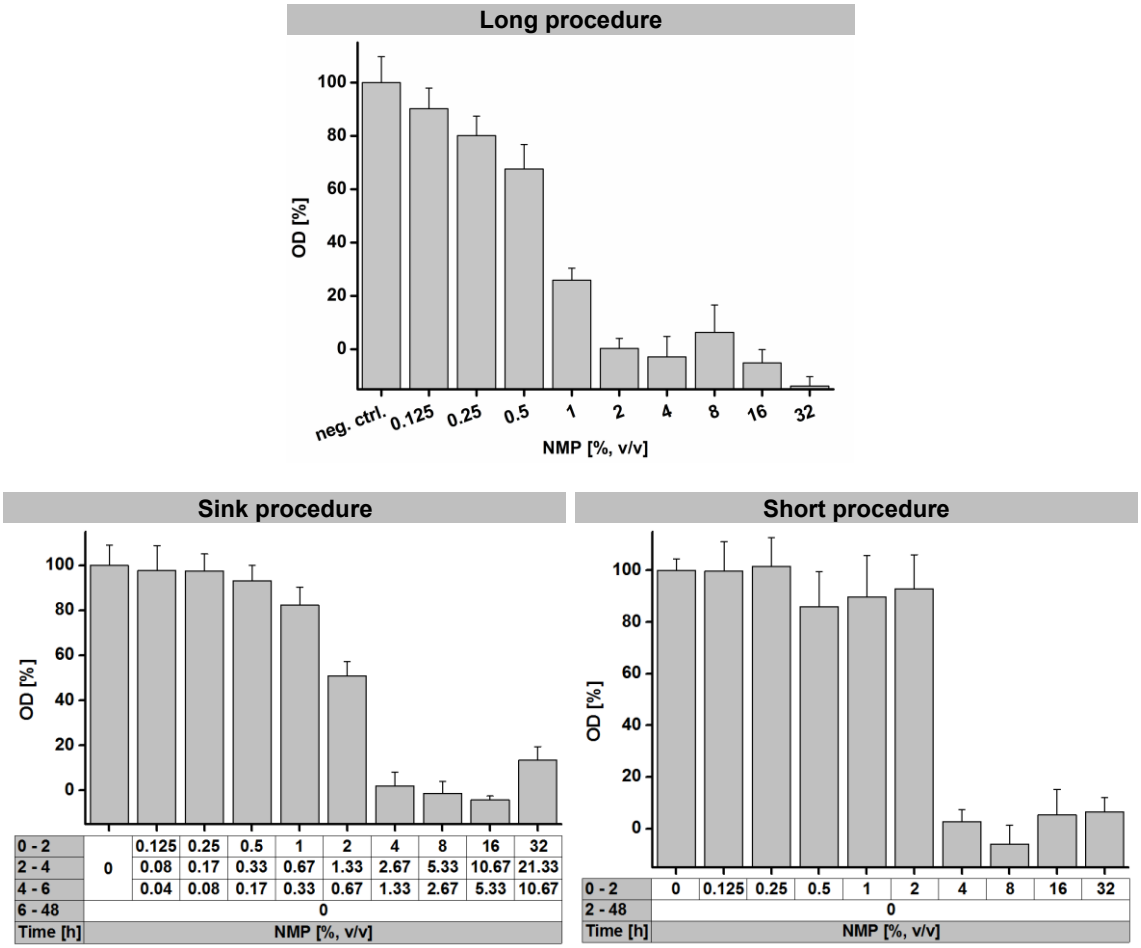

Figure 25 ***Resazurin assay: Optical densities measured after incubation of CCD-18Co cells with mMEM containing different NMP concentrations. Cells in mMEM were used as negative control. Top: Constant concentration of NMP for 48 h (long procedure). Bottom left: Decreasing concentration of NMP over 6 h, then 42 h mMEM (sink procedure). Bottom right: 2 h NMP exposition, then 46 h mMEM (short procedure). Data represent means ± SD, n=8.***

The results are consistent with the metabolic activities determined in the MTT assay. Time and concentration dependence of the NMP toxicity are quite pronounced. By applying *sink* and *short procedure*, 4 % [v/v] of NMP led to a complete failure of the metabolic activity (at the *sink procedure* with concern for the first two hours), as for the MTT assay. This, in turn, confirms the assumption of an immediate fixation of the cells on the ground of the plate after adding highly concentrated solutions of NMP.

SUMMARY OF CYTOTOXICITY EXPERIMENTS

Table 18 (p. 78) summarizes the estimated IC_{50} values derived from the cytotoxic experiments. IC_{50} indicates the concentration of NMP which causes the half-maximal

inhibition of the cells (*i.e.* protein concentration or metabolic activity). Low IC_{50} values are considered to be critical, whereas high IC_{50} values indicate better tolerability. For an exposition period of 48 h (*long procedure*), about 0.5 % [v/v] of NMP is confirmed as acceptable. For short periods up to 2 h, the IC_{50} increases to 2 % [v/v] of NMP. Under sink conditions, the IC_{50} values fit in between.

Table 18 ***Estimated IC_{50} values (%, [v/v]) of NMP on the basis of the cytotoxicological results. For explanation of the procedures see Figure 22 (p. 73).***

Assay	Long procedure	Sink procedure[a]	Short procedure
SRB	0.5	2-4	2-4
MTT	0.25-0.5	1-2	2
Resazurin	0.5-1	2	2-4

[a] Values relate to the concentration of NMP during the first two hours.

The following calculation example is intended to classify these values in terms of the practical benefit of the ISFOs. In the interest of simplification it is assumed that the cytotoxicological results are directly transferable to human side effects and the entire quantity of NMP is released abruptly from the formulations into the surrounding tissue. Thus, each single dose of the 4-month depot drug Eligard, which contains 258.5 mg of NMP, would require a *s.c.* acceptor volume of 51.4 mL (based on the IC_{50} of 0.5 % [v/v] of NMP) or of 12.7 mL (based on the IC_{50} of 2 % [v/v] of NMP). In contrast, the 7 % ISFO with an identical mass of matrix material contains only 38 mg of NMP and thus requires only 7.6 mL (based on the IC_{50} of 0.5 % [v/v] of NMP) or 1.9 mL (based on the IC_{50} of 2 % [v/v] of NMP) of *s.c.* acceptor volume. In spite of all that, this calculation is just an oversimplification and neglects the complex distribution and metabolization processes *in vivo*. However, the example clearly illustrates the potential benefits of the developed ISFOs with regard to reduced side effects originating from NMP at the site of injection. Moreover, the 3 % ISFO contains only slightly more than half of the NMP amount of the 7 % ISFO and therefore offers a further reduction in the *s.c.* acceptor volume and also promises an improved side-effect profile.

4.2.6 ENZYMATIC DEGRADATION

LPLs (lipoprotein lipases) are water-soluble enzymes, which hydrolyze triglycerides. They can be found in all tissues of the human body, especially in the skeletal muscles, the adipose tissue and the serum fluid.[161–163] The hydrolysis of the ester bonds of lipids

occurs at the oil-water interface.[64,164] Unfortunately, the postulated *in vivo* degradation of lipid-based drug carriers via phagocytosis and subsequent lymphatic removal cannot be simulated *in vitro*. LPL assays potentially enable the determination of the biodegradation of lipid-based dosage forms.[22,163,165] Enzyme activity refers to the rate of enzymatic conversion of the reactants into products and is expressed as enzyme units (U). The LPL activity in the *s.c.* adipose tissue is specified with 0.01 U/mL.[161] In case of the LPL applied for the experiments conducted, 1 U corresponds to the amount of enzyme which liberates 1 *µ*mol of oleic acid of triolein per min at pH 8.0 and 40 °C. However, these standard conditions are slightly different from both the experimental *in vitro* and *in vivo* conditions. Hence, the stated activities are to be understood as approximations.

Assuming a *s.c.* lipase activity of 0.01 U/mL, the entire hydrolysis of 500 mg of triolein in a volume of 3 mL would take about 13 days (500 mg of triolein corr. to 565 *µ*mol of oleic acid). This period of time approximates to the dosage recommendation for 1 mL of an oily depot formulation for testosterone substitution of 2-3 weeks.[133] However, since this drug is administered *i.m.* instead of *s.c.*, the local LPL activity possibly differs. In addition, lipophilic and hence dissolved APIs are primarily released via diffusion. Oil hydrolysis is, therefore, not essential for these APIs' release. Furthermore, oily carriers for parenteral use (*e.g.* peanut oil, sesame oil, soybean oil) are more complex in their composition than the reference substance triolein. Hence, the rate of the substrate conversion is not completely transferable.

The general principle of organogelation is to delay the degradation of the oil and thus the release of the API. For parenteral depot drug formulations, a degradation period between a few weeks and several months is often desired. To examine the ISFOs' degradation characteristics, they were hydrolyzed *in vitro* using different concentrations of LPL. As Figure 26 (p. 80) shows, lowering the concentration of 12-HSA in the ISFOs and increasing the concentration of LPL led to accelerated degradation of the implants. All implants degraded layer-by-layer from the surface. Mass erosion and rupture did not occur. Therefore, a correlating release of API particles or dissolved API with a low diffusion coefficient (*i.e.* molecules with a high molecular weight or hydrodynamic radius) appears feasible.

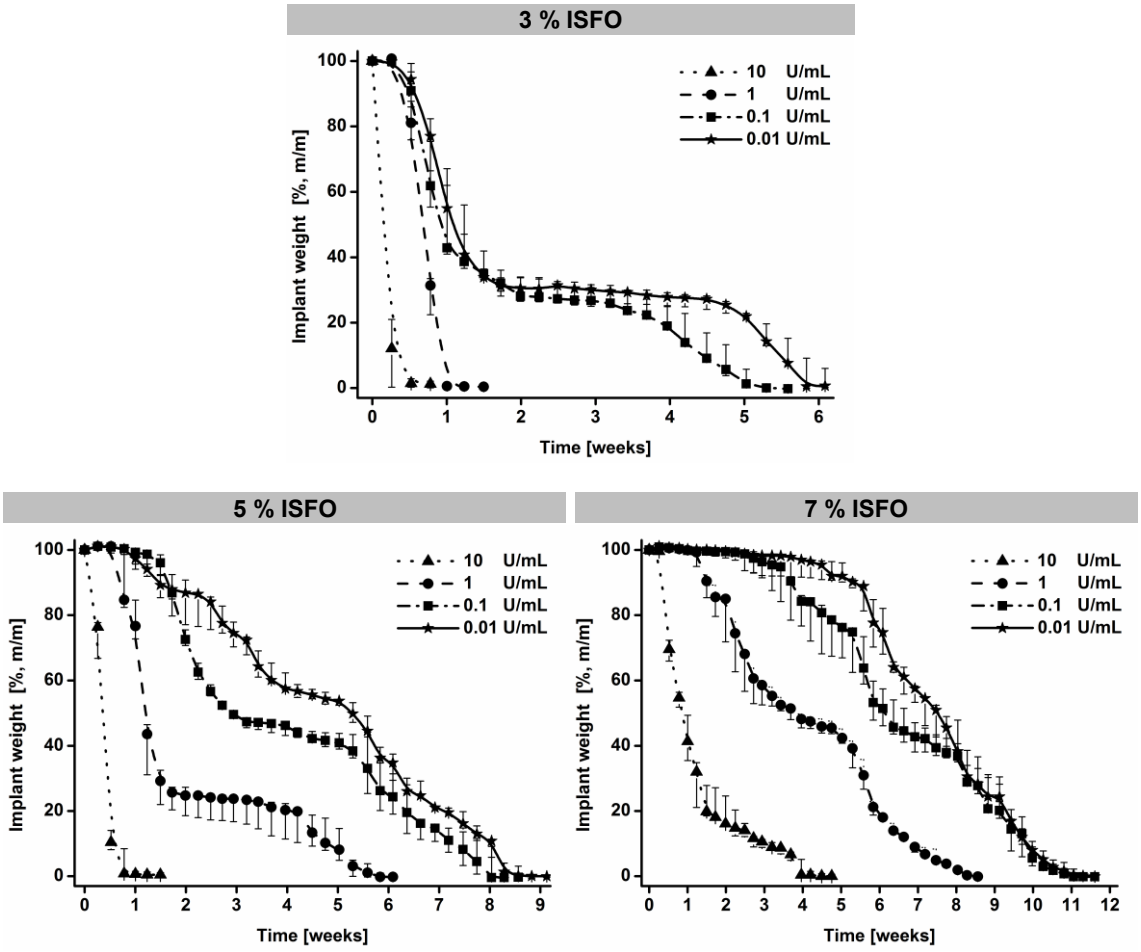

Figure 26 ***Time-dependent degradation of the 3 % ISFO (top), 5 % ISFO (bottom left) and 7 % ISFO (bottom right) in PBS at 37 °C using different activities of LPL. Data represent medians ± ranges, n=3.***

Interestingly, dependent on both 12-HSA and LPL concentration, a lag time was observed at the beginning of the experiment with almost no loss of the implant weight. The higher the concentration of 12-HSA and the lower the concentration of LPL, the longer the lag time was. By applying 7 % ISFO at the human concentration of LPL of 0.01 U/mL, this lag time covered a 4-weeks timeframe. Since the LPL containing medium has always been prepared freshly, a loss of enzymatic activity is unlikely. These lag times may be explained by the denser fibrillar network structure near the implants' surface, whereas the peanut oil is protected from the hydrolysis of the LPL.

Furthermore, in some cases, a plateau was observed after the initial accelerated degradation of the oil. However, a predictable forecast concerning the applied concentrations of 12-HSA and LPL is not apparent. This effect could be due to the

accumulation of 12-HSA making the surface of the implant denser and leading to a kind of shield effect. The re-increase of the degradation rate after the plateau could be explained by the resulting fatty acids and di-/ monoglycerides from the oil hydrolysis, which slowly but steadily detach the water-insoluble 12-HSA molecules from the surface. Also, these degradation products reduce surface tension at the oil-water interface which might increase the rate of lipolysis. Both effects will not play a major role for the *in vivo* degradation because degradation products are being constantly absorbed. Therefore, the results only provide an approximate idea regarding the release of the API *in vivo*.

In terms of the human *s.c.* LPL concentration of 0.01 U/mL, the degradation of the 3 % ISFO displays biphasic degradation (Figure 26, p. 80, top). 70 % [m/m] of the implant was degraded constantly during the first two weeks. The remaining 30 % [m/m] of the implant was finally hydrolyzed between week 4 and 6.

In contrast, there is a more continuous degradation of the 5 % ISFO and the 7 % ISFO (Figure 26, p. 80, bottom). After an initial lag time of about one week and 4 weeks, respectively, both formulations have been degraded at 0.01 U/mL of LPL over a period of 7 weeks with approximately zero-order kinetics. In other words, the concentration of 12-HSA does not affect the degradation time but the duration of the lag time. It is reported in the literature that precipitation of the gelling agent at the implant surface can cause incomplete implant degradation due to the limited access of the lipase to the oil.[163] This does not appear to be the case here. The developed 12-HSA-based ISFOs have completely been degraded, which complies with previous studies concerning 12-HSA-based organogels.[91] It is assumed that the release rate of API particles would be identical to the degradation rate of the oily carrier. By applying oil-soluble (*i.e.* mostly lipophilic) APIs, which can diffuse inside of the peanut oil through the fiber meshes of the 12-HSA network, the release rate would depend on the sizes of the API molecules. The higher their hydrodynamic radius, the lower the diffusion coefficient is and the more significant the release based on the surface degradation of the oily carrier will be. Despite the phenomena of lag times and plateau phases, the solidified peanut oil implants appear to be more favorable depot formulations than their solid lipid counterparts (*e.g.* compressed glyceryl-trimyristate, -tripalmitate, -tristearate implants), which merely degrade *in vitro* (below 1 % [m/m] within 30 days, even at an irrationally high concentration of lipase of 50 U/mL).[165]

For depot drug delivery systems, *in vitro* release and degradation experiments only provide a rough idea in terms of the *in vivo* situation. The composition of the surrounding *s.c.* fluid as well as metabolic and immunological processes can lead to large deviations. For instance, the fasted state, obesity and the release of insulin cause up-regulation of the human *s.c.* concentration of LPL. With regard to the release of testosterone enanthate, down-regulation of the LPL is commonly known, whereby the oil hydrolysis slows down.[166] Furthermore, the presence of polyvalent cations (*e.g.* calcium, magnesium) could lead to the formation of non-polar complexes with the split fatty acids, which could re-diffuse into the implant and affect the oil degradation. In addition, free fatty acids could attach to and thereby charge the implant's interface and thus influence the action of the lipase. The cytotoxicity of NMP (chapter 4.2.5, p. 68 ff.) may further cause local inflammation or edema and consequently change the properties of the surrounding fluid and the tissue. Another aspect is the *s.c.* tissue pressure, which may lead to the spreading of the liquid formulations directly after injection resulting in non-reproducible implant shapes. Finally, the *in vitro* release of poorly water-soluble APIs (*e.g.* testosterone enanthate) mostly requires the addition of a solubilizing excipient in the release medium in order to maintain sink conditions. This procedure will fail since the oily implant will be attacked by the solubilizer, which affects both the degradation of the carrier and the release of the API.

Due to the variety of factors influencing the *in vitro* degradation and also their superimposition, *in vivo/ in vitro* correlations of the API's release can hardly be displayed. Despite the need, no standard method exists for testing oil-based injectables. Floating-, dialysis- and continuous flow techniques have been reported.[22,64] However, the obtained release data are not comparable since the surface area of the oil, the stirring conditions and the sink conditions between these approaches are not uniform. Furthermore, even the *in vitro* release of the API from compressed and dimensionally stable triglyceride implants is significantly affected by the experimental setup, which is also true for polymer-based microparticulate formulations.[167] Moreover, ISFOs based on L-alanine showed a weight loss *in vitro* of 15 % [m/m] within 30 days, whereas *in vivo* about 90 % [m/m] have been degraded in the same time. This indicates the ambivalence of *in vitro* release experiments.[168] For the reasons mentioned, *in vitro* API release experiments have intentionally been excluded from this thesis.

4.3 *IN VIVO* CHARACTERIZATION

Pharmaceutical development of novel dosage forms always aims at the successful administration to living organisms. In this thesis, comprehensive *in vitro* investigations primarily served to understand the physico-chemical properties of the ISFOs. However, the complex interactions between the formulations and their surrounding at the injection site can be displayed *in vivo* only. Quite often *in vivo* results are seemingly contrasting to *in vitro* findings. This contradiction is explained by the change of a variety of parameters by the transition from well-controlled *in vitro* conditions to complex and only partially known *in vivo* conditions. Crucial *in vivo* factors concerning the examined ISFOs are primarily:

- Influence of the *s.c.* tissue pressure and animal movement directly after injection to the spreading characteristics of the formulation and thus the implant shape and consequently the rate of degradation and the release of the API;
- Physico-chemical irritation, immune responses and histological alterations due to implant components or degradation products, which may cause local and/ or systemic reactions (*e.g.* edema, fever, necrosis, fibrosis) and lead to
- Accelerated or inhibited as well as incomplete implant degradation due to factors influencing lipase activity and/ or lymphatic absorption and thus affect the release of the API.

To examine the behavior of the ISFOs *in vivo*, they were *s.c.* injected and the degradation was monitored. Figure 27 (p. 84) shows the injection site of the ISFOs, the inguinal region (lat. *regio inguinalis*) of mice. For administration, the cannula was punctured into the skin from distal and then guided underneath to the site of injection. The distance between puncture site and the area of injection prevented an undesirable outflow of the still liquid formulations directly after injection. The site of injection has been chosen for three reasons: 1) low tissue tension (compared to the often selected nuchal fold); 2) low-noise area with respect to MRI and USI (*i.e.* less motional interferences than cardiac and pulmonary near structures); 3) possibility of bilateral implantation (*i.e.* halving the mouse number by the use of placebo ISFOs).

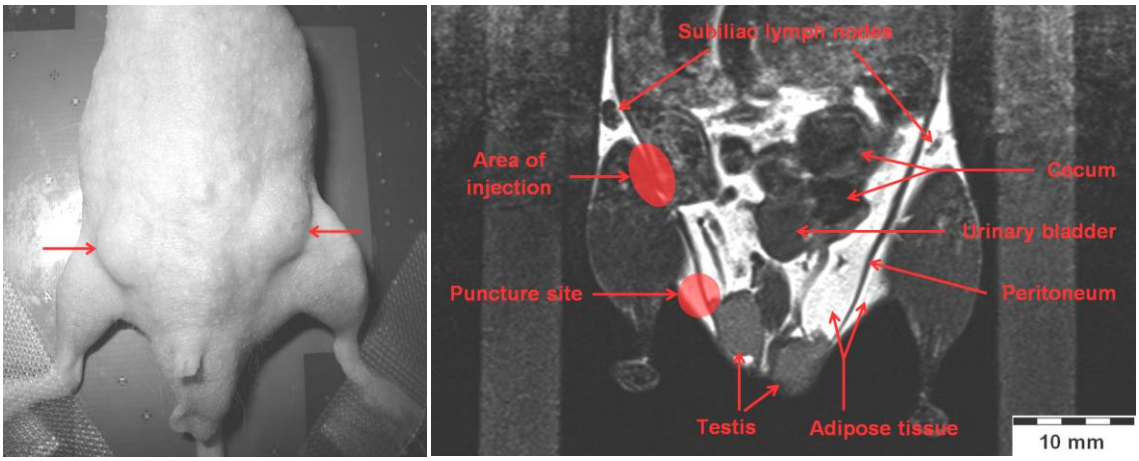

Figure 27 ***Left: Anesthetized male SKH1-Hr^{hr} nude mouse in supine position after s.c. injection of 150 µL of the ISFOs into both sides (arrows). Right: Coronal T_1-weighted MR image from the lower body part of an untreated mouse. Formulations were injected from distal into the inguinal region.***

4.3.1 IMPLANT DEGRADATION

MAGNET RESONANCE IMAGING (MRI)

T_1 relaxation times depend on structure and composition of the tissue. After excitation, the antiparallel spins in the adipose tissue rapidly change back into parallel position. In contrast, highly hydrated tissues emit the absorbed energy more slowly. For high-contrast visualization of structures with a short T_1 relaxation time, T_R must be in the range of the T_1 relaxation time (T_1-weighted image). Fast relaxing spins of the adipose tissue as well as the ISFO can then be excited again by the following rf-pulse. Not yet relaxed spins of hydrated structures cannot be excited again, which leads to a reduced MR signal. T_E should be as low as possible to reduce the influence of the T_2 relaxation.[169] Hence, for T_1-weighted images, fat and ISFOs (T_1 short) are hyperintense, whereas hydrated or inflamed tissues (T_1 long) appear hypointense. By using TSE sequences, multiple echoes can be received per excitation by means of additional 180° pulses. This allows the reduction in measurement duration and increases the signals of adipose tissue and ISFOs.[170]

Figure 28 (p. 86 ff.) shows T_1-weighted *in vivo* images of the ISFOs and peanut oil as a control during an observation period of 22 weeks. Each image shows the mouse's hind leg and the inguinal region into which the formulations have been injected. The high quantity of peanut oil contained in the ISFOs complicates the distinction between the *s.c.* adipose tissue. For a sharp distinction, transverse planes have additionally been

recorded (data not shown). Based on the implants' shape and position the degradation-time course could be monitored.

After injection, the 7 % ISFO solidifies into one spherical implant (week 1 and 2). During the first three weeks, there is no reduction in the implant size observable (lag phase). However, a broad hypointense area around the implant is striking (week 1, 2 and 3). This may be an edematous swelling due to a local inflammatory response caused by NMP or degradation products of the implant. However, externally the mice showed neither irritation nor inflammation at the site of injection. During the following 16 weeks, the implant gradually degraded until it was not further detectable. Thus, the initial lag phase is followed by a degradation period over about 13 weeks. Interestingly and contrary to expectations, the degradation did not happen in layers from outside to inside as observed *in vitro* (chapter 4.2.6, p. 78 ff.). Rather mass rupture and the formation of smaller separate gel depots, which finally degrade, occurred (compare week 2, 3, 5 and 6). The continuous and complete degradation of the 7 % ISFO appears to be promising in terms of a controlled release of API over a period of 3-4 months.

The 5 % ISFO shows identical degradation characteristics to the 7 % ISFO concerning both lag time (about 2 weeks) and the duration of the residue-free degradation (about 16 weeks). However, three smaller gel depots have directly been formed after injection. The largest is located in the desired area of injection, whereas the two smaller ones developed by spreading during pull out of the cannula. This is probably caused by the lower concentration of 12-HSA compared to the 7 % ISFO, leading to a lower robustness of the implant. Likewise to the 7 % ISFO, but to a smaller extent, hypodense areas around the implant depots were observed (week 1 and 2). This could be related to the lower content of NMP compared to the 7 % ISFO (Table 8, p. 25). Over time, the three gel depots split further (compare week 2, 3 and 5) and are completely degraded between week 16 and 19. Generally, an increased spreading tendency results in less reproducible implant shapes leading to higher deviations in the rate of degradation and ultimately in a varying release of the API. On the other hand, a certain degree of fluidity of the implants may reduce foreign body reactions and thus improves the implants' tolerability.

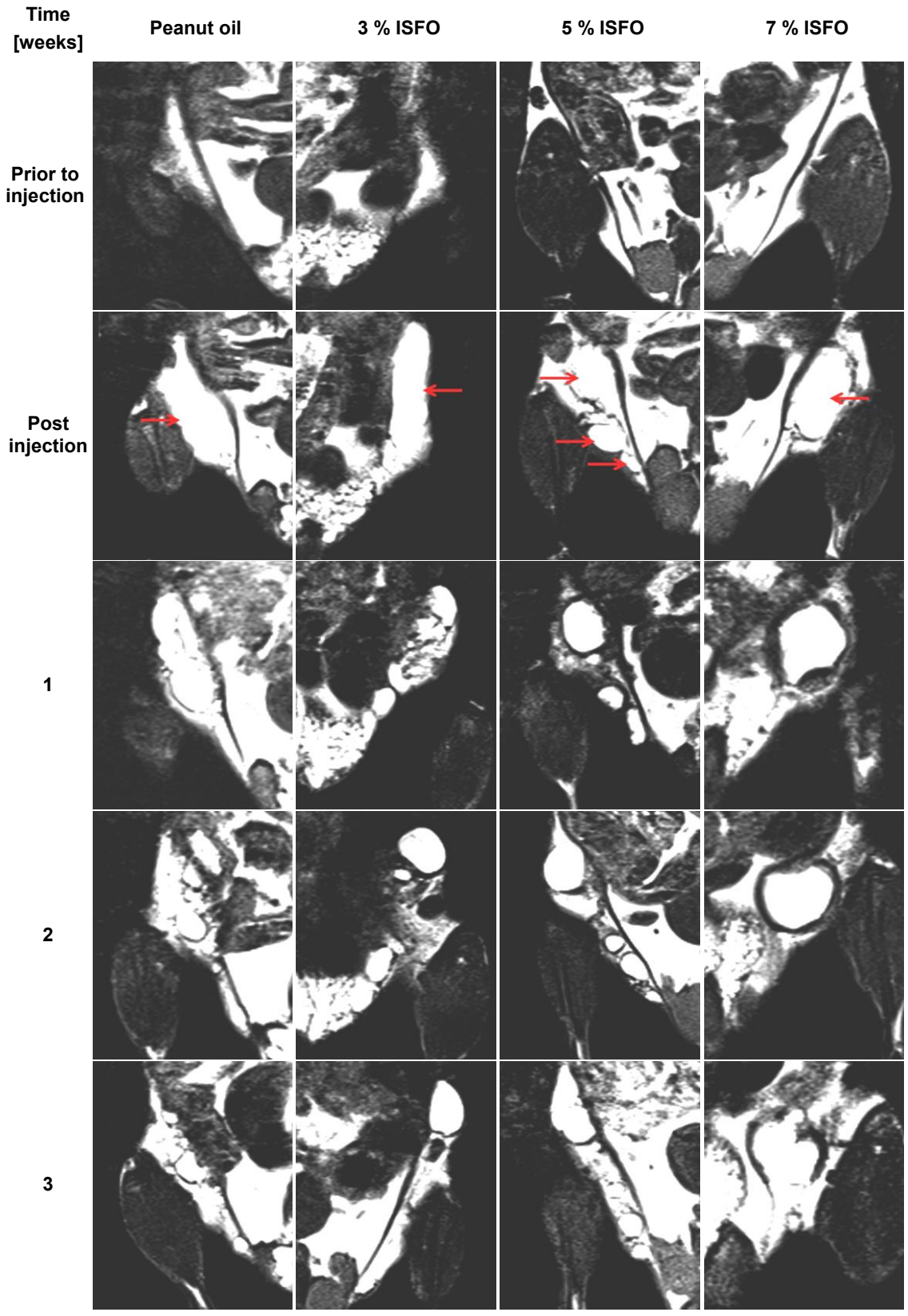
Time [weeks]
Peanut oil
3 % ISFO
5 % ISFO
7 % ISFO
Prior to injection
Post injection
1
2
3

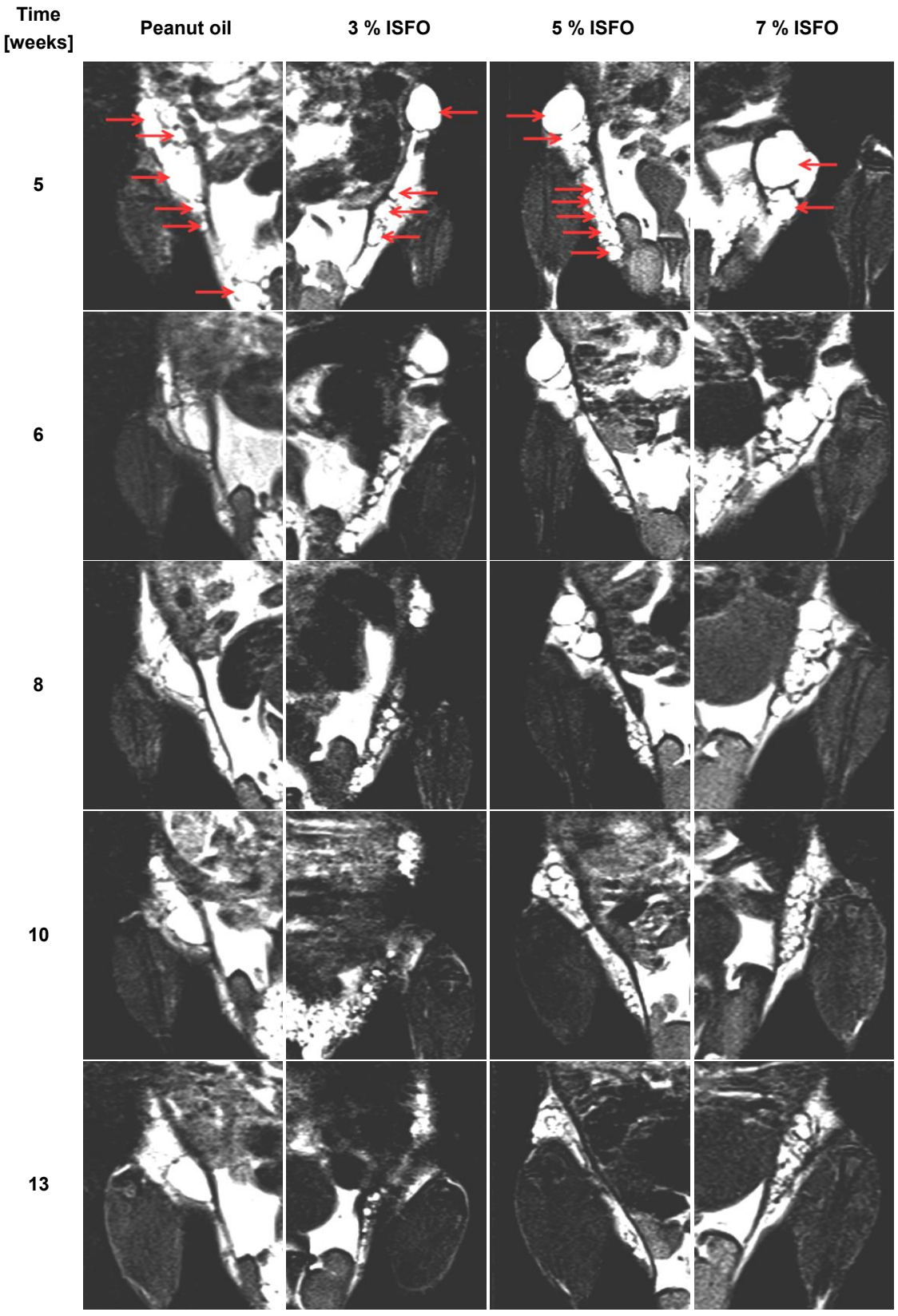
Time [weeks]
Peanut oil
3 % ISFO
5 % ISFO
7 % ISFO
5
6
8
10
13

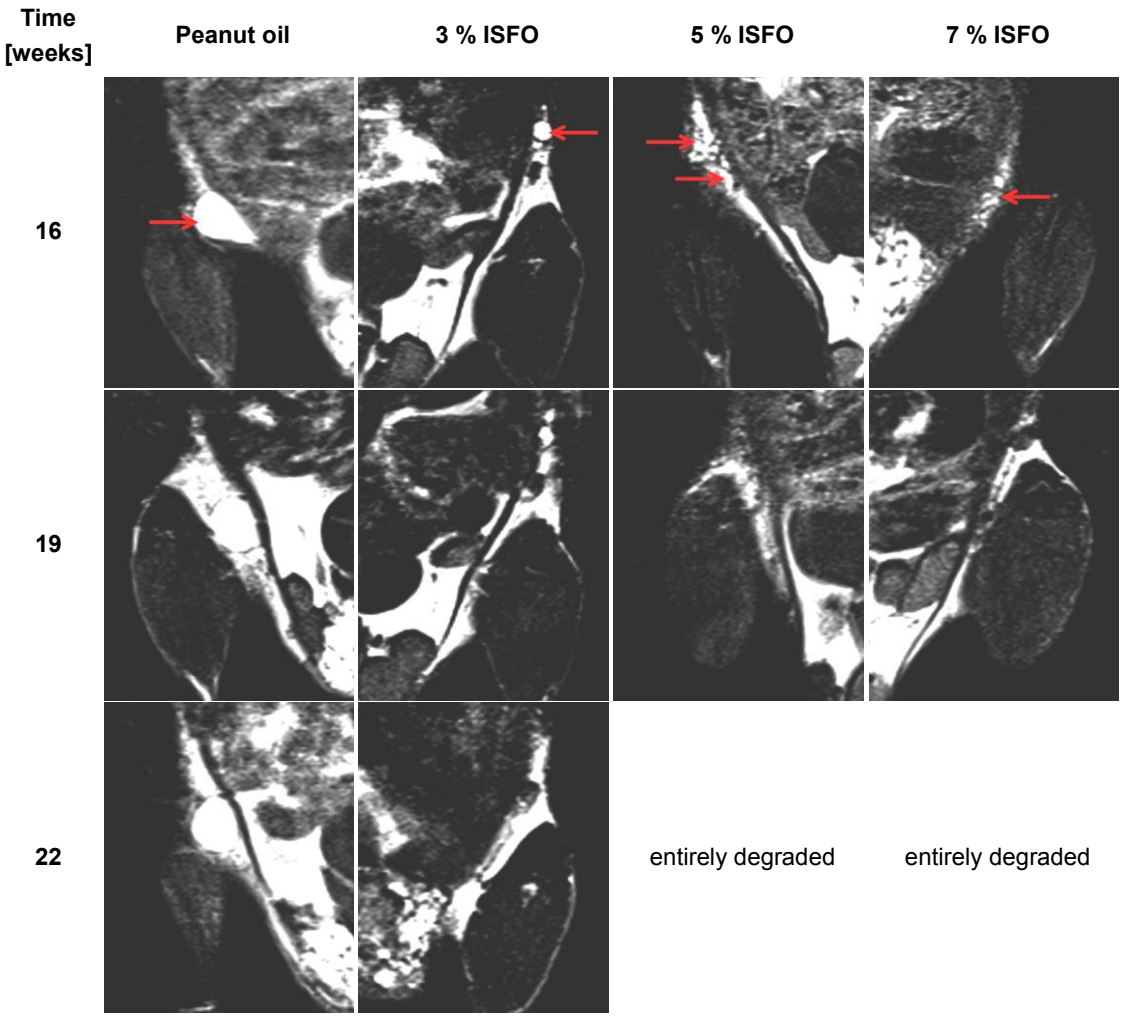

Figure 28 ***Exemplary coronal T_1-weighted MR images from the lower body part of SKH1-Hr^{hr} mice in the untreated state and after injection of peanut oil (control) and the ISFOs (n=3). The arrows at the beginning of each page (p. 86-88) indicate the position of the depot.***

The 3 % ISFO also shows a similar tendency to spread after injection, which led to the formation of several small gel depots between puncture and injection site (compare post injection and week 1). The largest depot at the site of injection hardly changed in size between week 2 and 5. In the following, this large depot fissured slowly. However, even after 22 weeks, residues have still been apparent, while the initially smaller depots had disappeared completely after 16 weeks. Probably the lower macroviscosity of this formulation contributes to its constant deformation by the movement of the mouse, which affects the degradation of the implant.

Pure peanut oil does not undergo solidification after injection. The dark border around the bright oil droplets is narrower compared to the ISFOs (week 1). As already shown in the cytotoxicological experiments (chapter 4.2.5, p. 68 ff.) and other studies by various authors, it is likely that the solvent NMP causes concentration dependent irritation *in vivo*.[45,171] The resulting peanut oil chambers repeatedly change in both size and shape over the duration of the implant degradation. Hence, assessing the degradation rate on the basis of the MR images is difficult. One large oil chamber is striking with nearly the same size after 22 weeks compared to the beginning. However, analyzing the surrounding tissue *post mortem* showed no fibrotic encapsulation, as it is often observed in connection with implants.[111,171,172]

The root cause of the slow or incomplete degradation of the low-viscous formulations (peanut oil and 3 % ISFO) is not fully understood. Possibly, more solid implant surfaces cause a facilitated attack of the *s.c.* lipase and therefore a more continuous implant degradation. Moreover, half-lives of oil vehicles after *s.c.* and *i.m.* administration directly depend on the organism. For instance, the quantity of sesame oil is eliminated by half within 23 days in pigs, but within 63 days in rats.[64] In addition, also the type of oil affects the rate of degradation. By using rabbits, the half-time of the semi-synthetic oil MCT is 8 days, whereas half-times of sesame oil and peanut oil are approximately similar (27 days *vs.* 25 days), which is due to their nearly identical fatty acid finger prints (Table 16, p. 49).[22] Currently approved drugs with peanut oil as carrier contain only lipophilic APIs (*e.g.* testosterone enanthate), which diffuse out of the oily carrier. Thereby, the kinetics of the degradation of peanut oil plays a subordinate role. However, by applying solid API particles, the entire degradation of the developed ISFOs is decisive to ensure a continuous release of the API. Therefore, the 5 % ISFO and the 7 % ISFO appear more suitable.

ULTRASOUND IMAGING (USI)

USI is a powerful tool to non-invasively quantify the *in vivo* degradation properties of *s.c.* drug delivery systems, such as polymer-based implants and ISFOs.[173,174] MRI studies revealed that the ISFOs are likely to spread in the *s.c.* tissue with lower concentrations of 12-HSA (Figure 28, p. 86 ff.). Usually, ultrasound transducers were put directly onto the skin of the object after applying a thin layer of ultrasonic contact gel. In order to suppress the influence of the ultrasound transducer to the shape of the lower-viscous implants, the transducer was installed free-floating above the anatomical

region to be examined. Consequently, using plenty of ultrasonic contact gel provided the necessary transmission of the sound waves between both mouse and transducer. Using fur-free mice as model organism primarily served for the better spreadability of the contact gel without the inclusion of interfering air bubbles in the hair interstices. Furthermore, the first measurement has been done 24 h after injecting the ISFOs. Thereby, the implants have already been solidified and their shape was not affected by the measurement. Based on the apparent external skin bulges at the sites of injection, the transducer could easily be adjusted in the measuring position.

Figure 29 (p. 91) shows the decreasing volumes of the ISFOs and peanut oil (control) over time. 100 % [v/v] corresponds to the initial volume on the first day after *s.c.* injection of 150 µL. In all cases, this recovered volume has been between 100-140 µL. The volumes of spread formulations consisting of several small depot chambers have been added up. As demonstrated by MRI (Figure 28, p. 86 ff.), this was primarily the case for the peanut oil control and to a lesser extent for the 3 % ISFO. Comparing the USI results of all the 4 formulations clearly shows the decreasing variation of the degradation with increasing the concentration of 12-HSA. By applying pure peanut oil (Figure 29, p. 91, top left), the degradation period ranges from an immediately occurring and continuous volume reduction over 4-6 weeks (mouse #11) up to a 3-week lag time with subsequent continuous degradation and still 10 % [v/v] of peanut oil remaining after 22 weeks (mouse #8). In contrast, all mice bearing the 7 % ISFO (bottom right) show a lag time of 3 weeks, followed by a continuous degradation period of another 9 weeks (except mouse #9 with a degradation time of 13 weeks).

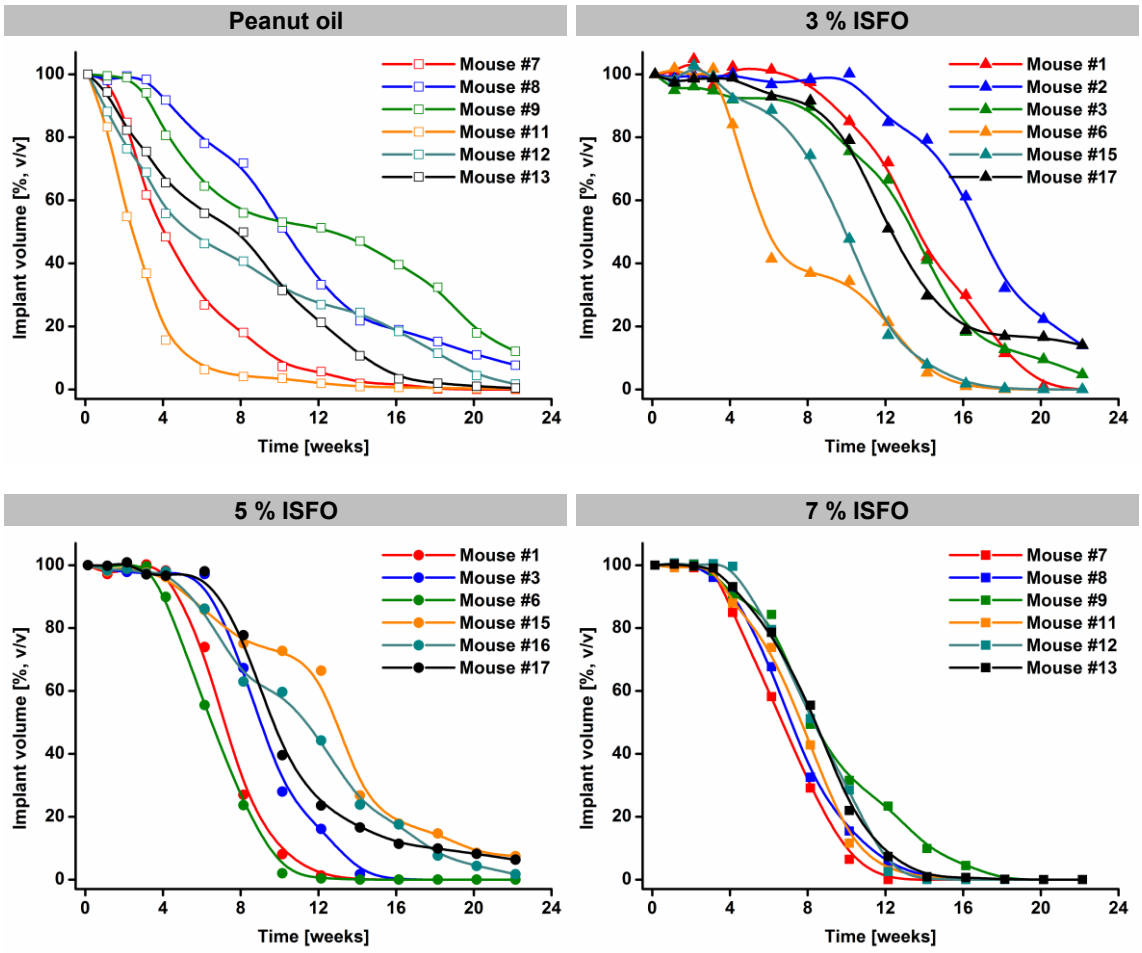

Figure 29 ***Time-dependent degradation of peanut oil (top left), 3 % ISFO (top right), 5 % ISFO (bottom left) and 7 % ISFO (bottom right) after s.c. injection of 150 µL. Each mouse received two injections (both legs). Data represent the courses of each injection.***

The major cause of the varying degradation of the implants is the increased spreadability with decreasing the concentration of 12-HSA. The 7 % ISFOs form large stable depots, whereas liquid peanut oil results in several smaller depots already starting to degrade with the first day after injection (Figure 30, p. 93). Over time, both shape and size of the implant made of pure peanut oil change by the movement of the mouse, as already demonstrated in the MR images (Figure 28, p. 86 ff.) and other studies.[22] The interaction of coalescence and spreading leads to a permanent change of the implant surface and possibly prevents a predictable degradation of the pure peanut oil. In contrast, the solidified ISFOs are more resistant to mechanical strain. The higher the concentration of 12-HSA, the more stable the depots are and the more uniform and reproducible the implants' surface is. This leads to a more consistent degradation characteristic.

Moreover, the different degradation curves of peanut oil and ISFOs during the first month after injection are remarkable (Figure 29, p. 91). The degradation of peanut oil usually starts immediately, whereas all of the 18 ISFOs investigated show a lag time of about 3-4 weeks. One explanation for this phenomenon seems to be the irritative and cytotoxic effect of the solvent NMP (chapter 4.2.5, p. 68 ff.). NMP as well as degradation products of the ISFO might cause inflammation around the organogels and thus change some local physico-chemical properties, which consequently affect the lipase's activity. Immunological reactions or encapsulation phenomena by fibrosis are also possible, as they are often observed in connection with implants.[111,171,172] However, implant enveloping tissue layers have neither been noticed in the MR images nor *ex vivo*. In addition, the complete *in vivo* degradation of all ISFOs militates against a long-term encapsulation. It rather might be a local tissue irritation during the first weeks after injection, which has to be overcome in order to allow the implants' degradation. The different lag times *in vitro* caused by different concentrations of 12-HSA (Figure 26, p. 80) may be superimposed *in vivo* by this inflammation. Thus, the lag times of all the ISFOs have the same duration *in vivo*, although the concentrations of 12-HSA are different.

Figure 30 (p. 93) also shows that the *in vivo* degradation of the ISFOs did not proceed in layers from the surface, but only after fragmentation into smaller depots, which ultimately degrade. This observation confirms the results obtained by MRI (Figure 28, p. 86 ff.), but differs from the layer-by-layer degradation observed *in vitro* (chapter 4.2.6, p. 78 ff.). These different types of degradation (*i.e.* surface erosion and fragmentation) probably cause different implant degradation rates. In this context, the comparison with the *in vitro* degradation is of great interest (Figure 26, p. 80). By applying 0.01 U/mL of LPL, the *in vitro* degradation of the 5 % ISFO and the 7 % ISFO corresponds very well to the *in vivo* degradation (Figure 29, p. 91), but with a slightly shorter *in vitro* lag phase of the 5 % ISFO. However, the *in vivo* degradation of the 3 % ISFO does not match to any concentration of LPL tested *in vitro*. Due to the fundamentally divergent degradation types *in vitro* and *in vivo*, a reliable correlation is not feasible. In addition, it is not clear yet which process contributes more to the ISFOs' degradation. Both phagocytosis and subsequent lymphatic absorption as well as enzymatic degradation by lipases are conceivable. Therefore, *in vivo* release predictions can hardly be made on the basis of the *in vitro* results.

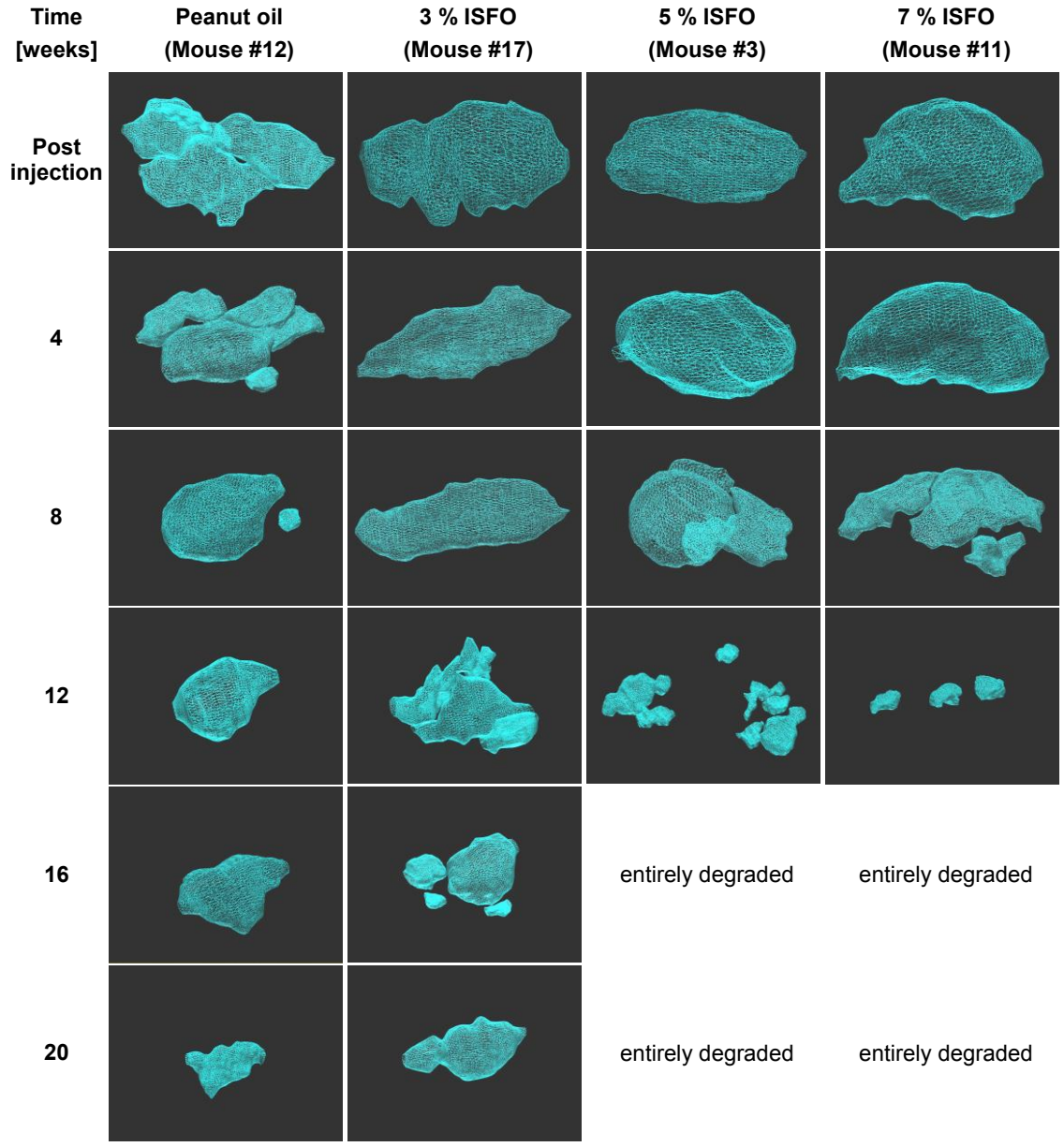

Figure 30 ***Exemplary 3D-projections of the degrading ISFOs and peanut oil (control) from Figure 29 (p. 91).***

4.3.2 RELEASE OF APIs

Testosterone enanthate and leuprolide acetate have been selected as model APIs with different physico-chemical properties in order to investigate the release characteristics of the ISFOs. Both of them are of great therapeutic relevance concerning a continuous release over periods of several weeks up to months. Testosterone is used against testosterone deficiency of diverse causes, which is an endocrinological problem in men.[175] Predominantly long-acting esters of testosterone (mostly enanthate) are

administered *s.c.* and *i.m.* due to their improved efficiency and lower toxicity compared to the oral therapy with testosterone.[175] Testosterone enanthate is characterized by its pronounced lipophilicity. Hence, this API occurs dissolved in oil-based depot formulations. Therefore, its primarily diffusion-controlled release is based on the distribution between the oil and the aqueous tissue fluid.[15,22,64] Testosterone enanthate is a prodrug and requires saponification of the ester to the pharmacologically active substance testosterone. Thus, a half-life extension after the release of the API is obtained.

Leuprolide acetate has been studied as an additional model API in a further experiment in order to induce down-regulation of the endogenous testosterone plasma level. It is primarily used against hormonal related disorders, including prostate and mammary cancer, endometriosis and precocious puberty.[176,177] Its nonapeptide structure makes it highly water-soluble and consequently, this API occurs in a particulate form inside of oily depot formulations (*i.e.* suspension). Thus, its release is theoretically hardly controlled by diffusion, but by the degradation of the oily gel depot. Since both APIs, testosterone enanthate and leuprolide acetate, affect the testosterone blood level, only one analytic test procedure is required to measure the release of testosterone enanthate and to correlate the leuprolide acetate release with the testosterone serum concentration.

Figure 31 (p. 95, left) shows the testosterone serum concentration of 66 untreated male SKH1-*Hr*^{hr} nude mice between 1-3 p.m. as box plot. Interestingly, the measured concentrations are not normally (Gaussian) distributed. Half of the values are between 0.1-1.2 ng/mL, while the other half is distributed between 1.2-24.6 ng/mL. Hence, the exponential distribution excludes the calculation of means and standard deviations. Instead, medians have been presented as location parameters and ranges as dispersion parameters. Figure 31 (p. 95, right) shows the testosterone serum concentration of 6 mice, which have been injected the API-free 5 % ISFO (placebo reference). As expected, large fluctuations of the physiological testosterone serum concentration are apparent. The median values of the measurements are distributed around the physiological median of 1.2 ng/mL, but with a large total fluctuation of 0.2 ng/mL (week 6) to 5.8 ng/mL (week 20). Obviously, the sample size of 6 mice is insufficient to characterize the population adequately. Therefore, the following release results of the APIs have to be regarded as a pilot study in order to provide information

on the release characteristics and to substantiate the ISFOs' potential as depot dosage forms.

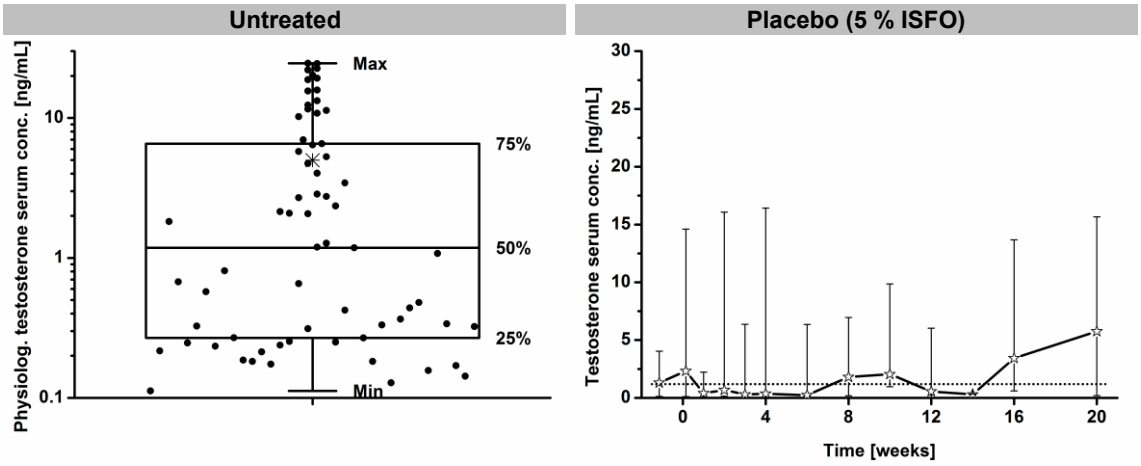

Figure 31 ***Left: Box-Plot diagram showing the physiological testosterone serum concentration of 66 untreated male SKH1-Hr^{hr} nude mice. The cross at 5.0 ng/mL indicates the mean. Right: Time-dependent testosterone serum concentration after s.c. injection of 150 µL of the 5 % ISFO without API (placebo reference). The dotted line indicates the physiological median testosterone serum concentration measured. Data represent medians ± ranges, n=6.***

RELEASE OF TESTOSTERONE ENANTATE

Figure 32 (p. 96) presents the testosterone serum concentration profiles of mice, which have been treated with testosterone enanthate containing ISFOs or peanut oil. At first glance, the curves of all the 4 formulations do not show a continuous and consistent release of the API. However, to assess the large deviations of testosterone serum concentration, the untreated mice should also be considered (Figure 31). Upon closer examination, the largely deviating concentrations of all 4 formulations on day 8 *before* injection strike out, although all these mice are still regarded as identical (*i.e.* untreated). In addition, the diffusion-controlled release of the API from the dimensionally unstable or shear sensitive depots (especially peanut oil and 3 % ISFO) raise expectations of large concentration fluctuations. Within 9 days, precisely, from day 8 before injection until day 1 after injection, the median of the peanut oil control (Figure 32, p. 96, top left) paradoxically decreases from 5.0 ng/mL to 2.3 ng/mL. The values then fluctuate around the physiological median of 1.2 ng/mL. However, the strong fluctuations hardly allow exact statements regarding release characteristics.

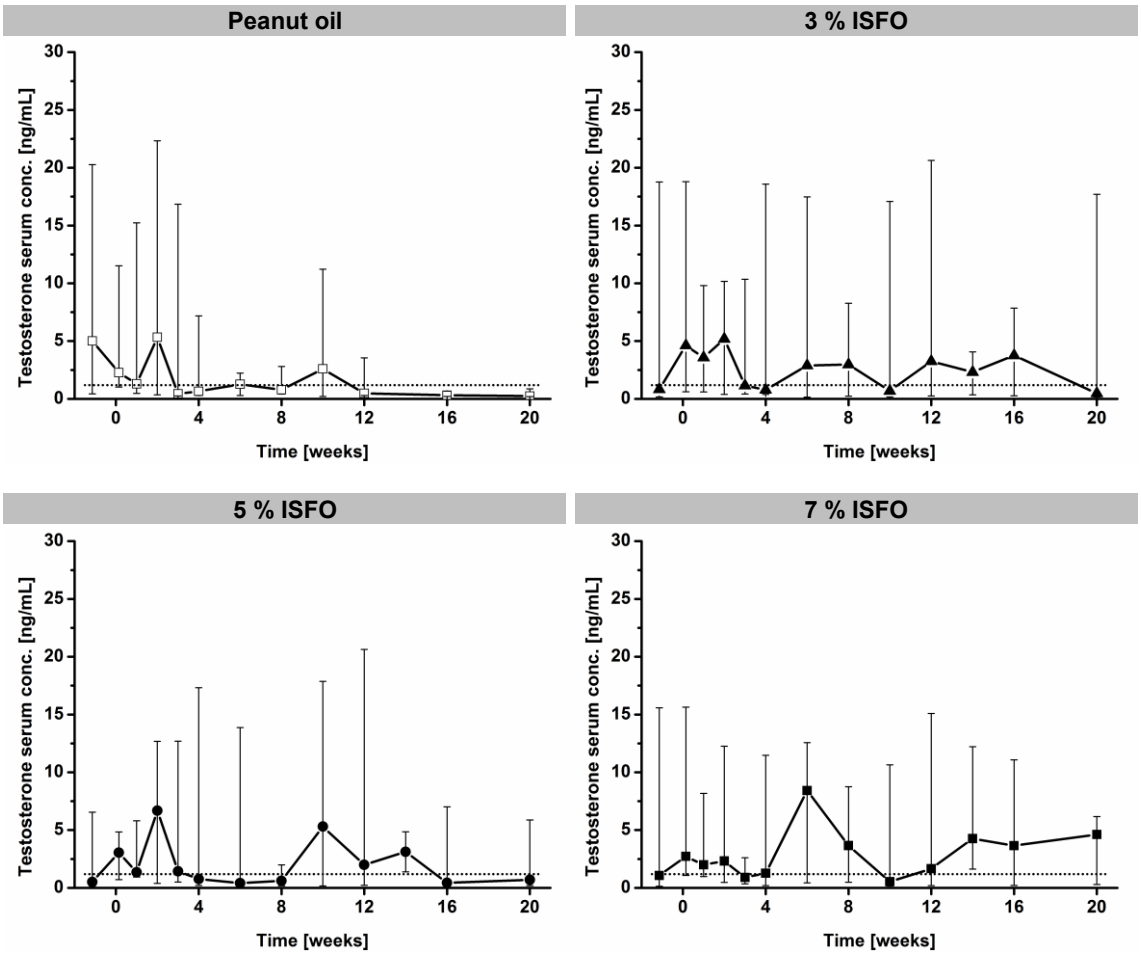

Figure 32 ***Time-dependent testosterone serum concentration in male SKH1-Hr^{hr} nude mice after s.c. injection of 150 µL of peanut oil (top left), 3 % ISFO (top right), 5 % ISFO (bottom left) and 7 % ISFO (bottom right), each containing a single dose of 17 mg/kg testosterone enanthate. The dotted lines indicate the physiological median testosterone serum concentration measured previously with 66 untreated mice. Data represent medians ± ranges, n=6.***

In contrast, all ISFOs show an increased testosterone serum concentration above the physiological value almost during the entire observation period. However, the number of animals is too low to make statistically reliable statements. A correlation of the release curves with the matrix degradation of the ultrasound experiments (Figure 29, p. 91) is also indiscernible, but this has not been expected concerning diffusion-controlled release processes. By applying the 7 % ISFO (Figure 32, bottom right), the testosterone serum concentration is still increased even after the 12th week, although this formulation has completely been degraded to this point in time in the ultrasound examinations. A note of caution is due here since the formation of a *second depot* is reported in the literature, especially with regard to poorly water-soluble APIs.[2]

Thereby, after the API is released from the dosage form, it can precipitate in the surrounding tissue or concentrate itself inside. Its release into the systemic circulation depends then on the solubility and the dissolution rate. In case of the ISFOs, the extraction of NMP causes an initial burst effect, whereby the implants are solidified. This effect could lead to the transport of a certain amount of dissolved API outside of the gel depot. While the NMP is mixed with aqueous tissue fluid, the lipophilic API may precipitate. Thus, distribution processes play a major role, which can hardly be simulated *in vitro*.

RELEASE OF LEUPROLIDE ACETATE

Testosterone and its active metabolite dihydrotestosterone constitute endogenous risk factors for the development of prostate cancer.[178] Their plasma levels are controlled by the functional unit of hypothalamus and pituitary. The pulsatile-released hypothalamic hormone GnRH (gonadotropin-releasing hormone) stimulates in males the release of the LH (luteinizing hormone) from the pituitary into the bloodstream. In the testes, LH stimulates, in turn, the production of testosterone.[179]

Leuprolide acetate is a synthetic GnRH analogue, which (apparently contradictory) leads to suppression of testosterone. After a transient increase of the testosterone serum concentration (flare-up phenomenon), the continuous administration of leuprolide acetate results in a chronic overstimulation of GnRH receptors and consequently a down-regulation of the LH levels followed by a suppression of the testicular steroid biosynthesis.[157] The initial increase of the testosterone level may take up to one week.[178] The reduction of testosterone levels in humans below the castration level (< 0.5 ng/mL) is achieved 2-5 weeks after starting the treatment.[157,179] For the treatment of hormone-dependent prostate cancer, GnRH analogs are the first choice medication for the metastatic phase. Available depot formulations have to be injected *s.c.* or *i.m.* every 4 weeks or in intervals of several months.[176]

Figure 33 (p. 98) presents the testosterone serum concentration profiles of mice, which have been treated with leuprolide acetate containing ISFOs and peanut oil. All 4 formulations initially showed the discussed flare-up phenomenon. On day 1 after injection, all mice had significantly increased testosterone serum concentrations higher than 17 ng/mL compared to day 8 prior to the injection. In the following course, the testosterone serum concentrations decreased due to the therapeutic effect of the API.

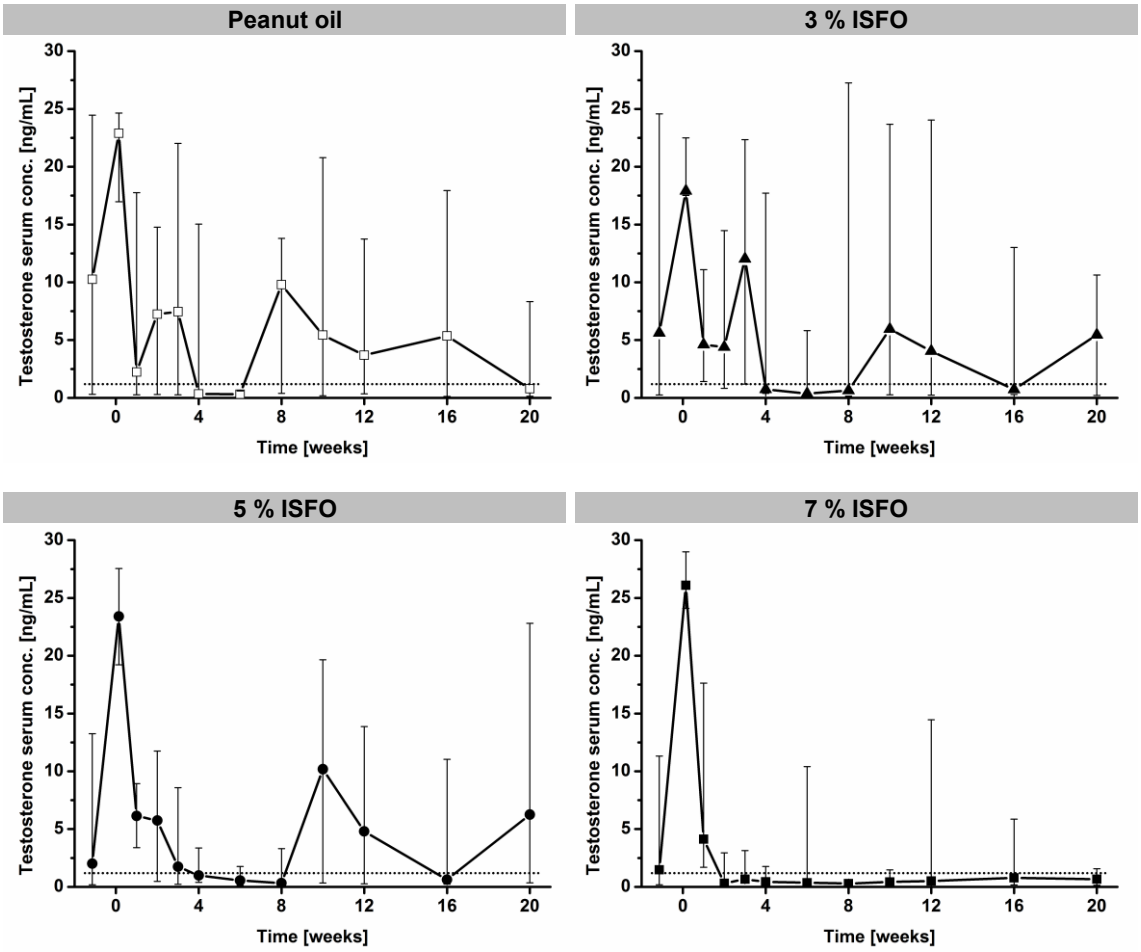

Figure 33 ***Time-dependent testosterone serum concentration in male SKH1-Hr^{hr} nude mice after s.c. injection of 150 µL of peanut oil (top left), 3 % ISFO (top right), 5 % ISFO (bottom left) and 7 % ISFO (bottom right), each containing a single dose of 50 mg/kg leuprolide acetate. The dotted lines indicate the physiological median testosterone serum concentration measured previously with 66 untreated mice. Data represent medians ± ranges, n=6.***

Interestingly, using pure peanut oil as matrix carrier (Figure 33, top left) results in a re-increase of the testosterone serum concentration in week 2 and 3. However, the fluctuations in total are very large. In week 4 and 5, the testosterone serum concentrations eventually fall below the physiological median value of 1.2 ng/mL. Not later than 8 weeks after injection, the leuprolide acetate effect on the testosterone serum concentration does not longer exist. To sum up, the physiological value has fallen below 1.2 ng/mL at least for 2 weeks (week 4-6) and maximally for 3 weeks (week 4-7) and thus achieving suppression of testosterone. As the investigations by MRI and USI already confirmed, once pure peanut oil is injected, it is subjected to a constant deformation due to its liquid state (chapter 4.3.1, p. 84 ff.). Thereby, also the

oil-insoluble leuprolide acetate particles are able to change their position continuously. After contact with the *s.c.* tissue fluid at the interface of the peanut oil, the particles are released by dissolution and delivered to the systemic circulation. Thus, the fluidity of peanut oil promotes the release of leuprolide acetate and restricts the duration of the effective period of this liquid formulation.[22,48]

As for the peanut oil, the suppression of testosterone starts after 4 weeks also for the 3 % ISFO (Figure 33, p. 98, top right) and for the 5 % ISFO (Figure 33, p. 98, bottom left). In order to interpret the release of leuprolide acetate from the ISFOs, a distinction between the release during the phase of *in situ* solidification and the release from the solidified implants has to be made. In the first phase, besides the immediate release of interfacial-related API particles an additional initial burst effect by the extraction of NMP occurs. Thus, an additional amount of leuprolide acetate is released, which is at least partially soluble in pure NMP. This process is proven by the USI results (Figure 29, p. 91), where all the ISFOs show a 4-week lag phase without degradation of the implant matrix. Thus, only the burst effect of the solvent and the initial release of peripheral API from the still liquid ISFOs may cause the flare-up phenomenon on day 1. Moreover, the implants' fragmentation during the first 4 weeks led to an accelerated release of API particles. Increasing the surface-to-volume ratio by dividing one large implant into a few smaller fragments consequently led to a larger proportion of peripheral API particles, which were available for the surface erosion-based release. In the second phase, the release of API from the solidified implants, the release is driven by simultaneous surface erosion and further fragmentation of the matrix carrier as it is clearly traceable by the MR images (Figure 28, p. 86 ff.). Thereby, undissolved particles of leuprolide acetate are released until the implant matrix material is entirely absorbed. Both the 3 % ISFO and the 5 % ISFO enable suppressions of testosterone for at least 4 weeks (week 4-8) and maximally for 5 weeks (week 4-9). The longer duration compared to pure peanut oil is based on the increased robustness of the implants' bodies, retarding the release of the API.

Testosterone serum concentrations resulting from the release of leuprolide acetate from the 7 % ISFO (Figure 33, p. 98, bottom right) significantly differ compared to both 3 % ISFO and 5 % ISFO. Firstly, the suppression of testosterone already starts after two weeks instead of four. Secondly, the testosterone serum concentration remains below the physiological median value of 1.2 ng/mL during the entire observation period of 20 weeks. However, interpreting this curve is just as difficult as the variations are still

high. Nevertheless, the high dimensional stability of this formulation (highest content of 12-HSA) obviously leads to a more controlled leuprolide acetate release compared to the 3 % ISFO and the 5 % ISFO. Falling below the castration level after approximately 14 days is also observed for polymer-based ISFIs.[176] Even with these formulations, the initial release of leuprolide acetate is due to the initial burst effect coming from the extraction of the organic solvent. By applying ISFMs, this effect can cause a 40 % *in vitro* release of API directly after injection, whereas the remaining 60 % were released within the following 45 days.[180] In this context it is also notable that once the GnRH receptors are down-regulated, only a minimum amount of leuprolide acetate is necessary to sustain the suppression.[181] However, leuprolide acetate causes no long-term effect. Once the API is entirely released, the testosterone serum concentration immediately starts to rise again.[82] Conversely and applicable for the 7 % ISFO, as long as the testosterone serum concentration is low, leuprolide acetate is released from the implant. However, it is not fully understood why the testosterone serum concentration is decreased over the entire observation period of 20 weeks, although the USI investigation showed a complete degradation of this implant already after 12 weeks (Figure 29, p. 91). Perhaps the NMP exposure induces a reversible aggregation of the API and hence delays the absorption. This assumption is supported by the two-chamber syringe packaging concept of the ISFI product Eligard. One syringe contains the NMP dissolved matrix polymer and the other one is filled with leuprolide acetate powder.[157] In order to reduce premature aggregation of the API, the content of both syringes is mixed by means of a connector directly prior to the injection.[41] On the other hand, studies show only about 15 % of aggregation of leuprolide acetate in NMP after 6 months.[182]

Generally, concerning release data of both, leuprolide acetate as well as testosterone enanthate, a convincing interpretation is difficult because of several factors. Besides the statistical variations (*i.e.* small sample sizes, serious variations of the physiological testosterone serum concentration), there are additional factors resulting from the formulations themselves:

- First of all, the change of the release mechanism based on the changing implant state from liquid to solid directly after injection (*in situ* solidification);
- In combination with the initial burst effect caused by the extraction of NMP there is the changing solubility of the APIs inside of the organogel matrix;

- Furthermore, the parallel occurrence of surface erosion and fragmentation as well as a certain degree of deformability of the implants, which make predictions concerning the release of APIs more ambivalent;
- In theory, it is also conceivable that the release of the APIs is temporarily influenced by local inflammatory reactions coming from degradation products of the implant carrier and/ or the exposition of NMP.

5 SUMMARY AND PERSPECTIVES

In the present work, organogel-based depot formulations were developed and tested *in vitro* and *in vivo* with respect to their suitability as parenteral drug delivery systems. During formulation development, the *in situ* gelling effect was of prime importance. The desired formulations should contain the gelling agent 12-HSA (12-Hydroxystearic acid), an oil, which acts as matrix lipid and a gelation inhibitor to prevent premature gelation between production and administration. Initially, various commercially available raw materials of 12-HSA were examined with regard to their purity and their gelling properties by means of HTPLC and texture analysis. Thereby, purified substances (analytical grade) had the advantage over products of technical quality. Among a variety of organic solvents, NMP (*N*-Methyl-2-pyrrolidone) proved to be an excellent gelation inhibitor. Besides a high solubility for 12-HSA, NMP showed a complete miscibility with both water and the tested oils. Thus, it enabled its economical use and the *in situ* solidification of the formulations inside of the subcutaneous tissue. In order to obtain solid and form-stable gel bodies, peanut oil afforded the lowest quantities of 12-HSA and NMP. These three components are already contained in medicinal products for use in humans and allowed the production of liquid dosage forms, which formed stable implants after injection into buffer and subsequent extraction of NMP (*in situ* solidification). The straightforward and heat-free preparation of the formulations compared to the complex production of microparticles or preformed solid implants is of particular importance. In contrast to aqueous formulations, isotonicity and pH adjustments can be neglected. Furthermore, polymer-based *in situ* forming implants (*e.g.* commercial product Eligard) require more than 50 % of NMP to receive injectable formulations, whereas less than 15 % of NMP is sufficient to fluidize the organogels. With regard to the known toxicity of NMP, this reduced amount of solvent can already be considered as a milestone. In addition, degradation reactions of polymeric substrates (mostly PLGA and derivatives) during manufacturing and storage are of no concern when using the LMOG (low molecular weight organogelator) 12-HSA.

Three selected formulations containing 3 %, 5 % and 7 % of 12-HSA were studied in detail *in vitro* for their physico-chemical properties. Measurements by texture analysis indicated an excellent and effortless injectability of the liquid formulations, even when using narrow, patient-friendly cannulas (27 Gauge). Compared to preformed solid implants (14-16 Gauge) and polymer-based *in situ* forming implants (18-20 Gauge), the ISFOs (*In Situ* Forming Organogels) showed a significantly lower viscosity and are,

therefore, easier and less painful to inject. Conductometric determinations after ejecting the formulations into buffer led to the complete extraction of NMP within 6-12 h, independent of the concentration of 12-HSA. Thereby, the gelling agent 12-HSA forms a 3D network penetrated by coherent peanut oil (bulk gel structure). NMP, which is dissolved in the oil, can freely diffuse through the meshes of the scaffold to the interface of the implant. This causal relation was also confirmed by EPR studies. After the extraction of NMP, the mobility of the spin probe dissolved in the oil was identical for all the implants and was independent of the concentration of 12-HSA. Thus, the probe can diffuse freely inside of the oil and is unaffected by the network of the 12-HSA. The bulk gel structure was also substantiated by relaxometric ^{1}H-NMR measurements. T_2 relaxation time of the gelled oil matched the relaxation time of free oil. Despite gelation, no interaction between 12-HSA and peanut oil occurred. Thus, the oil viscosity was unaffected by the solidification. Although the microviscosity of the oil between the meshes of the scaffold corresponds to the viscosity of pure liquid peanut oil, the solidified implants macroscopically still correspond to solid state bodies. The macroscopically clearly perceptible improvement of rigidity of the implants was quantified by rheological studies. The solid-state character, expressed as storage modulus, significantly increased with increasing concentrations of 12-HSA. However, already at a low deformation, the yield points of the implants were exceeded and rheodestruction occurred, whereby the 12-HSA network structure collapsed. On the one hand, this particular fluidity of the formulations may affect the *in vivo* release of the API. On the other hand, a certain degree of fluidity reduces the foreign body reaction and thus contributes to the implants' biocompatibility. Studies on cellular toxicity resulted in a complete compatibility of the solidified implants containing 12-HSA and peanut oil. However, NMP showed a concentration and exposure time-associated toxicity. Thus, the economical use of the solvent in the developed ISFOs is a decisive criterion for their potential as an alternative to the approved polymer-based *in situ* forming implants. Studies on *in vitro* degradation by the use of lipase showed a continuous and surface erosion-controlled degradation of the implants containing 5 % and 7 % of 12-HSA within 7 weeks after a one and four week lag phase, respectively.

Ultimately, the promising results of the *in vitro* degradation led to two implant degradation studies and two therapy studies *in vivo*. In general, all ISFOs were well-tolerated by all mice. Degradation investigations by MRI and USI showed a 4-week lag phase, probably caused by an NMP associated local tissue irritation. Subsequently,

continuous implant degradation occurred over 7 weeks. Parallel to surface erosion also fragmentation of larger implant bodies into several smaller was observed. In addition, by increasing the concentration of 12-HSA and based on the greater dimensional stability, the interindividual fluctuations of the degradation of the implants were significantly reduced. Finally, release studies of two model APIs delivered only a vague idea of the release profile, the duration of the lag phase and the completeness of the implant degradation due to high fluctuations of the physiological murine testosterone serum concentration. The release of testosterone enanthate from the implants was measurable, but the release period did not significantly elongate compared to pure peanut oil. Fortunately, by the use of leuprolide acetate in the implant containing 7 % of 12-HSA, a down-regulation of the endogenous teststosteron serum concentration could be achieved over 4 months. These promising results contribute substantially to a further development of this still largely unknown class of *in situ* forming organogels as parenteral depot dosage forms.

In the future, more API candidates and larger sample sizes should be considered and tested for their *in vivo* release characteristics. In particular, the initial lag phase observed should be analyzed by histological experiments and the assumptive connection to the solvent NMP should be demonstrated. In general, the lack of a consistent and recognized *in vitro* release method should lead to the establishment of valid testing procedures concerning *in situ* formulations. Furthermore, long-term tests for the stability of the formulations and the development of a suitable primary packaging are mandatory. Two-chamber syringes, for example, should be taken into consideration as they isolate and protect the API from the carrier during storage and guarantee the immediate homogenization of both of them prior to the administration.

REFERENCES

1 EDQM (ed.) (2016) Ph. Eur.: Parenteral Preparations (#0520), 8th edn.

2 J. C. Wright, D. J. Burgess (2012) Long acting injections and implants: Springer

3 C. E. Adams, M. K. P. Fenton, S. Quraishi, A. S. David (2001) Systematic meta-review of depot antipsychotic drugs for people with schizophrenia. The British Journal of Psychiatry 179(4), 290–299

4 S. Nema, J. D. Ludwig (2010) Pharmaceutical dosage forms., 3rd edn.: Informa Healthcare

5 D. J. Burgess, A. S. Hussain, T. S. Ingallinera, M.-L. Chen (2002) Assuring Quality and Performance of Sustained and Controlled Release Parenterals. Pharmaceutical Research 19(11), 1761–1768

6 S. S. Lee, P. Hughes, A. D. Ross, M. R. Robinson (2010) Biodegradable implants for sustained drug release in the eye. Pharmaceutical Research 27(10), 2043–2053

7 M. P. Do, C. Neut, H. Metz, E. Delcourt, K. Mäder, J. Siepmann, F. Siepmann (2015) In-situ forming composite implants for periodontitis treatment: How the formulation determines system performance. International Journal of Pharmaceutics 486(1-2), 38–51

8 M. P. Do, C. Neut, H. Metz, E. Delcourt, J. Siepmann, K. Mäder, F. Siepmann (2015) Mechanistic analysis of PLGA/HPMC-based in-situ forming implants for periodontitis treatment. European Journal of Pharmaceutics and Biopharmaceutics 94, 273–283

9 G. A. Brazeau, B. Cooper, K. A. Svetic, C. L. Smith, P. Gupta (1998) Current perspectives on pain upon injection of drugs. Journal of Pharmaceutical Sciences 87(6), 667–677

10 FDA (2004) Guidance for Industry: Sterile Drug Products Produced by Aseptic Processing - Current Good Manufacturing Practice

11 FDA (2006) Guidance for Industry: Quality Systems Approach to Pharmaceutical CGMP Regulations

12 FDA (2004) Guidance for Industry: PAT - A Framework for Innovative Pharmaceutical Development, Manufacturing, and Quality Assurance

13 FDA (2004) Pharmaceutical cGMPs for the 21th century - a risk-based approach: Final report

14 D. Hussong (2010) Sterile products: advances and challenges in formulation, manufacturing and regulatory aspects - a regulatory review perspective. AAPS PharmSciTech 11(3), 1482–1484

15 C. Larsen, S. W. Larsen, H. Jensen, A. Yaghmur, J. Østergaard (2009) Role of in vitro release models in formulation development and quality control of parenteral depots. Expert opinion on drug delivery 6(12), 1283–1295

16 J. T. Jastak, J. A. Yagiela (1983) Vasoconstrictors and Local Anesthesia: A Review and Rationale for Use. The Journal of the American Dental Association 107(4), 623–630

17 D. Butler (2005) Wartime tactic doubles power of scarce bird-flu drug. Nature 438(3), 6

18 D. A. Scott, A. M. Fisher (1935) The effect of zinc salts on the action of insulin. Journal of Pharmacology and Experimental Therapeutics 55(2), 206–221

19 M. W. Jann, L. Ereshefsky, S. R. Saklad (1985) Clinical pharmacokinetics of the depot antipsychotics. Clinical pharmacokinetics 10(4), 315–333

20 V. J. Stella, W. N. A. Charman, V. H. Naringrekar (1985) Prodrugs: Do They Have Advantages in Clinical Practice? Drugs 29(5), 455–473

21 Y. Shi, L. Li (2005) Current advances in sustained-release systems for parenteral drug delivery. Expert opinion on drug delivery 2(6), 1039–1058

22 A. Rutz (2007) Ölige Suspensionen als parenterale Depotsysteme für rekombinante Proteine

23 Y.-S. Rhee, C.-W. Park, P. P. DeLuca, H. M. Mansour (2010) Sustained-Release Injectable Drug Delivery: A review on the current status of long-acting injectables, including commercially marketed products. Pharmaceutical Technology 2010(6), 6–13

24 A. Göpferich (1996) Mechanisms of polymer degradation and erosion. The Biomaterials: Silver Jubilee Compendium, 117–128

25 F. Alexis (2005) Factors affecting the degradation and drug-release mechanism of poly(lactic acid) and poly[(lactic acid)-co-(glycolic acid)]. Polymer International 54(1), 36–46

26 K. Mäder, B. Bittner, Y. Li, W. Wohlauf, T. Kissel (1998) Monitoring Microviscosity and Microacidity of the Albumin Microenvironment Inside Degrading Microparticles from Poly(lactide-co-glycolide) (PLG) or ABA-triblock Polymers Containing

Hydrophobic Poly(lactide-co-glycolide) A Blocks and Hydrophilic Poly(ethyleneoxide) B Blocks. Pharmaceutical Research 15(6), 787–793

27 A. Schädlich, S. Kempe, K. Mäder (2014) Non-invasive in vivo characterization of microclimate pH inside in situ forming PLGA implants using multispectral fluorescence imaging. Journal of Controlled Release 179, 52–62

28 K. Mäder, B. Gallez, K. J. Liu, H. M.Swartz (1996) Non-invasive in vivo characterization of release processes in biodegradable polymers by low-frequency electron paramagnetic resonance spectroscopy. Biomaterials 17(4), 457–461

29 M. L. Houchin, E. M. Topp (2008) Chemical degradation of peptides and proteins in PLGA: a review of reactions and mechanisms. Journal of Pharmaceutical Sciences 97(7), 2395–2404

30 A. Brunner, K. Mäder, A. Göpferich (1999) pH and Osmotic Pressure Inside Biodegradable Microspheres During Erosion. Pharmaceutical Research 16(6), 847–853

31 T. Estey, J. Kang, S. P. Schwendeman, J. F. Carpenter (2006) BSA degradation under acidic conditions: a model for protein instability during release from PLGA delivery systems. Journal of Pharmaceutical Sciences 95(7), 1626–1639

32 S. Fredenberg, M. Wahlgren, M. Reslow, A. Axelsson (2011) The mechanisms of drug release in poly(lactic-co-glycolic acid)-based drug delivery systems - a review. International Journal of Pharmaceutics 415(1-2), 34–52

33 J. Siepmann, K. Elkharraz, F. Siepmann, D. Klose (2005) How autocatalysis accelerates drug release from PLGA-based microparticles: a quantitative treatment. Biomacromolecules 6(4), 2312–2319

34 R. Jalil, J. R. Nixon (1990) Biodegradable poly(lactic acid) and poly(lactide-co-glycolide) microcapsules: problems associated with preparative techniques and release properties. Journal of microencapsulation 7(3), 297–325

35 H. Kranz, R. Bodmeier (2008) Structure formation and characterization of injectable drug loaded biodegradable devices: In situ implants versus in situ microparticles. European Journal of Pharmaceutical Sciences 34(2-3), 164–172

36 Takeda (2012) Fachinformation: Enantone Monats-Depot 3,75 mg Retardmikrokapseln und Suspensionsmittel

37 MSD (2016) Fachinformation: Implanon NXT

38 Rote Liste. http://www.rote-liste.de/. Accessed 3 January 2017

39 Gelbe Liste. https://www.gelbe-liste.de/. Accessed 3 January 2017

40 O. Sartor (2003) Eligard: Leuprolide acetate in a novel sustained-release delivery system. Urology 61(2), 25–31

41 C. B. Packhaeuser, J. Schnieders, C. G. Oster, T. Kissel (2004) In situ forming parenteral drug delivery systems: an overview. European Journal of Pharmaceutics and Biopharmaceutics 58(2), 445–455

42 E. A. Yapar, Ö. İnal, Y. Özkan, T. Baykara (2012) Injectable In Situ Forming Microparticles: A Novel Drug Delivery System. Tropical Journal of Pharmaceutical Research 11(2), 307–318

43 R. R. S. Thakur, H. L. McMillan, D. S. Jones (2014) Solvent induced phase inversion-based in situ forming controlled release drug delivery implants. Journal of Controlled Release 176, 8–23

44 P. Agarwal, I. D. Rupenthal (2013) Injectable implants for the sustained release of protein and peptide drugs. Drug Discovery Today 18(7-8), 337–349

45 M. A. Royals, S. M. Fujita, G. L. Yewey, J. Rodriguez, P. C. Schultheiss, R. L. Dunn (1999) Biocompatibility of a biodegradable in situ forming implant system in rhesus monkeys. Journal of Biomedical Materials Research 45(3), 231–239

46 O. Sartor (2006) Eligard 6: A New Form of Treatment for Prostate Cancer. European Urology Supplements 5(18), 905–910

47 S. Kempe, K. Mäder (2012) In situ forming implants - an attractive formulation principle for parenteral depot formulations. Journal of Controlled Release 161(2), 668–679

48 H. Kranz, R. Bodmeier (2007) A novel in situ forming drug delivery system for controlled parenteral drug delivery. International Journal of Pharmaceutics 332(1-2), 107–114

49 A. Hatefi, B. Amsden (2002) Biodegradable injectable in situ forming drug delivery systems. Journal of Controlled Release 80, 9–28

50 W. Rungseevijitprapa, G. A. Brazeau, J. W. Simkins, R. Bodmeier (2008) Myotoxicity studies of O/W-in situ forming microparticle systems. European Journal of Pharmaceutics and Biopharmaceutics 69(1), 126–133

51 M. Körber (2007) In situ forming biodegradable microparticles for sustained parenteral delivery of protein drugs

52 S. J. Bae, M. K. Joo, Y. Jeong, S. W. Kim, W.-K. Lee, Y. S. Sohn, B. Jeong (2006) Gelation Behavior of Poly(ethylene glycol) and Polycaprolactone Triblock and Multiblock Copolymer Aqueous Solutions. Macromolecules 39(14), 4873–4879

53 F. A. Ismail, J. Napaporn, J. A. Hughes, G. A. Brazeau (2000) In situ gel formulations for gene delivery: release and myotoxicity studies. Pharmaceutical development and technology 5(3), 391–397

54 S. Kempe, H. Metz, P. G. C. Pereira, K. Mäder (2010) Non-invasive in vivo evaluation of in situ forming PLGA implants by benchtop magnetic resonance imaging (BT-MRI) and EPR spectroscopy. European Journal of Pharmaceutics and Biopharmaceutics 74(1), 102–108

55 R. Astaneh, M. Erfan, H. Moghimi, H. Mobedi (2009) Changes in morphology of in situ forming PLGA implant prepared by different polymer molecular weight and its effect on release behavior. Journal of Pharmaceutical Sciences 98(1), 135–145

56 E. Pamula, E. Menaszek (2008) In vitro and in vivo degradation of poly(L-lactide-co-glycolide) films and scaffolds. Journal of materials science. Materials in medicine 19(5), 2063–2070

57 Sanofi-Aventis (2009) Fachinformation: ELIGARD (leuprolide acetate for injectable suspension)

58 Y. W. Chien (1981) Long-acting parenteral drug formulations. Journal of parenteral science and technology 35(3), 106–139

59 H. A. E. Benson, R. J. Prankerd (1998) Optimisation of Drug Delivery 6. Modified-Release Parenterals. The Australian Journal of Hospital Pharmacy 28(2), 99–104

60 R. G. Strickley (2014) Solubilizing Excipients in Oral and Injectable Formulations. Pharmaceutical Research 21(2), 201–230

61 A. Schieber (2017) Ranzigkeit, Ranzigwerden. https://roempp.thieme.de/roempp4.0/do/data/RD-18-00268. Accessed 7 January 2017

62 J. Senior, M. Radomsky (2000) Sustained-Release Injectable Products: Interpharm Press

63 K. Hirano, T. Ichihashi, H. Yamada (1982) Studies on the absorption of practically water-insoluble drugs following injection V: Subcutaneous absorption in rats from solutions in water immiscible oils. Journal of Pharmaceutical Sciences 71(5), 495–500

64 S. W. Larsen, C. Larsen (2009) Critical Factors Influencing the In Vivo Performance of Long-acting Lipophilic Solutions - Impact on In Vitro Release Method Design. The AAPS Journal 11(4), 762–770

65 S. W. Larsen, A. E. Thomsen, E. Rinvar, G. J. Friis, C. Larsen (2001) Effect of drug lipophilicity on in vitro release rate from oil vehicles using nicotinic acid esters as model prodrug derivatives. International Journal of Pharmaceutics 216(1-2), 83–93

66 J. Zuidema, F. Kadir, H. A. C. Titulaer, C. Oussoren (1994) Release and absorption rates of intramuscularly and subcutaneously injected pharmaceuticals (II). International Journal of Pharmaceutics 105(3), 189–207

67 J. Rømsing, J. T. Jørgensen, M. Rasmussen, J. Sonnergaard, L. Vang, L. Musæus (1996) Pain assessment of subcutaneous injections. Annals of Pharmacotherapy 30, 729–732

68 Jenapharm (2015) Fachinformation: Nebido 100 mg Injektionslösung

69 J. Häseler, A. Behler (2017) Organogelatoren. https://roempp.thieme.de/roempp4.0/do/data/RD-15-01654. Accessed 3 January 2017

70 A. Vintiloiu, J.-C. Leroux (2008) Organogels and their use in drug delivery - A review. Journal of Controlled Release 125(3), 179–192

71 S. S. Sagiri, B. Behera, R. R. Rafanan, C. Bhattacharya, K. Pal, I. Banerjee, D. Rousseau (2013) Organogels as Matrices for Controlled Drug Delivery: A Review on the Current State. Soft Materials 12(1), 47–72

72 L. Lukyanova, S. Franceschi-Messant, P. Vicendo, E. Perez, I. Rico-Lattes, R. Weinkamer (2010) Preparation and evaluation of microporous organogel scaffolds for cell viability and proliferation. Colloids and Surfaces B: Biointerfaces 79(1), 105–112

73 T. A. Stortz, A. K. Zetzl, S. Barbut, A. Cattaruzza, A. G. Marangoni (2012) Edible oleogels in food products to help maximize health benefits and improve nutritional profiles. Lipid Technology 24(7), 151–154

74 M. A. Rogers, T. Strober, A. Bot, J. F. Toro-Vazquez, T. Stortz, A. G. Marangoni (2014) Edible oleogels in molecular gastronomy. International Journal of Gastronomy and Food Science 2(1), 22–31

75 S. Barbut, J. Wood, A. G. Marangoni (2016) Effects of Organogel Hardness and Formulation on Acceptance of Frankfurters. Journal of food science 81(9), C2183-C2188

76 Y. E. Shapiro (2011) Structure and dynamics of hydrogels and organogels: An NMR spectroscopy approach. Progress in Polymer Science 36(9), 1184–1253

77 D. J. Abdallah, R. G. Weiss (2000) Organogels and Low Molecular Mass Organic Gelators. Advanced Materials 12(17), 1237–1247

78 J. H. van Esch, B. L. Feringa (2000) New Functional Materials Based on Self-Assembling Organogels: From Serendipity towards Design. Angewandte Chemie International Edition 39(13), 2263–2266

79 S. Wu, J. Gao, T. J. Emge, M. A. Rogers (2013) Solvent-Induced Polymorphic Nanoscale Transitions for 12-Hydroxyoctadecanoic Acid Molecular Gels. Crystal Growth & Design 13(3), 1360–1366

80 J. Bonnet, G. Suissa, M. Raynal, L. Bouteiller (2015) Organogel formation rationalized by Hansen solubility parameters: influence of gelator structure. Soft Matter 11(11), 2308–2312

81 P. Terech, R. G. Weiss (1997) Low Molecular Mass Gelators of Organic Liquids and the Properties of Their Gels. Chemical Reviews 97(8), 3133–3159

82 F. Plourde, A. Motulsky, A.-C. Couffin-Hoarau, D. Hoarau, H. Ong, J.-C. Leroux (2005) First report on the efficacy of -alanine-based in situ-forming implants for the long-term parenteral delivery of drugs. Journal of Controlled Release 108(2-3), 433–441

83 A.-C. Couffin-Hoarau, A. Motulsky, P. Delmas, J.-C. Leroux (2004) In situ-Forming Pharmaceutical Organogels Based on the Self-Assembly of L-Alanine Derivatives. Pharmaceutical Research, 21(3), 454–457

84 A. Vintiloiu, M. Lafleur, G. Bastiat, J.-C. Leroux (2008) In Situ-Forming Oleogel Implant for Rivastigmine Delivery. Pharmaceutical Research 25(4), 845–852

85 H. Heydt (2016) 12-Hydroxystearinsäure. https://roempp.thieme.de/roempp4.0/do/data/RD-08-02523. Accessed 12 January 2016

86 V. A. Mallia, R. G. Weiss (2014) Self-assembled fibrillar networks and molecular gels employing 12-hydroxystearic acid and its isomers and derivatives. Journal of Physical Organic Chemistry 27(4), 310–315

87 E. Co, A. G. Marangoni (2013) The Formation of a 12-Hydroxystearic Acid/Vegetable Oil Organogel Under Shear and Thermal Fields. Journal of the American Oil Chemists' Society 90(4), 529–544

88 Y. Han, D. Shchukin, J. Yang, C. R. Simon, H. Fuchs, H. Möhwald (2010) Biocompatible Protein Nanocontainers for Controlled Drugs Release. ACS Nano 4(5), 2838–2844

89 E. Co, A. G. Marangoni (2012) Organogels: An Alternative Edible Oil-Structuring Method. Journal of the American Oil Chemists' Society 89(5), 749–780

90 K. Iwanaga, T. Sumizawa, M. Miyazaki, M. Kakemi (2010) Characterization of organogel as a novel oral controlled release formulation for lipophilic compounds. International Journal of Pharmaceutics 388(1-2), 123–128

91 L. Lukyanova, R. Castangia, S. Franceschi-Messant, E. Perez, I. Rico-Lattes (2008) Soft Microporous Green Materials from Natural Soybean Oil. ChemSusChem 1(6), 514–518

92 H. Takeno, M. Yanagita, Y. Motegi, S. Kondo (2015) Relationship between helical aggregates and polymorphs in a 12-hydroxystearic acid gel: their thermal stability and formation kinetics. Colloid and Polymer Science 293(1), 199–207

93 V. A. Mallia, M. George, D. L. Blair, R. G. Weiss (2009) Robust Organogels from Nitrogen-Containing Derivatives of (R)-12-Hydroxystearic Acid as Gelators: Comparisons with Gels from Stearic Acid Derivatives. Langmuir 25(15), 8615–8625

94 C. M. O'Sullivan, S. Barbut, A. G. Marangoni (2016) Edible oleogels for the oral delivery of lipid soluble molecules: Composition and structural design considerations. Trends in Food Science & Technology 57, 59–73

95 D. A. S. Grahame, C. Olauson, R. S. H. Lam, T. Pedersen, F. Borondics, S. Abraham, R. G. Weiss, M. A. Rogers (2011) Influence of chirality on the modes of self-assembly of 12-hydroxystearic acid in molecular gels of mineral oil. Soft Matter 7(16), 7359–7365

96 J.-L. Li, R.-Y. Wang, X.-Y. Liu, H.-H. Pan (2009) Nanoengineering of a Biocompatible Organogel by Thermal Processing. The Journal of Physical Chemistry B 113(15), 5011–5015

97 S. Abraham, Y. Lan, R. S. H. Lam, D. A. S. Grahame, J. J. H. Kim, R. G. Weiss, M. A. Rogers (2012) Influence of Positional Isomers on the Macroscale and Nanoscale Architectures of Aggregates of Racemic Hydroxyoctadecanoic Acids in Their Molecular Gel, Dispersion, and Solid States. Langmuir 28(11), 4955–4964

98 L. S. K. Dassanayake, D. R. Kodali, S. Ueno (2011) Formation of oleogels based on edible lipid materials. Current Opinion in Colloid & Interface Science 16(5), 432–439

99 M. Burkhardt, S. Kinzel, M. Gradzielski (2009) Macroscopic properties and microstructure of HSA based organogels: sensitivity to polar additives. Journal of colloid and interface science 331(2), 514–521

100 M. A. Rogers, A. J. Wright, A. G. Marangoni (2009) Nanostructuring fiber morphology and solvent inclusions in 12-hydroxystearic acid / canola oil organogels. Current Opinion in Colloid & Interface Science 14(1), 33–42

101 T. Tamuraa, T. Suetake, T. Ohkubo, K. Ohbu (1994) Effect of alkali metal ions on gel formation in the 12-hydroxystearic acid/soybean oil system. Journal of the American Oil Chemists' Society 71(8), 857–861

102 X. Yu, L. Chen, M. Zhanga, T. Yi (2014) Low-molecular-mass gels responding to ultrasound and mechanical stress: towards self-healing materials. Chemical Society reviews 43(15), 5346–5371

103 O. T. Bloom (1925) Machine for testing jelly strength of glues, gelatins, and the like-(US1540979)

104 J. H. Hudson, S. E. Sheppard (1929) A Contribution to the Preparation of Standard Gelatin. Journal of the Franklin Institute 207(5), 699

105 J. Kutza (2014) Oleogele auf 12-Hydroxystearinsaeurebasis als injizierbare Implantate zur kontrollierten Proteinfreisetzung

106 U. Massing, S. Cicko, V. Ziroli (2008) Dual asymmetric centrifugation (DAC) - A new technique for liposome preparation. Journal of Controlled Release 125(1), 16–24

107 N. M. Atherton (1993) Principles of electron spin resonance: PTR Prentice Hall

108 J. A. Weil, J. R. Bolton (2007) Electron paramagnetic resonance: Elementary theory and practical applications, 2nd edn.: Wiley-Interscience

109 W. Gordy (1980) Theory and applications of electron spin resonance: Wiley

110 S. S. Eaton, G. R. Eaton (2012) Electron Paramagnetic Resonance Spectroscopy, in: E. N. Kaufmann (ed.) Characterization of materials, 2nd edn.: Wiley

111 S. Kempe (2012) Non-invasive characterization of in situ forming implants

112 V. V. Khramtsov, I. A. Grigor'ev, M. A. Foster, D. J. Lurie, I. Nicholson (2000) Biological applications of spin pH probes. Cellular and molecular biology 46(8), 1361–1374

113 N. Khan, B. B. Williams, H. Hou, H. Li, H. M. Swartz (2007) Repetitive tissue pO2 measurements by electron paramagnetic resonance oximetry: current status and

future potential for experimental and clinical studies. Antioxidants & redox signaling 9(8), 1169–1182

114 D. J. Lurie, K. Mäder (2005) Monitoring drug delivery processes by EPR and related techniques - principles and applications. Advanced drug delivery reviews 57(8), 1171–1190

115 S. Kempe, H. Metz, K. Mäder (2010) Application of electron paramagnetic resonance (EPR) spectroscopy and imaging in drug delivery research - chances and challenges. European Journal of Pharmaceutics and Biopharmaceutics 74(1), 55–66

116 I. Katzhendler, K. Mäder, M. Friedmann (1999) Correlation between drug release kinetics from proteineous matrix and matrix structure: EPR and NMR study. Journal of Pharmaceutical Sciences 89(3), 365–381

117 R. Kimmich (1997) NMR - Tomography, Diffusometry, Relaxometry: Springer

118 A. Abragam (1983) The principles of nuclear magnetism: Oxford University Press

119 J. C. Richardson, R. W. Bowtell, K. Mäder, C. D. Melia (2005) Pharmaceutical applications of magnetic resonance imaging (MRI). Advanced drug delivery reviews 57(8), 1191–1209

120 M. Rudin, N. Beckmann, R. Porszasz, T. Reese, D. Bochelen, A. Sauter (1999) In vivo magnetic resonance methods in pharmaceutical research: current status and perspectives. NMR in biomedicine 12(2), 69–97

121 H. Metz, K. Mäder (2008) Benchtop-NMR and MRI - a new analytical tool in drug delivery research. International Journal of Pharmaceutics 364(2), 170–175

122 M. Bastrop (2010) Physico-chemical characterization of a novel class of bolaamphiphilic hydrogelators

123 R. Winter, F. Noll, C. Czeslik (2011) Methoden der biophysikalischen Chemie, 2nd edn.: Vieweg + Teubner

124 Ausschuss für Tierschutzbeauftragte in der GV-SOLAS und Arbeitskreis 4 in der TVT (2009) Empfehlung zur Blutentnahme bei Versuchstieren, insbesondere kleinen Versuchstieren

125 Demeditec Diagnostics (2013) User´s Manual: Testosterone rat/mouse ELISA

126 O. Dössel (2000) Bildgebende Verfahren in der Medizin: Von der Technik zur medizinischen Anwendung: Springer

127 H. Morneburg (1995) Bildgebende Systeme für die medizinische Diagnostik: Röntgendiagnostik und Angiographie, Computertomographie, Nuklearmedizin,

Magnetresonanztomographie, Sonographie, Integrierte Informationssysteme, 3rd edn.: Publicis MCD Verlag

128 F. W. Kremkau, F. Forsberg (2011) Sonography principles and instruments, 8th edn.: Elsevier/Saunders

129 D. Rallan, C. C. Harland (2003) Ultrasound in dermatology - basic principles and applications. Clinical and Experimental Dermatology 28(6), 632–638

130 C. R. Hill, J. C. Bamber, G. R. ter Haar (ed.) (2004) Physical principles of medical ultrasonics, 2nd edn.: John Wiley & Sons

131 L. S. Karfeld-Sulzer, C. Ghayor, B. Siegenthaler, M. de Wild, J.-C. Leroux, F. E. Weber (2015) N-methyl pyrrolidone/bone morphogenetic protein-2 double delivery with in situ forming implants. Journal of Controlled Release 203, 181–188

132 M. Bockisch (1993) Nahrungsfette und -öle: Eugen Ulmer

133 Jenapharm (2013) Gebrauchsinformation: Testosteron-Depot Jenapharm 250 mg/1 ml Injektionslösung

134 Deutsche Lebensmittelbuch-Kommission (2011) Neufassung der Leitsätze für Speisefette und Speiseöle

135 H. Kranz, G. A. Brazeau, J. Napaporn, R. L. Martin, W. Millard, R. Bodmeier (2001) Myotoxicity studies of injectable biodegradable in-situ forming drug delivery systems. International Journal of Pharmaceutics 212, 11–18

136 D. Swern, R. Wieder, M. McDonough, D. R. Meranze, M. B. Shimkin (1970) Investigation of Fatty Acids and Derivatives for Carcinogenic Activity. Cancer Research 30, 1037–1046

137 P. Schreier, R. Carle, M. Gänzle (2016) Fettraffination. https://roempp.thieme.de/roempp4.0/do/data/RD-06-00652. Accessed 4 February 2016

138 Deutsche Pharmazeutische Gesellschaft e.V. (2015) Pharmakon - Arzneimittel in Wissenschaft und Praxis: Allergie 3(2)

139 W. Rungseevijitprapaa, R. Bodmeier (2009) Injectability of biodegradable in situ forming microparticle systems (ISM). European Journal of Pharmaceutical Sciences 36(4-5), 524–531

140 S. Nippe (2014) Injectable drug delivery systems for steroids

141 B. Braun Melsungen (2013) Produktbrochüre: Präzision in der Injektion - Sicherheit in der Applikation

142 K. Mäder, U. Weidenauer (2010) Innovative Arzneiformen: Ein Lehrbuch für Studium und Praxis: Wiss. Verl.-Ges

143 A. Rübe (2006) Development and physico-chemical characterization of nanocapsules

144 S. Kempe, B. Schreier, S. Ruhs, I. Wollert, M. B. Teixeira, M. Gekle, K. Mäder (2013) Development and Noninvasive Characterization of Hormone Releasing In Situ Forming Implants. Macromolecular Symposia 334(1), 98–105

145 K. Schoenhammer, H. Petersen, F. Guethlein, A. Göpferich (2009) Poly(ethyleneglycol) 500 dimethylether as novel solvent for injectable in situ forming depots. Pharmaceutical Research 26(12), 2568–2577

146 EDQM (ed.) (2016) Ph. Eur.: Topical semi-solid preparations (#0132), 8th edn.

147 G. Schramm (2004) Einführung in Rheologie und Rheometrie, 2nd edn.: Thermo Fisher Scientific

148 P. Skehan, R. Storeng, D. Scudiero, A. Monks, J. McMahon, D. Vistica, J. T. Warren, H. Bokesch, S. Kenney, M. R. Boyd (1990) New Colorimetric Cytotoxicity Assay for Anticancer-Drug Screening. Journal of the National Cancer Institute 82(13), 1107–1112

149 V. Vichai, K. Kirtikara (2006) Sulforhodamine B colorimetric assay for cytotoxicity screening. Nature protocols 1(3), 1112–1116

150 BASF (2012) Technical Information: Kolliphor HS 15

151 BASF (2011) Technical Information: Kolliphor RH 40

152 A. Jouyban, M. A. A. Fakhree, A. Shayanfar (2010) Review of Pharmaceutical Applications of N-Methyl-2-Pyrrolidone. Journal of Pharmaceutical Sciences 13(4), 524–535

153 G. Schliecker (2003) Biodegradable polyesters for veterinary drug delivery systems Characterization, in vitro degradation and release behavior of Oligolactides and Polytartrate

154 A. Motulsky, M. Lafleur, A.-C. Couffin-Hoarau, D. Hoarau, F. Boury, J.-P. Benoit, J.-C. Leroux (2005) Characterization and biocompatibility of organogels based on l-alanine for parenteral drug delivery implants. Biomaterials 26(31), 6242–6253

155 J. P. Moreau, P. J. Vachon, M. C. Huneau (2001) Elevated glycemia and local inflammation after injecting N-methyl-2-pyrrolidone (NMP) into the marginal ear vein of rabbits. Contemporary topics in laboratory animal science 40(1), 38–40

156 J.-P. Payan (2002) Toxicokinetics and Metabolism of N-[14C]Methylpyrrolidone in Male Sprague-Dawley Rats. A Saturable NMP Elimination Process. Drug Metabolism and Disposition 30(12), 1418–1424

157 Astellas (2011) Fachinformation: ELIGARD 45 mg Pulver und Lösungsmittel zur Herstellung einer Injektionslösung

158 T. Mosmann (1983) Rapid colorimetric assay for cellular growth and survival: Application to proliferation and cytotoxicity assays. Journal of Immunological Methods 65(1-2), 55–63

159 R. S. Twigg (1945) Oxidation-Reduction Aspects of Resazurin. Nature 155, 401–402

160 K. L. Pesch, U. Simmert (1929) Combined assays for lactose and galactose by enzymatic reactions. Milchw. Forsch. 8, 551

161 M. Schwab, G. Sax, S. Schulze, G. Winter (2009) Studies on the lipase induced degradation of lipid based drug delivery systems. Journal of Controlled Release 140(1), 27–33

162 H. Wang, R. H. Eckel (2012) Lipoprotein Lipase in the Brain and Nervous System. Annual Review of Nutrition 32(1), 147–160

163 M.-H. Dufresne, E. Marouf, Y. Kränzlin, M. A. Gauthier, J.-C. Leroux (2012) Lipase Is Essential for the Study of in Vitro Release Kinetics from Organogels. Molecular Pharmaceutics 9(6), 1803–1811

164 K. Saulich (2008) Reaktionskinetische Experimente zur Lipase-katalysierten Hydrolyse von Rapsöl in Wasser-in-Öl-Emulsionen

165 M. Schwab, C. M. McGoverin, K. C. Gordon, G. Winter, T. Rades, J. Myschik, C. J. Strachan (2013) Studies on the lipase-induced degradation of lipid-based drug delivery systems. Part II – Investigations on the mechanisms leading to collapse of the lipid structure. European Journal of Pharmaceutics and Biopharmaceutics 84(3), 456–463

166 T. Kolter, B. Weinhold (2016) Lipoprotein-Lipase. https://roempp.thieme.de/roempp4.0/do/data/RD-12-01292. Accessed 14 March 2016

167 C. Delplace, F. Kreye, D. Klose, F. Danède, M. Descamps, J. Siepmann, F. Siepmann (2012) Impact of the experimental conditions on drug release from parenteral depot systems: From negligible to significant. International Journal of Pharmaceutics 432(1-2), 11–22

168 K. Wang, Q. Jia, F. Han, H. Liu, S. Li (2010) Self-assembled L-alanine derivative organogel as in situ drug delivery implant: characterization, biodegradability, and biocompatibility. Drug Development and Industrial Pharmacy 36(12), 1511–1521

169 R. W. Brown,Y.-C. N. Cheng, E. M. Haacke, M. R. Thompson, R. Venkatesan (2014) Magnetic Resonance Imaging: Physical Properties and Sequence Design, 2nd edn.: Wiley

170 D. Weishaupt, V. D. Köchli, B. Marincek (2014) Wie funktioniert MRI?: Eine Einführung in Physik und Funktionsweise der Magnetresonanzbildgebung, 7th edn.: Springer

171 V. Weiss (2014) Parenteral drug delivery systems based on fatty acid modified poly(glycerol adipate)

172 G. Sax, B. Kessler, E. Wolf, G. Winter (2012) In-vivo biodegradation of extruded lipid implants in rabbits. Journal of Controlled Release 163(2), 195–202

173 R. B. Patel, L. Solorio, H. Wu, T. Krupka, A. A. Exner (2010) Effect of injection site on in situ implant formation and drug release in vivo. Journal of Controlled Release 147(3), 350–358

174 L. Solorio, B. M. Babin, R. B. Patel, J. Mach, N. Azar, A. A. Exner (2010) Noninvasive characterization of in situ forming implants using diagnostic ultrasound. Journal of Controlled Release 143(2), 183–190

175 P. J. Snyder, D. A. Lawrence (1980) Treatment of Male Hypogonadism with Testosterone Enanthate. Journal of Clinical Endocrinology and Metabolism 51(6), 1335–1339

176 H. B. Ravivarapu, K. L. Moyer, R. L. Dunn (2000) Sustained activity and release of leuprolide acetate from an in situ forming polymeric implant. AAPS PharmSciTech 1(1), 1–8

177 G. L. Plosker, R. N. Brogden (2012) Leuprorelin. A Review of its Pharmacology and Therapeutic Use in Prostatic Cancer, Endometriosis and Other Sex Hormone-Related Disorders. Drugs 48(6), 930–967

178 G. Heyn (2016) Prostatakarzinom. Neue Therapien für Männer. Pharmazeutische Zeitung 161(13), 20–25

179 Takeda (2012) Fachinformation: Sixantone 30 mg Retardmikrokapseln und Suspensionsmittel

180 X. Luan, R. Bodmeier (2006) In situ forming microparticle system for controlled delivery of leuprolide acetate: Influence of the formulation and processing parameters. European Journal of Pharmaceutical Sciences 27(2-3), 143–149

181 U. W. Tunn, U. Bargelloni, S. Cosciani, G. Fiaccavento, S. Guazzieri, F. Pagano (1998) Comparison of LH-RH Analogue 1-Month Depot and 3-Month Depot by Their Hormone Levels and Pharmacokinetic Profile in Patients with Advanced Prostate Cancer. Urologia Internationalis 60(1), 9–17

182 W. Y. Dong, M. Körber, V. López Esguerra, R. Bodmeier (2006) Stability of poly(d,l-lactide-co-glycolide) and leuprolide acetate in in-situ forming drug delivery systems. Journal of Controlled Release 115(2), 158–167

DEUTSCHE ZUSAMMENFASSUNG

In der vorliegenden Arbeit wurden Organogel-basierte Depotformulierungen entwickelt und sowohl *in vitro* als auch *in vivo* hinsichtlich ihrer Eignung als parenterale Arzneiträgersysteme untersucht. Bei der Rezepturentwicklung stand der *in situ*-gelierende Effekt im Vordergrund. Die gesuchten Formulierungen sollten folgende Bestandteile enthalten: den Gelbildner 12-HSA (12-Hydroxystearinsäure), ein Öl, welches als Matrixlipid fungiert sowie einen Gelierungs-Hemmer zur Verhinderung der vorzeitigen Gelierung zwischen Herstellung und Verabreichung. Anfänglich wurden mittels HTPLC und Texturanalyse verschiedene kommerziell erhältliche 12-HSA-Ausgangsstoffe auf ihre Reinheit und ihr Gelbildungsvermögen hin untersucht. Dabei stellten sich die aufgereinigten Produkte (analytical grade) als vorteilhafter gegenüber den Produkten technischer Qualität dar. Unter einer Vielzahl organischer Lösungsmittel erwies sich NMP (*N*-Methyl-2-pyrrolidon) als ausgezeichneter Gelierungs-Hemmer. Es besitzt ein hohes Lösungsvermögen für 12-HSA und ist sowohl mit den getesteten Ölen als auch mit Wasser vollständig mischbar. Somit ermöglichte es eine sparsame Verwendung sowie die *in situ*-Verfestigung der Formulierungen im subkutanen Gewebe. Zur Herstellung fester Gelkörper erlaubte Erdnussöl als Matrixöl den geringsten Bedarf an 12-HSA und NMP. Mit diesen drei Rezepturbestandteilen, welche allesamt in bereits zugelassenen Human-Arzneimitteln vorkommen, ließen sich flüssige Zubereitungen herstellen, die nach Ausspritzen in Puffer und der darauffolgenden NMP-Extraktion formstabile Implantate bildeten (*in situ* Verfestigung). Hervorzuheben ist vor allem die unkomplizierte und hitzefreie Herstellung der Formulierungen verglichen mit den apparativ- und prozesstechnisch aufwändigen Methoden zur Herstellung von Mikropartikeln und vorgeformten festen Implantaten. Gegenüber allen wässrigen Zubereitungen kann zudem auf die Anpassung von Isotonie und pH-Wert verzichtet werden. Im Vergleich zu polymer-basierten ISFIs (*In Situ* Forming Implants; z.B. Handelsprodukt Eligard), bei dem über 50 % NMP zur Herstellung einer injizierbaren Formulierung notwendig sind, genügten weniger als 15 % NMP, um die entwickelten Organogele zu fluidisieren. Im Hinblick auf die bekannte NMP-Toxizität kann dies bereits als Erfolg angesehen werden. Zudem spielen Abbaureaktionen polymerer Trägermaterialien (meist PLGA und Derivate) während der Herstellung und Lagerung der Zubereitungen bei Verwendung von 12-HSA als LMOG (low molecular weight organogelator) keine Rolle.

Drei ausgewählte Zubereitungen mit einem 12-HSA-Gehalt von 3 %, 5 % und 7 % wurden *in vitro* ausführlich auf ihre physiko-chemischen Eigenschaften hin untersucht. Messungen mittels Texturanalyse zeigten, dass sich die flüssigen Formulierungen bei Verwendung schmaler, patientenfreundlicher Kanülen (27 Gauge) mit äußerst geringem Kraftaufwand applizieren lassen. Verglichen mit vorgeformten festen Implantaten (14-16 Gauge) und polymer-basierten ISFIs (18-20 Gauge) zeigten die ISFOs (*In Situ* Forming Organogels) eine deutlich geringere Viskosität und sind somit leichter sowie schmerzärmer injizierbar. Konduktometrische Bestimmungen nach Ausspritzen der Zubereitungen in Puffer ergaben eine vollständige NMP-Extraktion innerhalb von 6-12 h, unabhängig von der verwendeten 12-HSA-Konzentration. Dies lässt den Schluss auf eine Bulkgel-Struktur zu, wobei der Gelbildner 12-HSA ein dreidimensionales Gerüst bildet, welches von frei beweglichem Erdnussöl penetriert wird (Bikohärenz). Das im Öl gelöste NMP kann ungehindert durch die Gerüstmaschen zur Grenzfläche der Implantate diffundieren. Dies bestätigten auch EPR-Untersuchungen. Nach der NMP-Extraktion war die Mobilität der im Öl gelösten Spinsonde in allen Implantaten, trotz unterschiedlicher 12-HSA-Konzentration, identisch. Demnach kann die Sonde innerhalb des Öls frei diffundieren und wird dabei nicht durch das Gelbildnergerüst behindert. Das Vorliegen dieser Bulkgelstruktur wurde zudem durch relaxometrische ^{1}H-NMR-Bestimmungen untermauert. Die T_2-Relaxationszeiten der gelierten Öle entsprachen der von reinem Öl. Trotz Gelierung findet demnach zwischen 12-HSA und Erdnussöl keine Wechselwirkung statt, durch welche die Viskosität des Öls beeinflusst wird. Während die Mikroviskosität des Öls im Gel (d.h. zwischen den Gerüstmaschen) mit der von reinem Erdnussöl identisch war, entsprachen die Implantate makroskopisch trotzdem Festkörpern. Die makroskopisch deutlich wahrnehmbare Festigkeitserhöhung der Implantate mit steigender 12-HSA-Konzentration wurde mittels rheologischer Untersuchungen, bei denen der Gesamtverbund aus 12-HSA und Erdnussöl untersucht wird, beziffert. Die Festkörpereigenschaft, ausgedrückt als Speichermodul, nahm mit steigender 12-HSA-Konzentration deutlich zu. Jedoch zeigte sich auch, dass schon bei geringer Deformation die Fließgrenze der Systeme überschritten wird und Rheodestruktion einsetzt, wodurch das 12-HSA-Gerüst aufgebrochen wird. Diese gewisse Fluidität der Formulierungen mag einerseits die Arzneistofffreisetzung *in vivo* beeinflussen, andererseits aber auch zur Verträglichkeit beitragen indem sie das Fremdkörpergefühl verringert. Untersuchungen zur Zelltoxizität ergaben eine vollständige Verträglichkeit

der aus 12-HSA und Erdnussöl bestehenden verfestigten Implantate. Jedoch weist NMP eine konzentrations- und auch Expositionszeit-assoziierte Zelltoxizität auf. Somit ist die sparsame Verwendung des Lösungsmittels in den entwickelten ISFOs ein wichtiges Kriterium für deren Potential als Alternative zu den bislang einzigen zugelassenen ISFIs auf Polymer-Basis. Untersuchungen zum *in vitro*-Abbau mittels Lipase zeigten bei Verwendung von 5 % und 7 % 12-HSA nach ein- bzw. vierwöchiger lag-Phase einen kontinuierlichen und oberflächenerosions-gesteuerten Abbau der Implantate innerhalb von 7 Wochen.

Die vielversprechenden Ergebnisse zum *in vitro*-Abbau mündeten schließlich in zwei Abbau- und zwei Therapiestudien *in vivo*. Generell wurden die Formulierungen sehr gut von allen Mäusen vertragen. Wie die Untersuchungen zum Abbauverhalten mittels MRI und USI eindrucksvoll zeigten, gab es auch *in vivo* eine 4-wöchige lag-Phase, vermutlich verursacht durch lokale NMP-Gewebsreizungen, gefolgt von einem 7-wöchigen kontinuierlichen Implantatabbau. Parallel zur Oberflächenerosion fand interessanterweise auch eine Zerteilung großer Implantatkörper in mehrere kleine statt. Zudem nehmen aufgrund der besseren Formstabilität mit steigender 12-HSA-Konzentration die interindividuellen Schwankungen beim Abbau deutlich ab. Abschließende Freisetzungsuntersuchungen zweier Modellarzneistoffe lieferten aufgrund hoher Schwankungen nur eine vage Vorstellung über Freisetzungszeitraum, lag-Phase und die Vollständigkeit des Abbaus. Während bei Verwendung von Testosteronenanthat eine messbare, aber nicht signifikante Verlängerung der Freisetzung aus den entwickelten ISFOs im Vergleich zu reinem Erdnussöl sichtbar war, konnte durch Verwendung von Leuprorelinacetat in der Formulierung mit 7 % 12-HSA eine Downregulierung der endogenen Teststosteron-Serumkonzentration über 4 Monate erzielt werden. Diese aussichtsreichen Resultate liefern einen wichtigen Beitrag zur weiteren Entwicklung dieser noch weitgehend unbekannten Klasse der *In Situ* Forming Organogels als parenterale Depotarzneiformen.

Zukünftig sollten weitere Arzneistoffe auf ihr *in vivo*-Freisetzungsverhalten untersucht und dabei größere Fallzahlen herangezogen werden. Insbesondere die beobachtete initiale lag-Phase sollte mit histologischen Experimenten analysiert und der vermutete Zusammenhang mit dem Lösungsmittel NMP hergestellt werden. Das Fehlen einer einheitlichen und anerkannten *in vitro*-Freisetzungsmethode sollte zur Etablierung einer validen Untersuchungsmethode führen. Obligatorisch sind zudem Langzeittests zur

Stabilität der Formulierungen sowie die Entwicklung einer geeigneten Primärverpackung, bei der z.B. in Form einer Zweikammerspritze der Arzneistoff getrennt von der Formulierung aufbewahrt und somit vor ungewünschten Einflüssen z.B. durch NMP geschützt ist.

DANKSAGUNG

Mein Dank gilt jedem, der mich bei der Entstehung dieser Arbeit unterstützt hat.

Allen voran danke ich meinem Doktorvater und Betreuer Prof. Dr. Karsten Mäder für das mir stets entgegegebrachte Vertrauen, die immerwährende Unterstützung bei der Durchführung und Erstellung dieser Arbeit sowie für seine unkomplizierte Art, welche oft einen reibungslosen Verlauf der Dinge ermöglichte.

Zudem danke ich der gesamten Arbeitsgruppe Pharmazeutische Technologie für die großartige und spannende Zeit. Insbesondere danken möchte ich Dr. Hendrik Metz für zahlreiche Anregungen bei der Planung und Auswertungen von Experimenten; Dr. Manfrad Knörgen und Zhanna Svatko für ihre Hilfestellungen bei den MRI-Untersuchungen; Dr. Henrike Lucas für ihre Kompetenz bei den zelltoxikologischen Versuchen sowie der Organisation der *in vivo* Experimente; Dr. Sabine Kempe für die Unterstützung bei den EPR-Experimenten; Dr. Stefan Hoffmann, Johannes Stelzner und Erik Borski für viele wissenschaftliche Diskussionen und Ratschläge; Ute Menzel und Kerstin Schwarz für zahlreiche Erleichterungen im Laboralltag sowie die angenehme Arbeitsatmosphäre; Claudia Bertram für die Abwicklung organisatorischer Angelegenheiten sowie den Wahlpflichtfachstudenten Melanie Hedel, Marc Winderlich, Elisabeth Erler und Miriam Grundt für die Mithilfe bei Probenpräparationen und EPR-Experimenten. Außerdem danke ich Anja Windorf, Dr. Sabine Kempe und Dr. Stefan Hoffmann für viele nützliche Hinweise bei der Erstellung dieser Dissertation.

Ferner danke ich Dr. Bernhard Hiebl und Martina Hennicke für alle tierpflegerischen Maßnahmen sowie die Nutzung der Räumlichkeiten; Prof. Dr. Joachim Neumann und Dr. Barbara Schreier für die Ermöglichung der Ultraschalluntersuchungen; Dr. Michael Hacker für die Bereitstellung des Rheometers; Dieter Reese für die Hilfestellungen bei gerätebaulichen Anpassungen sowie dem Bundesministerium für Bildung und Forschung für die finanzielle Unterstützung.

Besonderer Dank gilt zudem meiner ganzen Famile für die jahrelange Unterstützung in jeder Hinsicht. Mein höchster Dank gilt meiner Frau Franziska, die mich allzeit unterstützt und motiviert hat, auch *wenn es mal wieder länger dauerte.* Vielen Dank.

LEBENSLAUF

PERSÖNLICHE DATEN

Name:	Martin Windorf
Geburtsdatum:	17.05.1988
Geburtsort:	Rudolstadt (Thür.)

AUSBILDUNG UND BERUFLICHE ENTWICKLUNG

Seit 02/2017	Head of Production - Hormone & Vial Products EVER Pharma Jena GmbH, Jena (Saale)
05/2016 - 01/2017	Production Trainee, EVER Pharma Jena GmbH, Jena (Saale)
06/2012 - 04/2016	Wissenschaftlicher Mitarbeiter, AG Pharmazeutische Technologie (Prof. Dr. K. Mäder), Martin-Luther-Universität, Halle (Saale)
04/2012 - 05/2012	Angestellter Apotheker, Schloss-Apotheke, Blankenhain (Thür.)
11/2011	Approbation als Apotheker
05/2011 - 10/2011	Pharmazeut im Praktikum, Rathaus-Apotheke, Frankfurt (Main)
11/2010 - 04/2011	Pharmazeut im Praktikum und Diplomand, Abt. Pharma Ingredients & Services, BASF SE, Ludwigshafen (Rhein)
10/2006 - 09/2010	Studium der Pharmazie, Martin-Luther-Universität, Halle (Saale)
05/2006	Allg. Hochschulreife, Staatl. Gymnasium Fridericianum, Rudolstadt (Thür.)

PUBLIKATIONSLISTE

PATENTE

K. Mäder, M. Windorf, J. Kutza; Injectable depot formulations for the controlled release of active ingredients; WO2015062571A1 (WIPO), DE102013018193A1 (DPMA), 2015

KONFERENZBEITRÄGE

K. Mäder, J. Kutza, M. Windorf; Oleogels as a New Alternative for Direct Injectable and Parenteral Controlled Release Formulations; 42nd Annual Meeting of the Controlled Release Society, July 26 - 29, 2015, Edinburgh, Scotland (Abstract & Poster)

M. Windorf, K. Mäder; Novel Carrier Systems for Protein Drug Delivery: *In Situ* Forming Oleogels; 5th Halle Conference on Recombinant Proteins, February 19 - 20, 2015, Halle (Saale), Germany (Poster)

K. Mäder, J. Kutza, M. Windorf, V. Weiss, A. Rodrigues, T. Naolou, M.H. Bilal, J. Kreßler; Direct injectable Lipid and Polymer based Carriers for Controlled Release Applications; 5th Halle Conference on Recombinant Proteins, February 19 - 20, 2015, Halle (Saale), Germany (Poster)

M. Windorf, K. Mäder; *In Situ* Forming Oleogels: *In Vitro* Investigation of Application, Solidification and Degradation; DPhG Annual Meeting, September 24 - 26, 2014, Frankfurt (Main), Germany (Abstract & Poster)

M. Windorf, Th. Cech, P. Hebestreit, K. Mäder; Investigating the underlying reason of the solubility enhancement of carbamazepine in the presence of Soluplus®; 10th Central European Symposium on Pharmaceutical Technology, September 18 - 20, 2014, Porotorz, Slovenia (Abstract & Poster)

M. Windorf, Th. Agnese, Th. Cech, S. Ganslmeier, P. Hebestreit, J. Hilzendegen, K. Mäder; Developing a reliable analytical method to determine the drug release characteristics of a formulated poorly soluble drug; 2nd Poorly Soluble Drugs Workshop, July 2, 2014, Lille, France (Abstract & Poster)

M. Windorf, Th. Cech, P. Hebestreit, K. Mäder; Preparing oral formulations of carbamazepine using the multifunctional solubilizer Soluplus®; 9th PBP World Meeting, March 31 - April 3, 2014, Lisbon, Portugal (Abstract & Poster)

M. Windorf; Injectable Lipid Formulations for Controlled Release of Proteins; 9. Gesamtarbeitsbesprechung, Protein-Kompetenznetzwerk-Halle, ProNet-T3, March 25 - 26, 2014, Halle (Saale), Germany (Vortrag)

SELBSTSTÄNDIGKEITSERKLÄRUNG

Hiermit erkläre ich an Eides statt, dass ich die vorliegende Arbeit selbstständig und ohne fremde Hilfe angefertigt und keine anderen als die angegebenen Quellen und Hilfsmittel benutzt sowie die den verwendeten Werken wörtlich oder inhaltlich entnommenen Stellen als solche kenntlich gemacht habe.

Ferner erkläre ich, dass ich mich mit dieser Dissertation erstmals um die Erlangung eines Doktorgrads bewerbe. Die vorliegende Arbeit ist weder im Inland noch im Ausland in gleicher oder ähnlicher Form einer anderen Prüfungsbehörde zum Zweck einer Promotion oder eines anderen Prüfungsverfahren vorgelegt worden.

sgd. Martin Windorf

Weimar, den 26.03.2017 Martin Windorf